NATIONAL INSTITUTE OF PUBLIC HEALTH AND THE ENVIRONMENT
BILTHOVEN, the NETHERLANDS

Report no. 722108006

European wet deposition maps based on measurements

E.P. van Leeuwen, J.W. Erisman, G.P.J. Draaijers,
C.J.M. Potma, W.A.J. van Pul

April 1995

THIS INVESTIGATION WAS CARRIED OUT ON BEHALF OF AND FOR THE ACCOUNT OF THE DIRECTORATE GENERAL OF ENVIRONMENT (DGM/LE) WITHIN THE FRAMEWORK OF PROJECT NO. 722108: "DEPOSITION RESEARCH".

Mailing list

1. Directeur Lucht en Energie, dr. G.M. van der Slikke
2. Plv.Directeur-Generaal Milieubeheer, dr.ir. B.C.J. Zoeteman
3. DGM, hoofd afd. Luchtkwaliteit en Verzuring, Drs. R.J.T. van Lint
4. W. Alexandra (UBA, Austria)
5. B. Artinaro (CIEMAT, Spain)
6. Dr. W. Asman (RISø, Denmark)
7. C. Baquero (CIEMAT, Spain)
8. E. Berge (EMEP, Norway)
9. M. Bíba (FGM, Czech Republic)
10. E. Bieber (UBA, Germany)
11. Dr. W. Bleuten (FG-UU)
12. E. O'Carroll (MS, Ireland)
13. R. Carvalho (IM, Portugal)
14. N. Cénac (MF, France)
15. P. Coddeville (MD, France)
16. E. Dambrine (INRA, France)
17. J.H. Duyzer (TNO)
18. A. Eliassen (EMEP, Norway)
19. D. Fottová (CGS, Czech Republic)
20. Dr. D. Fowler (ITE, United Kingdom)
21. M. Frolova (HA, Latvia)
22. Dr. J.Führer (ACEH, Switzerland)
23. Drs. T. Garritsen (MK-UU)
24. R. Gehrig (EMPA, Switzerland)
25. M. McGettigan (EPA, Ireland)
26. L. Granat (SU, Sweden)
27. P. Grennfelt (IVL, Sweden)
28. L. Horváth (HMS, Hungary)
29. D. Hrcek (MERP, Slovenia)
30. Z. Ikonomova (ME, Bulgaria)
31. J. Irwin (WSL, United Kingdom)
32. J. Iwanek (IEP, Poland)
33. O. Järvinen (NBWE, Finland)
34. D. Kallweit (UBA, Germany)
35. Drs. D.J. Karssenberg
36. K. Kindbom (IVL, Sweden)
37. A.Kovar (ECOSENSE, Austria)
38. R. Lavrinenko (MGO, Russia)
39. M. Mitosinkova (SHI, Slovak Republic)
40. D. Möller (FI, Germany)
41. R. Mosello (III, Italy)
42. H.Puxbaum (TUWien, Austria)
43. A. Reissell (MI, Finland)
44. M. Reuther (BLWF, Germany)
45. E. Roekens (VMM, Belgium)
46. Drs. W. Ruijgrok (KEMA)
47. L.Saare (EIC, Estonia)

48. J. Santroch (CHI, Czech Republic)
49. M. Semb (NILU, Norway)
50. V. Smirnioudi (ME, Greece)
51. Dr. J. Schaug (EMEP, Norway)
52. S. Slalina (ECN)
53. Dr. T. Spranger (UBA, Germany)
54. I. Stratan (EPNR, Moldava)
55. K. Torseth (NILU, Norway)
56. E.Ulrich (ONF, France)
57. Dr.ir W. de Vries (SC-DLO)
58. J. Vrubel (EMC, Czech Republic)
59. T. Vukovic (FHI, Yugoslavia)
60. H. Wielogorska (IMWM, Poland)
61. D.Wintermeyer (BGA, Germany)
62. G.P. Wyers (ECN)
63. Depot Nederlandse Publicaties en Nederlandse Bibliografie
64. Directie Rijksinstituut voor Volksgezondheid en Milieuhygiene
65. Dr. R.M. van Aalst (LLO)
66. Drs. J.M.M. Aben (LLO)
67. Ing. A. Bleeker (LLO)
68. Drs. E. Buijsman (LLO)
69. Ir. H.S.M.A. Diederen (LLO)
70. Ir. G.J. Heij (LWD)
71. J.P. Hettelingh (MTV)
72. Ing. J.A. van Jaarsveld (LLO)
73. Dr. L.H.J.M. Janssen (LLO)
74. Ir. F. Langeweg (SB7)
75. Dr. F.A.A.M. de Leeuw (LLO)
76. Dr. ir. D. van Lith (LLO)
77. Dr. D. Onderdelinden (LLO)
78. Drs. E.J. Pebesma (LBG)
79. Drs. R.J.C.F. Sluyter (LLO)
80. R.J. van de Velde (LBG)
81. Hoofd Bureau Voorlichting en Public Relations
82. Bureau Projekten- en Rapportenregistratie
83-87. Auteurs
88. Bibliotheek LLO
89-90. Bibliotheek RIVM
91-115. Reserve exemplaren t.b.v. Bureau Rapportenbeheer

CONTENTS

FIGURES:

APPENDICES:

TABLES:

MAPS:

SUMMARY

To date, wet deposition maps on a European scale have been based on long-range transport model results (e.g. the EMEP model). For most components wet deposition maps based on measurements are only available on national scales. However, it is desirable to derive wet deposition maps on a European scale from measurements. Although wet deposition is not a small-scale process, for effect-related studies (e.g. the determination of the exceedances of critical loads) the resolution of the maps based on models is generally too small (e.g. 150x150 km blocks for the EMEP model) in comparison with local variations in deposition. Maps derived from measurements solve this problem as the resolution of these maps can be larger. Additionally, these measurement-based maps can be used to evaluate the long-range transport models.

This report presents maps on concentration and wet deposition of non-marine sulphate, nitrate, ammonium, hydrogen, sodium, chloride, magnesium, potassium and calcium. These components, based on results of field measurements made at approximately 750 locations (the number of locations differs per component), are mapped on a 50x50 km scale over Europe for 1989. Point observations are interpolated to a field covering the whole of Europe using the Kriging interpolation technique. An extensive uncertainty analysis is performed to assess the quality of the maps. For sulphate, nitrate and ammonium wet deposition fluxes are compared with wet deposition fluxes as calculated by the EMEP long-range transport model.

Information on concentrations of ions in precipitation in 1989 was obtained from the EMEP database and from questionnaires which were sent to all organisations responsible for wet deposition monitoring in their countries. To obtain an indication of data quality, the ionic balance was calculated and a visual check was carried out by investigating scatter-plots of elements that exhibit a strong correlation. Concentrations measured with bulk samplers were corrected for the contribution of dry deposition onto the funnels of these samplers. Correction factors for different countries and for different elements were derived from literature.

Because data are distributed skew, they are transformed to their common logarithms. Spatial analysis based on regionalised variable theory revealed autocorrelation in all ions and reasonable bounded models were fitted to the experimental variograms. The variograms clearly showed that the measurements are spatially correlated, indicating kriging to be a good interpolation technique. A cross-validation procedure was carried out to investigate whether the fitted variogram models describe the spatial structure of the data correctly. Generally, results were found satisfactory.

Because concentrations in precipitation show smaller spatial variability than precipitation amounts, interpolation was performed on concentration data instead of fluxes. To obtain wet deposition fluxes, interpolated concentrations were multiplied by long-term mean precipitation amounts compiled by EPA (Environmental Protection Agency, U.S.A.), because this database contains a large number of measurements which are corrected for gauge-induced biases to remove systematic errors.

The patterns in the obtained concentration and flux maps agreed well with what would be expected from prior knowledge of European emissions and climate patterns. High sulphate deposition is observed in the border area between Germany, Poland and the Czech Republic, and Ukraine and former Yugoslavia, while nitrate deposition is highest in a zone ranging from southern Scandinavia to northern Italy. Ammonium fluxes are largest in Central Europe. The influence of salt water bodies is evident for sodium, chloride and magnesium. Large calcium fluxes are found in southeast Europe, probably caused by the influence of soil dust from calcareous soils and desert dust from the Sahara.

To assess the quality of the maps an extensive uncertainty analysis was performed. A large number of different sources of uncertainty could be recognised. The numbers presented here should therefore be regarded as a best guess based on expert judgement. To describe the uncertainty a division into three categories was made: *(a)* west, north-west and central Europe as 'good quality areas' where data quality is assumed to be high and sufficient (representative) data are present, *(b)* areas at the edges of the maps, i.e. east, south-east and south-west Europe as 'poor quality areas', where the representativeness and quality of the little data available can be questionable and *(c)* mountainous areas (e.g. the Alps) and upland areas (e.g. United Kingdom and Scandinavia), even though located in areas with many data, as 'complex terrain areas with additional uncertainties'. As the estimates are rather rough, no distinction between different components is made. Two cases were considered: first, a propagation of errors without correlation (conservative) and, second, a propagation with full positive correlation between precipitation amounts and concentrations in precipitation (worst case). Uncertainties refer to an average 50x50 km grid cell. In the conservative case *(1)*, the overall uncertainty is estimated to be 50% in west, north-west and central Europe, whereas in the worst case *(2)* the overall uncertainty is estimated to be 70% here. In areas at the edges of the maps, i.e. east, south-east and south-west Europe, *(1)* is estimated to be 60% and *(2)* 80%, whereas in complex terrain areas *(1)* is estimated to be 70% and *(2)* 100%.

Results are compared with EMEP model results by means of X-Y plots in which the averages of the new values within one EMEP grid cell of 150x150 km are plotted against the EMEP values. The fluxes obtained in this study are larger than those calculated by the EMEP long-range transport model. Average fluxes are about 75% larger for sulphate, 20% for nitrate and 55% for ammonium.

SAMENVATTING

Natte depositie kaarten van Europa zijn tot nu toe gebaseerd op resultaten die door lange afstands transport modellen zijn gegenereerd (b.v. het EMEP model; Iversen *et al.*, 1991). Natte depositie kaarten die op metingen zijn gebaseerd zijn voor de meeste componenten slechts op nationale schaal aanwezig. Het is echter noodzakelijk om natte depositie kaarten op Europese schaal te vervaardigen die gebaseerd zijn op metingen. Hoewel natte depositie geen kleinschalig proces is, is voor effect studies (de bepaling van de overschrijding van critische waarden) de resolutie van de op modellen gebaseerde kaarten over het algemeen te klein (bijvoorbeeld 150x150 km blokken voor het EMEP model) in vergelijking met locale variaties in depositie. Kaarten die uit metingen zijn verkregen lossen dit probleem op aangezien de resolutie van deze kaarten groter kan zijn. Daarnaast kunnen deze op metingen gebaseerde kaarten worden gebruikt om de lange afstands transport modellen te valideren.

In dit rapport worden concentratie en natte depositie kaarten van sulfaat, nitraat, ammonium, waterstof, chloride, natrium, magnesium, kalium en calcium gepresenteerd. De kartering van deze componenten op Europese schaal voor 1989 heeft plaatsgevonden met een resolutie van 50x50 km en was gebaseerd op resultaten van veld metingen die op ongeveer 750 locaties in Europa zijn uitgevoerd (het aantal locaties verschilt per component). Punt observaties zijn met behulp van de kriging interpolatie techniek geïnterpoleerd naar een veld dat heel Europa bestrijkt. Een uitgebreide onzekerheidsanalyse is uitgevoerd om de kwaliteit van de kaarten te beoordelen. De sulfaat, nitraat en ammonium natte depositie fluxen zijn vergeleken met natte depositie fluxen zoals die door het EMEP model zijn berekend.

Informatie over concentraties in de neerslag in 1989 zijn verkregen uit de EMEP database, en uit enquetes die waren verstuurd naar alle organisaties die verantwoordelijk zijn voor natte depositie metingen in hun land. Om een idee van de data kwaliteit te verkrijgen is de ionenbalans berekend en zijn visuele controles uitgevoerd aan de hand van grafieken tussen elementen die sterk gecorreleerd zijn. Concentraties die in bulk vangers zijn gemeten zijn gecorrigeerd voor de bijdrage van droge depositie op de trechters van deze vangers. Uit de literatuur zijn correctie factoren afgeleid voor verschillende elementen en voor verschillende landen.

Omdat de data scheef verdeeld waren zijn ze logarithmisch getransformeerd. Ruimtelijke analyse, gebaseerd op de theorie van de geregionaliseerde variabelen (Matheron, 1965) toonde voor alle ionen autocorrelatie aan zodat redelijke modellen door de experimentele variogrammen konden worden getekend. De variogrammen tonen duidelijk dat de data ruimtelijk gecorreleerd zijn, erop duidend dat kriging een goede interpolatietechniek is. Om te onderzoeken of de gebruikte variogram modellen de ruimtelijke structuur in de data correct beschrijven is een kruis-validatie procedure uitgevoerd. Over het algemeen waren de resultaten goed.

Aangezien concentraties in neerslag in de ruimte minder variëren dan neerslaghoeveelheden is een interpolatie uitgevoerd op concentraties i.p.v. fluxen. Om natte depositiefluxen te verkrijgen, zijn de geïnterpoleerde concentraties vermenigvuldigd met lange termijn-gemiddelde neerslaghoeveelheden, samengesteld door EPA (Environmental Protection Agency, USA), omdat deze dataset een groot

aantal metingen bevat waarbij systhematische fouten zijn verwijderd door te corrigeren voor afwijkingen die zijn veroorzaakt door het gebruik van verschillende trechters.

De waargenomen patronen in de concentratie en flux kaarten komen goed overeen met wat van te voren op basis van kennis over Europese emissies en klimaatspatronen kon worden verwacht. Hoge sulfaat fluxen zijn te zien in het grensgebied van Duitsland, Polen en de Tsjechische Republiek, en Oekraïne en voormalig Joegoslavië, terwijl de hoogste nitraat depositie in een zône van zuid-Scandinavië tot Noord-Italië is te vinden. Ammonium fluxen zijn het hoogst in Centraal Europa. De invloed van zeezout deeltjes is duidelijk te zien in de natrium, chloride en magnesium kaarten. Hoge calcium fluxen komen vooral voor in Zuid-Oost Europa, wat waarschijnlijk samenhangt met bodemstof van kalkrijke bodems en woestijnstof uit de Sahara.

Om de kwaliteit van de kaarten te beoordelen is een uitgebreide onzekerheidsanalyse uitgevoerd. De kaarten zijn aan een groot aantal verschillende onzekerheidsbronnen onderhevig. De gepresenteerde onzekerheidsgetallen zijn zelf ook aan onzekerheid onderhevig en dienen als een 'best guess' te worden beschouwd. Om de totale onzekerheid weer te geven is een onderverdeling in drie categorieën gemaakt: *(a)* West, Noord-West en Centraal Europa als 'goede kwaliteit' gebieden waar wordt aangenomen dat de datakwaliteit goed is en waar voldoende (representatieve) gegevens voorhanden zijn, *(b)* gebieden aan de randen van de kaarten, te weten Oost, Zuid-Oost en Zuid-West Europa als 'slechte kwaliteit' gebieden, waar minder gegevens beschikbaar zijn waarvan bovendien de kwaliteit en representativiteit minder groot kunnen zijn en *(c)* bergachtige gebieden (zoals de Alpen) en hooggelegen gebieden (zoals in het Verenigd Koninkrijk en Scandinavië), als 'complex landschap met aanvullende onzekerheden' (zelfs indien gelegen in gebieden met een goede data dekking). Aangezien de schattingen nogal grof zijn is er geen onderscheid gemaakt tussen de verschillende componenten. Er zijn twee gevallen beschouwd, ten eerste een foutenvoortplanting zonder correlatie (conservatief), en ten tweede een voortplanting met volledige correlatie tussen neerslaghoeveelheden en concentraties in neerslag ('worst case'). Onzekerheden hebben betrekking op een gemiddelde 50x50 km gridcel. In het conservatieve geval *(1)* is de totale onzekerheid in West, Noord-West en Centraal Europa op 50% geschat, terwijl in de 'worst case' *(2)* de totale onzekerheid hier op 70% is geschat. In gebieden aan de rand van de kaarten, te weten Oost, Zuid-Oost en Zuid-West Europa, is *(1)* op 60% geschat en *(2)* op 80%, terwijl in gebieden met complex landschap *(1)* geschat is op 70% en *(2)* op 100%.

De resultaten zijn vergeleken met door het EMEP model gegenereerde resultaten middels grafieken waarin de gemiddelden van de nieuwe waarden binnen 1 EMEP grid cel van 150x150 km zijn uitgezet tegen de EMEP waarden. De fluxen die in deze studie zijn verkregen zijn hoger dan de door het EMEP model gegenereerde fluxen. Gemiddeld zijn de fluxen ongeveer 75% hoger voor sulfaat, 20% voor nitraat en 55% voor ammonium.

1. INTRODUCTION

Acid deposition, acidifying soils and surface waters, is recognised as a serious threat to ecosystem stability. In Europe, sulphur compounds, and both reduced and oxidised nitrogen compounds, are thought to be the main precursors of acid deposition. Nitrogen deposition also causes eutrophication. A distinction can be made between dry deposition, cloud / fog water deposition and wet deposition.

Wet deposition is the process by which atmospheric pollutants are attached to and dissolved in cloud and precipitation droplets and as a result delivered to the earth's surface by rain, hail or snow. Wet deposition fluxes can be determined by measuring concentrations in rain and rainfall amounts. The wet deposition process is usually divided into in-cloud and below-cloud scavenging (Buijsman, 1982). In-cloud scavenging refers to scavenging of particles and gases in clouds, whereas below-cloud scavenging refers to below-cloud uptake of compounds by falling raindrops. In the in-cloud scavenging process, the particles may act as condensation nuclei for cloud droplets, whereas gases may be taken up by cloud droplets through absorption and subsequent dissolution. Below-cloud scavenging may play an important role when air concentrations of gases and particles below the cloud are much higher than concentrations in the cloud, as will be the case close to sources or source areas.

Up to now wet deposition maps on a European scale have been based on long-range transport model results (e.g. the EMEP model; Iversen *et al.*, 1991). However, it is desirable to derive wet deposition maps on this scale from measurements. Although wet deposition is not a small-scale process, for effect-related studies (e.g. the determination of the exceedances of critical loads) the resolution of the maps based on models is generally too small (e.g. 150x150 km blocks for the EMEP model) as local variations in deposition occur. Maps derived from measurements solve this problem as the resolution of these maps will be larger (50x50 km blocks). Additionally, the measurement based maps can be used to evaluate the long-range transport models. Up to now, wet deposition maps based on measurements have only been available on national scales (except for ammonium for which a map on a European scale was derived by Buijsman and Erisman, 1988). In the study reported here wet deposition fluxes are mapped on a European scale for 1989 with 50x50 km blocks, based on results from field measurements made at about 750 locations (numbers differing per component). In addition to maps of acidifying components maps of the base cations Ca^{2+}, Mg^{2+} and K^{+} are also made because they too play an integral role in the chemical processes of acid deposition (Barnard *et al.*, 1986; Gatz *et al.*, 1986; Munger and Eisenreich, 1983), since the acidity of any material is a function of both its acidic and basic content (Hendry and Brezonik, 1980).

The composition of precipitation is monitored in collectors throughout almost the whole of Europe. Information on concentrations of ions in precipitation in 1989 was obtained from the EMEP database (European Monitoring and Evaluation Program) and from questionnaires sent to all organisations responsible for wet deposition monitoring in their countries. To obtain an indication of data quality the ionic balance was calculated and a visual check was carried out by investigating scatter-plots of elements that exhibit a strong correlation (i.e. magnesium vs. chloride, magnesium vs sodium, sodium vs. chloride, sulphate vs. nitrate, sulphate vs. ammonium and nitrate

vs. ammonium). Data collection and data quality are described in chapter 2. Concentrations measured with bulk samplers were corrected for the contribution of dry deposition onto the funnels of these samplers. In chapter 3 correction factors for different countries and elements are derived from literature.

After data transformation (chapter 4), the spatial structures of the concentration data were analysed using geostatistics, and the data were interpolated using the Kriging interpolation technique. Using this technique, it is assumed that the sample data satisfy the intrinsic hypothesis (Cressie, 1993). For a description of theory and practical applications of Kriging, see chapter 5 and standard works by Cressie (1993), Journel and Huijbregts (1978) and Webster and Oliver (1990). In chapter 6 variogram modelling is described. Chapter 7 presents the interpolation procedure. To obtain wet deposition fluxes concentrations were multiplied by long-term mean precipitation amounts.

This report presents concentration- and wet deposition flux maps of non-marine sulphate, nitrate, ammonium, hydrogen, sodium, chloride, magnesium, potassium and calcium. In chapter 8 spatial patterns in the concentration and flux maps are described. An extensive uncertainty analysis is performed to assess the quality of the maps. For sulphate, nitrate and ammonium results are compared with wet deposition fluxes calculated by the EMEP long-range transport model. These topics are also described in chapter 8. The report terminates in chapter 9 with conclusions and recommendations for improving the wet deposition maps.

Compilation of wet deposition maps forms the sub-part of the project aiming at determining small-scale total deposition maps of acidifying components in Europe. This project, called **EDACS** (**E**uropean **D**eposition of **A**cidifying **C**omponents on a **S**mall scale) is described in Van Pul *et al.* (1995).

2. MONITORING NETWORK

2.1 Data collection

Information on the 1989 concentrations of ions in precipitation was obtained from EMEP (Schaug *et al.*, 1991) and from questionnaires (Appendix 1) sent to all organisations responsible for wet deposition monitoring in their countries. In many cases, not all information asked for was available, and only partially filled-in questionnaires were received. All data obtained by the questionnaires and reports were put together in a database containing the following: concentrations of the elements SO_4^{2-}, NO_3^-, NH_4^+, H^+, Na^+, Cl^-, Ca^{2+}, K^+, Mg^{2+}, precipitation amounts, information on location (co-ordinates) and type of rain sampler used (bulk or wet-only). Figure 1 shows a map of the locations of the measurement sites.

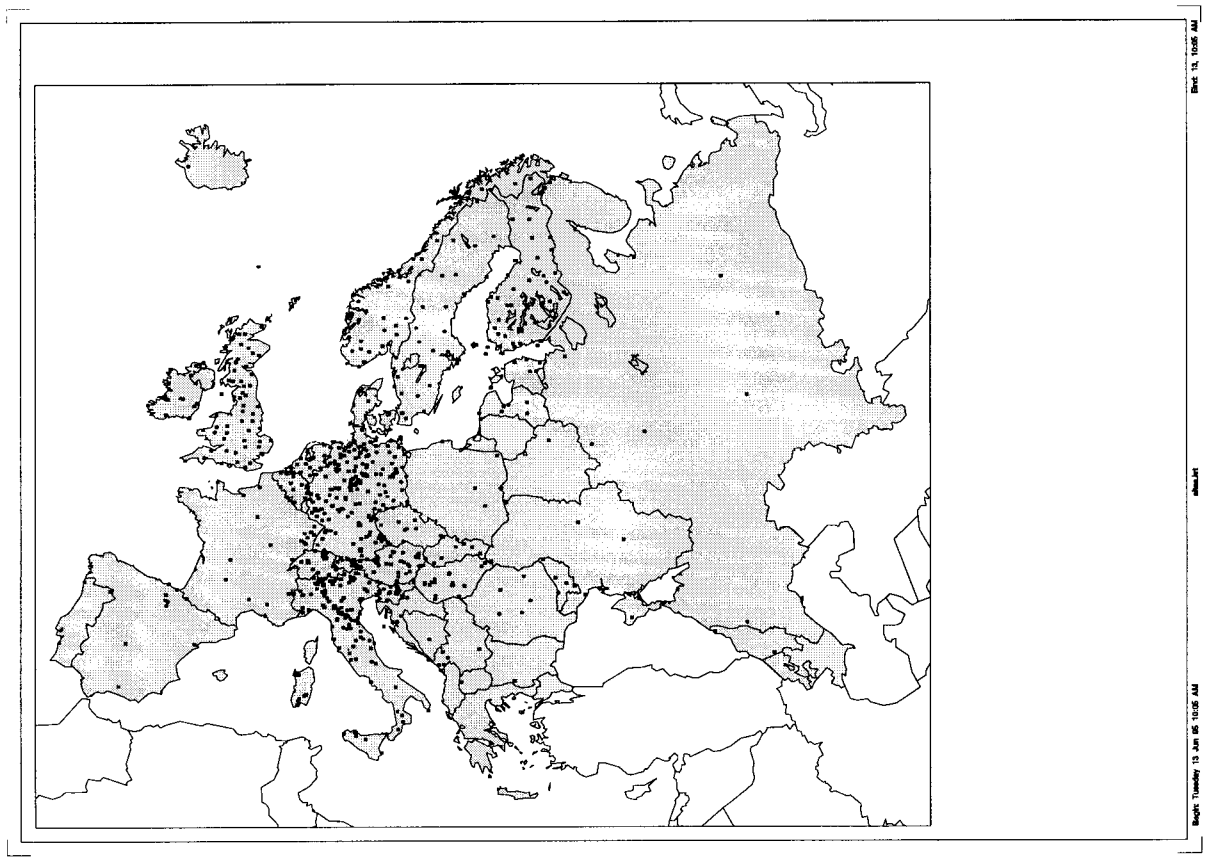

Figure 1: Locations of the wet deposition measurement sites.

It can be seen that the sites are not evenly spread over Europe. In east and south-west Europe the spacing between the sites is generally very large. Besides, not all elements were analysed at all sites (Table 1). The acidifying components SO_4^{2-}, NO_3^- and NH_4^+ were most frequently analysed. Although concentration data from 1989 were preferred, data from other years or the average of several years were used if 1989 data were not available. Information on approximately 300, of a total of 824 measurement sites in the database, did not originate from 1989.

Table 1: Total number of measurements of the various elements

Element:	SO_4^{2-}	NO_3^-	NH_4^+	H^+	Na^+	Cl^-	Mg^{2+}	K^+	Ca^{2+}
Number:	760	772	739	605	590	616	617	512	664

Sulphate concentrations were corrected for the contribution of sea salt, because only non-marine sulphate contributes to acidification. By assuming that the ratio of sodium to sulphate in sea spray is the same as in bulk sea water, and that all the sodium in a sample is of marine origin, it is possible to calculate non-marine sulphate (equation 1). When concentrations [x] are considered:

$$[\text{non-marine sulphate}] = [\text{sulphate}] - 0.06 * [\text{sodium}] \quad (1)$$

In background areas at small distances from the sea, this correction can cause a decrease of the sulphate concentration of up to 25%. However, at about 200 sites only information on the sulphate concentration was available and the sodium concentration was not measured. On these sites values from the interpolated sodium concentration map were used for correction.

2.2 Data quality

To get an idea about the quality of the data, two checks were carried out. First, a check on the ionic balance of the samples was performed. Of the total of 824 measurement sites, all major ions were measured at 478 sites. The balances for those sites were calculated according to equation 2:

$$\delta\ ion[\%] = \frac{\sum Kat - \sum An}{\sum Kat + \sum An} * 100 \quad (2)$$

Using this equation it can be calculated that 52% of the 478 samples have an ionic imbalance > 10%, and 13% of > 25%. In some cases there is a surplus of cations, while in others the anions dominate. This is also shown in the scatter-plot between the total sum of anion deposition and the total sum of cation deposition (Figure 2). The imbalance could have been caused by a measurement error in only one or few of the elements (not necessarily all elements have to be wrong). As it is not known what element(s) caused the imbalance, all data were maintained because excluding a site from the dataset would mean the loss of all data at that site. An ionic imbalance might also be caused by a particular element that was not measured but has a large impact on the balance locally. The imbalance was taken as uncertainty

The quality of the data was also checked by constructing scatter-plots of two elements should be strongly correlated, e.g. NH_4-SO_4, NO_3-NH_4, SO_4-NO_3, Na-Mg, Cl-Mg and Na-Cl. These plots are presented in Appendix 2. In Table 2 correlation coefficients as well as regression parameters for these ions are presented. For NH_4, SO_4 and NO_3 the

correlation between the elements is somewhat smaller than for Na, Cl and Mg as could be expected from the processes influencing these correlations. For these last three elements the relationship is only strong at high concentration levels. Outliers can only be excluded from the data set when correlation between elements is strong and additionally when data from certain sites deviate from the regression line to a large extent, preferably also in scatter plots for other elements. This does not seem to be the case. Because the Na-Cl correlation is rather good (r^2 is 0.87), it can be concluded that the outliers in the Cl-Mg and Na-Mg are probably caused by large magnesium concentrations. Outliers in these plots are not necessarily errors and may reflect local sources. Again this is treated as uncertainty.

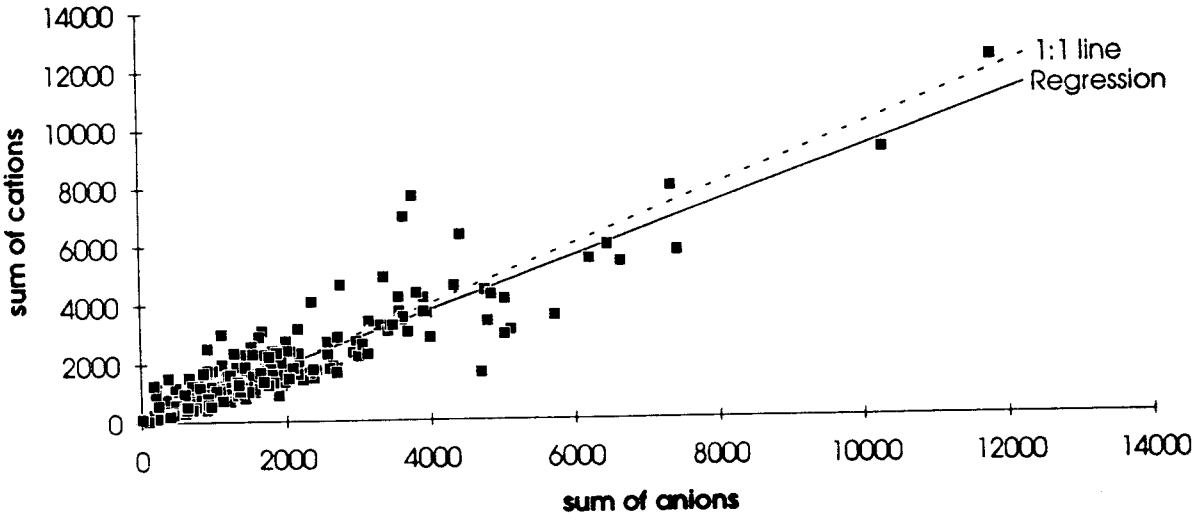

Figure 2: *Scatter-plot showing the difference between the sum of cation and the sum of anion deposition. (in mol/ha per year).*

Table 2: *Pearson correlation coefficients and regression parameters between highly correlated components.*

x	y	r^2	a	b
NO_3	SO_4	0.28	0.95	0.08
NO_3	NH_4	0.48	1.19	0.03
NH_4	SO_4	0.37	0.62	0.20
Cl	Na	0.87	0.75	0.07
Cl	Mg	0.49	0.08	0.05
Na	Mg	0.50	0.11	0.05

*r^2 is the Pearson correlation coefficient, **a** the slope and **b** the y-axis cut-off value in the equation $y = a\,x + b$.*

3. DIFFERENCE BETWEEN BULK AND WET-ONLY SAMPLERS

Wet deposition can be measured using bulk or wet-only samplers. Wet-only samplers are most accurate because the funnels are only open during precipitation events. The funnel surface of bulk samplers will also collect some dry deposition of gases and particles which will bias the samples. In the past, only bulk samplers were used, but recently wet-only samplers became more common practice. Because wet-only samplers are expensive, require a power source, and are relatively sensitive to disturbances, open funnels are still used to collect precipitation as well. The total deposition flux to such open funnels is called bulk precipitation flux, and consists of both wet deposition and some dry deposition onto the funnels. From parallel measurements with bulk samplers and wet-only samplers, correction factors for the contribution of dry deposition onto the funnels can be derived. These investigations were performed in different countries. An overview of the correction factors is presented in Table 3 as the ratio of wet-only to bulk precipitation fluxes. Each compound in the table shows a wide range of correction values, i.e. fairly large standard deviations. The amount of dry deposition onto the funnels will be influenced by the distance to sources, the collecting efficiency of the samplers and the frequency and amount of precipitation (Draaijers and Erisman, 1993). Small absolute concentration differences between samples analysed with bulk and wet-only samplers might have a large influence on the correction values when small concentrations of a compound occur in both wet-only and bulk precipitation. This might explain some very small values (e.g. smallest value for potassium is 0.25) and large values (e.g. largest value for calcium is 1.67). In most cases the ratio is smaller than 1, but the opposite is possible if the bulk sampler catches less precipitation than the wet-only sampler.

The ratios used in this study to correct bulk preciptation samples were derived using the criteria described below. First, the correction factors were averaged separately in each country, with exclusion of the values deviating more than 20% from the mean. By applying this selection criterion most German values as well as the values greater than 1 were excluded. Second, the 'mean country values' were averaged to obtain one factor for each element for the whole of Europe.

Table 3: Ratio of wet-only to bulk precipitation for each element in different countries

Ref.	Code	SO_4	NO_3	NH_4	Na_{cont}	Na_{coast}	Cl_{cont}	Cl_{coast}	Mg	Ca	K
1 NL	$a_{(4)}$	0.82	0.83	0.79	$0.87_{(3)}$	$0.63_{(1)}$	$0.87_{(3)}$	$0.63_{(1)}$	0.76	0.81	0.65
2 NL	b	0.74	0.78	0.77	0.77	-	0.83	-	0.65	0.45	0.71
3 NL	b	0.73	0.83	0.70	-	-	-	-	-	-	-
4 NL	c	0.82	0.82	0.73	-	0.73	-	0.75	0.65	0.69	0.64
Av.	$_{(7)}$	0.78	0.81	0.75	$0.82_{(4)}$	$0.68_{(2)}$	$0.85_{(4)}$	$0.69_{(2)}$	0.69	0.73	0.67
5 ITA	b	0.92	0.89	0.94	0.93	-	0.90	-	0.76	0.76	0.84
6 UK	b	0.92	0.95	0.93	0.85	-	0.87	-	0.86	0.80	0.83
7 UK	$a_{(11)}$	0.96	0.97	1.25	0.84	-	0.86	-	0.87	0.81	0.93
Av.	$a_{(12)}$	0.94	0.96	0.93	0.84	-	0.87	-	0.87	0.81	0.88
8 GER	$ba_{(3)}$	0.66	0.88	-	0.37	-	0.47	-	0.38	0.36	0.25
9 CZV	b	0.74	0.80	0.71	0.90	-	0.82	-	0.61	0.53	0.63
10 SWE	c	0.95	0.83	0.80	-	0.68	-	0.71	0.88	1.67	0.77
		SO_4	**NO_3**	**NH_4**	**Na_{cont}**	**Na_{coast}**	**Cl_{cont}**	**Cl_{coast}**	**Mg**	**Ca**	**K**
Average		**0.87**	**0.85**	**0.83**	**0.87**	**0.68**	**0.86**	**0.70**	**0.76**	**0.70**	**0.76**
SD		**0.09**	**0.04**	**0.10**	**0.07**	**0.00**	**0.05**	**0.01**	**0.10**	**0.11**	**0.09**

***a( )** is the average of (x) measurement sites (when measurement sites are considered as a pair of a bulk and a wet-only sampler), **b** is a continental measurement site and **c** a coastal measurement site. **Ref** refers to the literature as well as the concerned country.*

References:

1: KNMI/RIVM, 1989
2: Ridder *et al.*, 1984
3: Ruijgrok *et al.*, 1990
4: Slanina *et al.*, 1990
5: Mosello *et al.*, 1988
6: Clark&Lambert, 1987
7: Stedman *et al.*, 1990
8: Georgii *et al.*, 1986
9: Moldan, 1980
10: Grennfelt *et al.*, 1985

Country codes:

Nl: The Netherlands
UK: United Kingdom
CZV: Czechoslovakia
ITA: Italy
GER: Germany
SWE: Sweden

After data analysis one average correction factor for chloride and sodium for all measurement sites seemed to be inadequate, as the measured concentrations with 'corrected' bulk samplers at coastal sites were consequently higher than concentrations measured with wet-only samplers. Therefore coastal sites were corrected with another factor than continental sites. This 'distance to sea' effect was not clearly recognised for other elements. The correction factors for sodium and chloride (Table 3) were derived using a procedure in which the distance to the coast was determined for all available 'bulk vs. wet-only measurements'. The distance to the coast versus the ratio wet-only to bulk precipitation fluxes is presented in scatter-plots. In these plots (Figure 3), the influence of the distance to the coast on the ratio can be derived roughly. From a distance to the coast of about 50 km and more, a horizontal line through the points in the plots can be drawn, indicating that from 50 km the ratio remains constant. In the range from 0 to 50 km to the coast an increase in the ratio is observed, which implies that in this zone a different correction factor has to be applied. Therefore, a buffer zone of 50 km to the coast was constructed with ArcInfo. The average ratio of the available coastal measurements from Table 3 (the sites within a distance of 50 km to the coast) was calculated, as well as the average ratio of the other measurements (with a distance to the coast greater than 50 km). In this way, sites within the 'sea influenced zone' were corrected with a factor other than 'continental sites'. Although the width of the zone of sea influence may depend on the dominating wind direction and wind speed, this was not incorporated in the procedure.

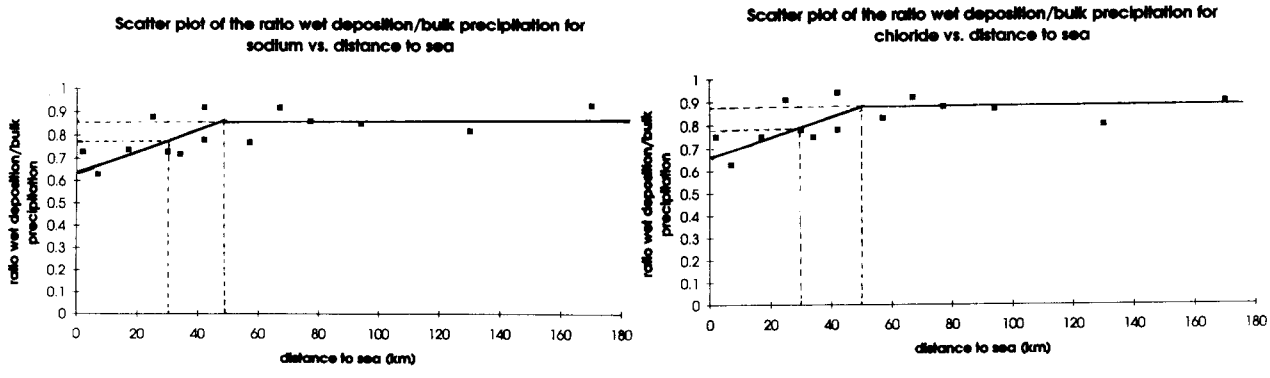

Figure 3: *Scatter plots of the ratio wet deposition / bulk precipitation vs. distance to sea for sodium and chloride.*

4. THEORY OF KRIGING

In order to map the distribution of the ionic concentrations in the most accurate way, kriging is used to estimate values on a fine mesh of grid cells (50x50 km blocks). Kriging is based on the *theory of regionalised variables* (Matheron, 1965). The theory rests on the recognition that the spatial variation of any natural property, known as a 'regionalised variable', is too irregular to be modelled by a smooth mathematical function, but can be described better by a stochastic surface. Concentrations in precipitation can be considered a regionalised variable as such. First, the stochastic aspects of the regionalised variable are explored and then modelled. The resulting information is used to estimate the λ_i weights for interpolation. The optimal interpolation technique kriging rests on the validity of assumptions about the statistical nature of the variation. Regionalised variable theory assumes that the spatial variation of any variable can be expressed as the sum of three major components. These are *(a)* a structural component, associated with a constant mean value or a constant trend; *(b)* a random, spatially correlated component; and *(c)* a random noise or residual error term (Burrough, 1986). The value of a variable Z at x (where x is a position in 1, 2 or 3 dimensions) is given by:

$$Z_{(x)} = m_{(x)} + \varepsilon'_{(x)} + \varepsilon''_{(x)} \qquad \textbf{(3)}$$

where $m_{(x)}$ is a deterministic function describing the 'structural' component of Z at x, $\varepsilon'_{(x)}$ is the term denoting the spatially dependent residuals from $m_{(x)}$, and ε'' is a residual, spatially independent Gaussian noise term having zero mean and variance σ^2. A more thorough description of the theoretical aspects of the kriging interpolation technique is presented in Appendix 3.

A variogram is used in an interpolation technique to give the best estimate of the concentration at point I, given measurements at points A, B, C, D, E and F (Figure 4; example taken from the UK Review Group on Acid Rain, 1990). The kriging interpolation technique uses the variogram model to estimate I:

$$\begin{aligned} &I = \lambda_a A + \lambda_b B + \lambda_c C + \lambda_d D + \lambda_e E + \lambda_f F \\ &\text{where} \sum \lambda_i = 1 \end{aligned} \qquad \textbf{(4)}$$

If the variogram is very steep near h = 0 and the nugget is small or zero, λ_e will be close to 1 since nearby measurements would tend to give similar answers. If, however the nugget was relatively large, λ_a, λ_b, λ_c and λ_d would increase relative to the former case. Another property of the kriging estimator is that λ_a and λ_b will be smaller than λ_d i.e. more weight would be given to a single measurement than to individuals of a pair of nearby measurements. λ_f will be smaller than λ_c because it is shielded from the unknown point by A and B.

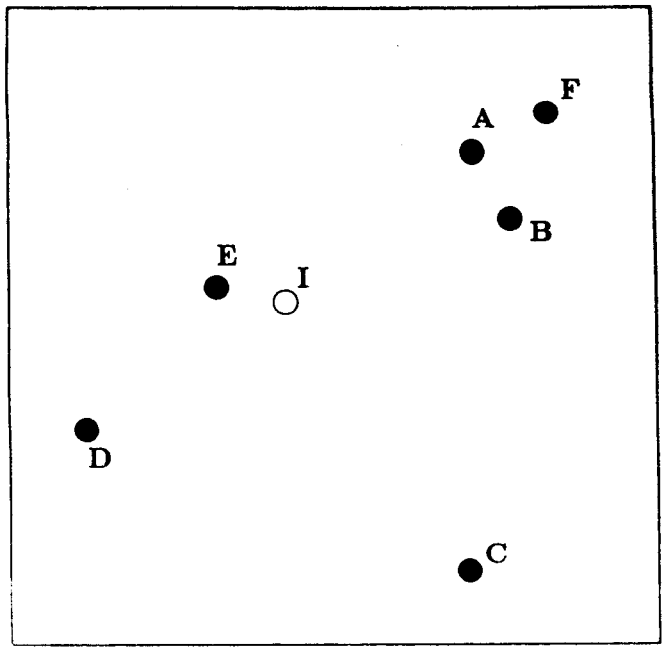

Figure 4: Illustration of the kriging interpolation procedure.

The kriging technique provides the best linear unbiased estimate. It is unbiased because the λ_i sum to 1, and the best in the sense that the error in the estimate is minimised. The kriging equations yield a value for the estimation error and this can be mapped to show the reliability of the interpolated map, which is another advantage of this method. The use of geostatistical analysis in mapping the composition of precipitation has been described, for example by Webster *et al.* (1991).

5. DATA TRANSFORMATION

Although a normal data distribution is not necessary for application of the kriging interpolation technique, interpolation results, just like other methods of least squares estimation, are most reliable when data are normally distributed. This is because extreme values carry much weight in the calculating procedure of the experimental semi-variograms, as these are determined by the squared differences between the values of two points separated by a distance **h** (Appendix 3). The frequency distributions (histograms) of the original data were examined and summary statistics (including coefficient of skewness) computed (Table 4). They show that for most components concentrations were distributed skew; in almost all cases the coefficient of skewness was greater than 1. Therefore data were transformed to their common logarithms. In Appendix 4 the histograms of the log-transformed variables are presented. Table 4 shows that skewness diminished after data transformation. Only nitrate did not improve, but for the sake of consistency the log-transformed nitrate values were interpolated. Of course, the maps of interpolated values derived in this way will represent log-normal values. These values were transformed back to the actual values later on in the procedure.

Table 4: Statistical summary of the annual mean composition of precipitation

Variate	**Mean** $10E^{-4}$ mol/l [ ]	**SD**	**Skew**	**Mean** $10E^{-4}$ mol/l log [ ]	**SD**	**Skew**
SO_4	0.43	0.35	3.61	-0.47	0.31	-0.28
NO_3	0.37	0.20	0.98	-0.51	0.30	-1.35
NH_4	0.46	0.33	2.27	-0.44	0.34	-1.05
H	0.25	0.20	0.88	-	-	-
Na	0.70	2.28	16.4	-0.52	0.50	0.47
Cl	0.749	2.05	12.3	-0.49	0.50	0.52
Mg	0.12	0.25	12.3	-1.20	0.44	0.40
K	0.08	0.19	10.6	-1.32	0.39	0.68
Ca	0.26	0.34	4.33	-0.84	0.48	-0.02

Skew *denotes the coefficient of skewness.*

6. VARIOGRAM MODELLING

Experimental variograms were calculated as described in Appendix 3. For this purpose the software package **GSTAT** 1.1 - **GeoSTA**tistical **T**oolbox (Pebesma, 1994) was used. GSTAT is a program for modelling, interpolation and simulation of multivariate geostatistical data. It only calculates the *experimental variogram.* To optimally fit a variogram model through the experimental variogram values, the computer program **WlSfit** - **W**eighted **L**east **S**quares **fit** (Pebesma, 1994) was used. The fit is optimal in the sense that the weighted residual sums of squares is minimized. The program can choose the type of variogram model to be fitted: spherical, circular, exponential, Gaussian, linear, linear with sill or Bessel (Pebesma, 1994). The resulting model is displayed, together with its parameter values and the value of the 'Sum of Squares due to Deviations' divided by the 'Total Sum of Squares' (SSD/TSS). The best model fitting the data is obtained when this value is lowest.

The nugget and shape of the variogram at small lag distances (**h**) were investigated in more detail by defining a short cut-off value (maximum distance for variogram modelling) and a smaller lag increment, and then recalculating the variogram. When modelling the variogram over a longer distance, the nugget value was set to the 'more exact' value determined with the short interval model. In this way the quality of the resulting variograms was improved. So the model with the lowest SSD/TSS ratio (best least squares fit) was chosen, with the nugget set to a particular value. In most cases the exponential model was used, whereas in some others the Gaussian model was applied. These models are defined by the following equations:

$$\textbf{Exponential:}\quad \gamma(\mathbf{h}) = c_0 + c_s \{1 - \exp(-\mathbf{h}/a)\} \tag{5}$$

$$\textbf{Gaussian:}\quad \gamma(\mathbf{h}) = c_0 + c_s \{1 - \exp(-\mathbf{h}^2/a^2) \tag{6}$$

where c_0 is the intercept or 'nugget' variance, c_s the 'sill' of the spatially dependent variance, **h** the 'lag' and a the 'range'. For the exponential model the effective range (r) is $3a$ and for the Gaussian model $r = \sqrt{3}a$ (Pebesma, 1994). Figure 5 presents the experimental variograms with the fitted models are presented. Table 5 lists the model types and their parameters.

Figure 5:
Variograms with estimated semi-variances plotted as points and fitted models as lines for (a) non-marine sulphate, (b) nitrate, (c) ammonium, (d) hydrogen, (e) sodium, (f) chloride, (g) magnesium,(h) potassium and (i) calcium.

semivariances γ(gamma) in $\log_{10}(10E^{-4}$ mol/l$)^2$ and lag (distance) in km.

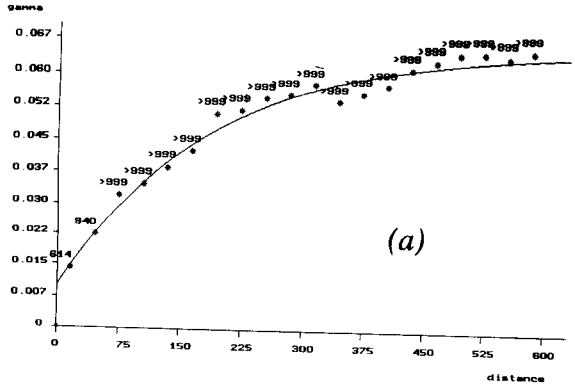

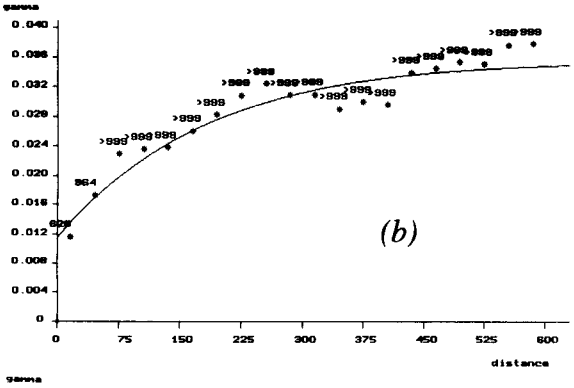

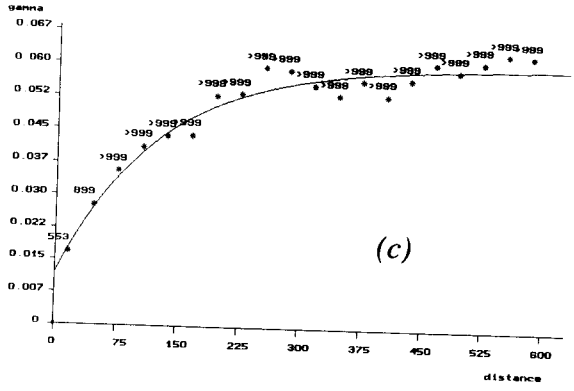

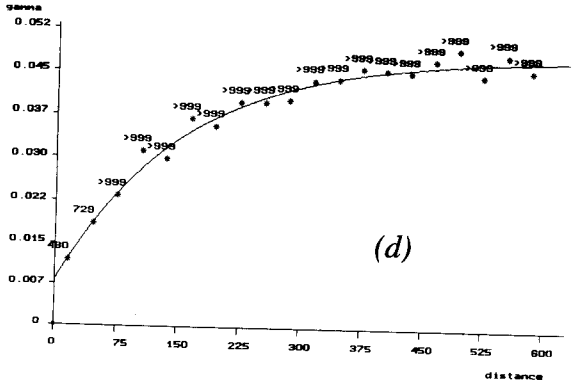

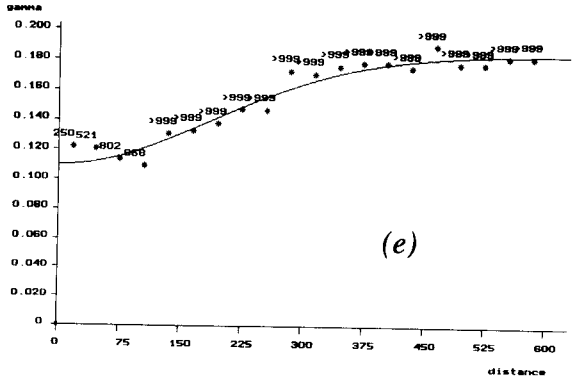

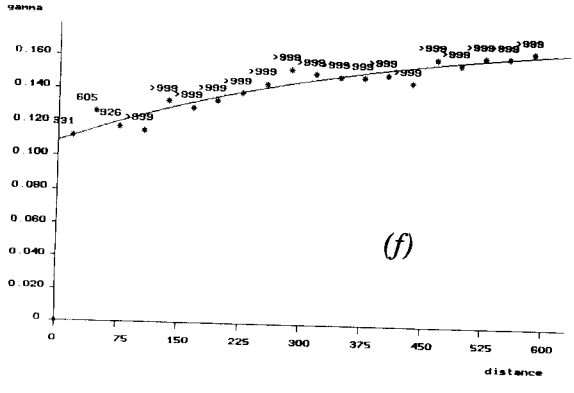

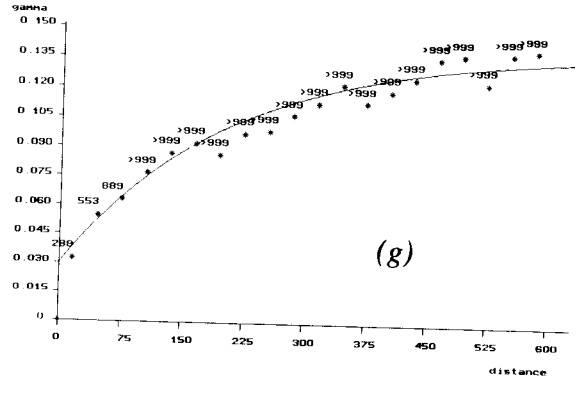

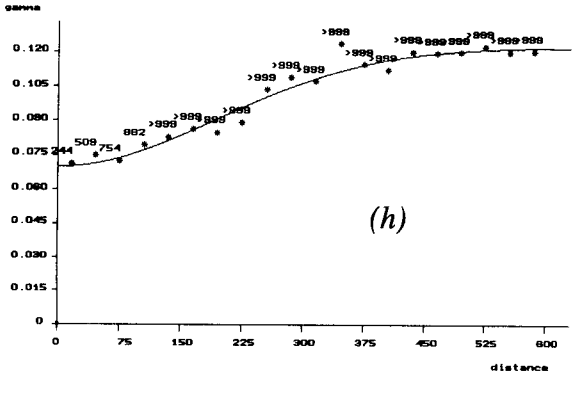

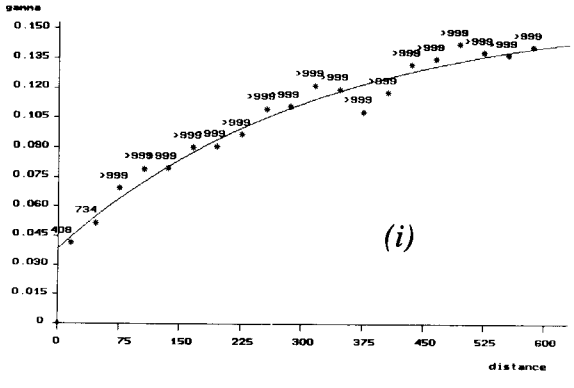

Table 5: Variogram models of the ions and their parameters

Ion	**Model**	**Nugget** (*co*)	**Sill** (*cs*)	**Range** (*a*)	**Effective range** (*r*)
		$\log_{10}(10E^{-4}mol/l)^2$		(km)	(km)
Sulphate	exponential	0.010	0.057	180	540
Nitrate	exponential	0.012	0.024	180	540
Ammonium	exponential	0.012	0.049	123	369
Hydrogen	exponential	0.008	0.040	152	456
Sodium	Gaussian	0.110	0.074	262	454
Chloride	exponential	0.109	0.072	413	1239
Magnesium	exponential	0.030	0.110	200	600
Potassium	Gaussian	0.070	0.053	275	476
Calcium	exponential	0.039	0.120	317	951

In Figure 5 the estimates of the semi-variance are indicated by a star (*), the number of pairs of points that contribute to an estimation is also presented here. This number is an indication of the reliability of the estimation (the larger the number, the better the estimation). All variograms fit the data fairly well (SSD/TSS values about 0.10 in most cases). The ammonium variogram has a smaller effective range (*r*) than the other ions, only about 369 km, indicating that the concentrations in precipitation of this ion varies more locally than concentrations of the other ions. The variograms are all convex upwards, with the sill larger than the nugget in most cases, indicating dominance of the stochastic element. For sodium, potassium and chloride, the nugget variances in the variograms are large in comparison to the sill variances because these elements exhibit a spatial trend near the coast, hampering the calculation of one appropriate variogram valid for the whole of Europe. Large nugget variances may occur for all elements because measurement errors make up a part of the nugget variance. Besides, the concentration of the ions may vary over shorter distances than those between the collectors. This variation appears in the nugget variance as well. To resolve this source of spatial variability, a denser network is required. Large nugget variances can also arise from a conservative fitting of the models to the sample semi-variances with too few data separated by short lags, with the result of overestimation at short lags (Webster *et al.*, 1991). Unfortunately, nothing is known about the shape of the variogram at lag distances less than the shortest sampling interval.

To investigate the quality of the variograms a cross validation procedure is carried out with the module Xvalid of the geostatistical package **GEO-EAS** (**GEO**statistical **E**nvironmental **A**ssessment **S**oftware) (Englund and Sparks, 1991). Cross-validation involves estimating values at each sampled location in an area by kriging with the neighbouring sample values, excluding the value of the point being estimated. The estimates are compared with the original observations in order to test if the hypothetical variogram and neighbourhood search parameters will accurately reproduce the spatial variability of the sampled observations. However, one of the difficulties in each cross validation procedure is the problem of clustering. If the original dataset is spatially clustered, then the cross validated residuals are so too. Ideally, the residuals should represent the entire area of interest and the complete range of values. In practice the residuals may be more representative of only certain regions or particular ranges of values (Isaaks and Srivastava, 1989). Another limitation is the fact that cross-validation can only generate pairs of true and estimated values at sample locations. Results usually do not accurately reflect the actual performance of the estimation method because estimation at sample locations is typically not representative of estimation at all the unsampled locations (Isaaks and Srivastava, 1989). Despite these objections, cross-validation is still a useful (and only) tool to investigate the quality of the variogram model performance.

Kriging gives an estimation ($\hat{Z}_{-j}(\mathbf{s}_j)$) and an estimation kriging standard deviation ($\sigma_{-j}(\mathbf{s}_j)$). The latter is the expected standard deviation of the error $\hat{Z}_{-j}(\mathbf{s}_j)$ - $Z(\mathbf{s}_j)$, estimated value minus measured value. The differences between the measured values and the estimated values are averaged and divided by $\sigma_{-j}(\mathbf{s}_j)$ (equation 5).

$$(1/n)\sum_{j=1}^{n}\left\{\left(Z(s_j)-\hat{Z}_{-j}(s_j)\right)/\sigma_{-j}(s_j)\right\} \qquad (7)$$

where n is number of samples;
$Z(\mathbf{s}_j)$ observed value at location $\mathbf{s}_j$;
$\hat{Z}_{-j}(\mathbf{s}_j)$ predicted value at location $\mathbf{s}_j$; Prediction made without use of $Z(\mathbf{s}_j)$;
$\sigma_{-j}(\mathbf{s}_j)$ kriging standard deviation at location $\mathbf{s}_j$ of $\hat{Z}_{-j}(\mathbf{s}_j)$

The squares of the differences are also divided by the kriging variances to give a ratio at each site and these ratios are averaged (equation 6).

$$\left[(1/n)\sum_{j=1}^{n}\left\{\left(Z(s_j)-\hat{Z}_{-j}(s_j)\right)^2/\sigma_{-j}(s_j)\right\}^2\right] \qquad (8)$$

If the mean in (5) is 0 and the mean square in (6) is 1 the data satisfy the intrinsic hypothesis and the variogram model is well chosen. Table 6 shows that these ideals are approximately approached with the fitted models. Generally, deviations from the 'ideal' values equal deviations found in other studies (e.g. Webster *et al.*, 1991).

Table 6: *Cross validation of variogram models of the log-transformed concentrations*

Ion	NO_3	NH_4	SO_4	Na	Cl	Ca	Mg	K	H
eq.(7)	-.001	.015	-.008	-.006	-.042	-.011	-.006	-.003	.001
eq.(8)	1.079	1.109	1.079	0.787	0.756	0.973	0.898	1.028	0.947

The value of equation (8) for sodium and chloride differ somewhat largely from the ideal values. This larger deviation might be explained by the sea influence described in section 3. A value less than 1 means that the kriging variance is larger than the actual variance. This is probably caused by large sodium and chloride concentrations (i.e. outliers) near the coast, in turn causing too high semi-variance estimations in the experimental variogram. To obtain a better interpolation for these elements, ideally, different variograms should be constructed for different regions, i.e. the coastal areas require other variograms than further inland. No attention was paid to this possibility because it is very difficult to link interpolations made with different variogram models for different regions (Karssenberg, 1994).

In Geo-eas some visual checks on the interpolation quality were also investigated:
(1) A graph of the kriging error, or 'differences', presented in a plot with the co-ordinates of the sites on the X and Y axis. Sample locations are marked with a '+' for overestimation (estimate - observed > 0), and an 'x' for negative differences, with the size of the symbol being proportional to the error, so that large positive or negative differences are easily noticed.
(2) Scatter-plots, i.e. 'Observed vs. Estimate' and 'Estimate vs. Error' plots. Figure 6 presents the ammonium plot as an example of an observed vs. estimate plot.
(3) Histograms (frequency distribution graph of the estimation error). Ideally the error has a normal distribution.

Generally, the variograms are in fairly good agreement with the data. The error maps show no areas with consequent over- or underestimation, and the frequency distributions of the estimation errors are almost normal. All 'Observed vs. Estimate' plots show a range comparable to Figure 6.

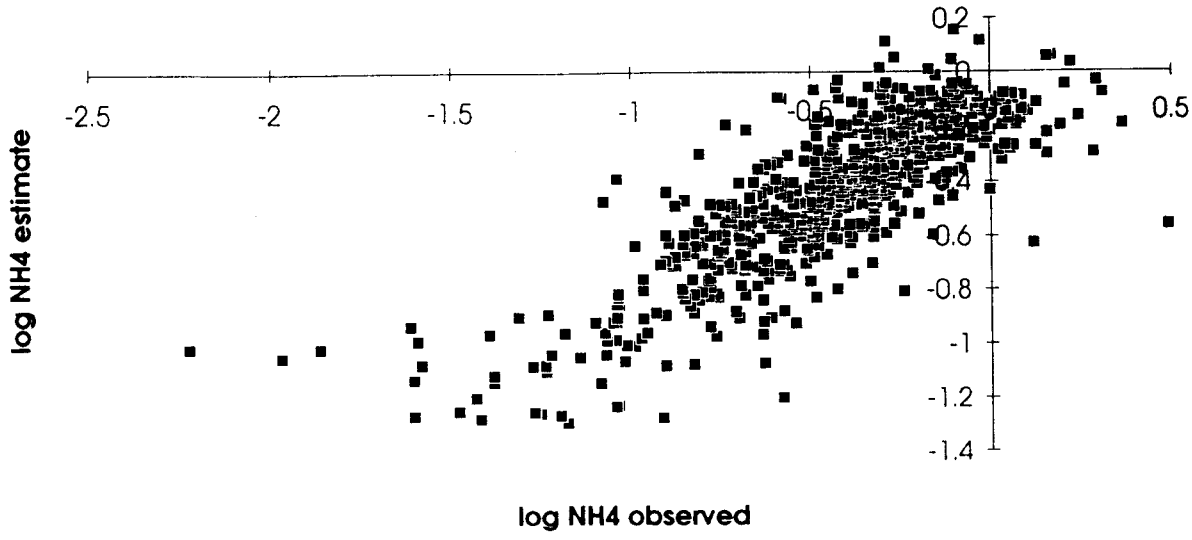

Figure 6: *Scatter-plot of the observed vs. estimated values for log ammonium concentration (in 10^{-4} mol/l).*

7. INTERPOLATION

7.1 Introduction

To create maps of all ions, estimates of the concentrations were made on a regular grid of 50x50 km by ordinary block kriging using the models specified in Table 5 and the data. The interpolations were performed using GSTAT. Maps were compiled using a Geographic Information System (GIS). The **PC-raster** package (Van Deursen and Wesseling, 1992) was used (because it is linked with GSTAT) as well as **Arc/Info** (for data management and presentation). The size of the grid cells used is determined by the confidentiality of the results. When kriging variances are large, using a more dense grid suggests a false reliability. With a dense grid, the boundary between two classes can be mapped very precisely but when kriging variances are large the boundary itself is very uncertain. Taking this into account and considering the total number of available measurements, the maps in this report were interpolated to a grid with blocks of 50x50 km. As concentration fields over Europe fluctuate less than precipitation fields, interpolation was performed on concentration data, instead of fluxes. This is the same procedure for mapping wet deposition fluxes as, for example, by Kovar *et al.* (1991) in the Alps and the UK Review Group on Acid Rain (1990) in the United Kingdom.

Concentration and flux maps for all components are presented in Appendix 5, except the sulphate, nitrate and ammonium flux maps which are presented in Figure 7. In some regions of Europe the distance between measurement sites is too large (i.e. larger than twice the effective range of the variograms, so no spatial relationship between the site to be predicted and the measurement sites exists) to obtain interpolated fields covering the whole of Europe. In the maps this can be seen by concentric circles around some data points. Interpolation proceeds until the maximum distance of spatial correlation, i.e. the effective range of the variogram, is reached.

7.2 Interpolation of precipitation amounts

Concentration data originated mainly from 1989. Because concentrations and precipitation amounts are physically linked, in principle, only precipitation amounts from 1989 should be used. An accurate interpolation of rainfall amounts with the data available in the dataset was not possible because actual values from 1989 were limited to approximately 450 measurement sites. As precipitation amounts can vary very much over short distances, several thousands of sites are necessary to describe the variation to a reasonable extent.

Therefore other actual data measured in 1989 were necessary. For this purpose, data from the Observational Data Set (ODS), which is a product of ECMWF (European Centre for Medium-range Weather Forecasts), were investigated. The ODS dataset contains 1297 measurement sites spread over Europe. At each site rainfall amounts were measured every 6-h period. Data are invalidated and therefore highly uncertain (Potma, 1993). For this reason, these data were also considered to be unsuitable to provide a precipitation map of Europe.

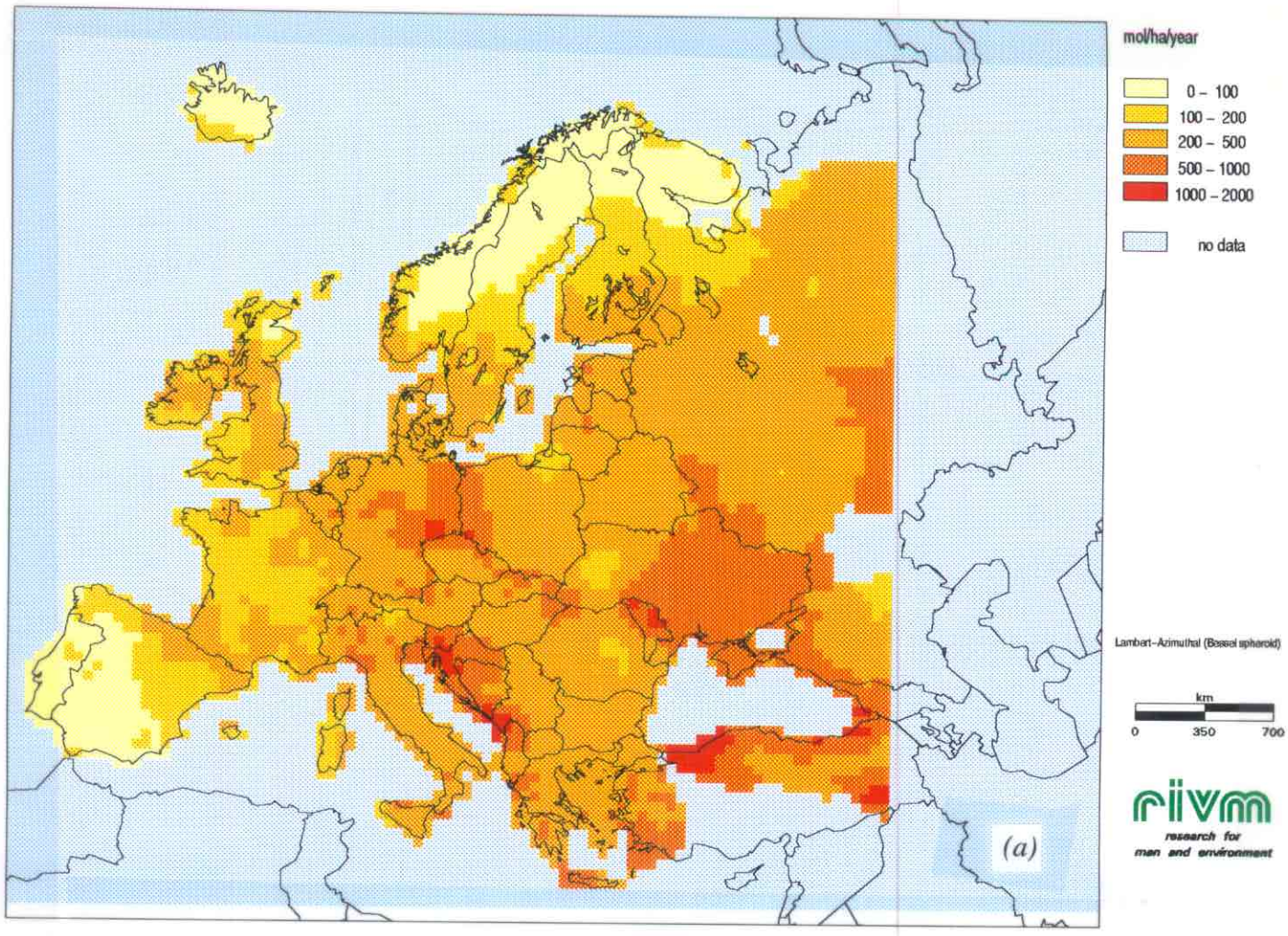

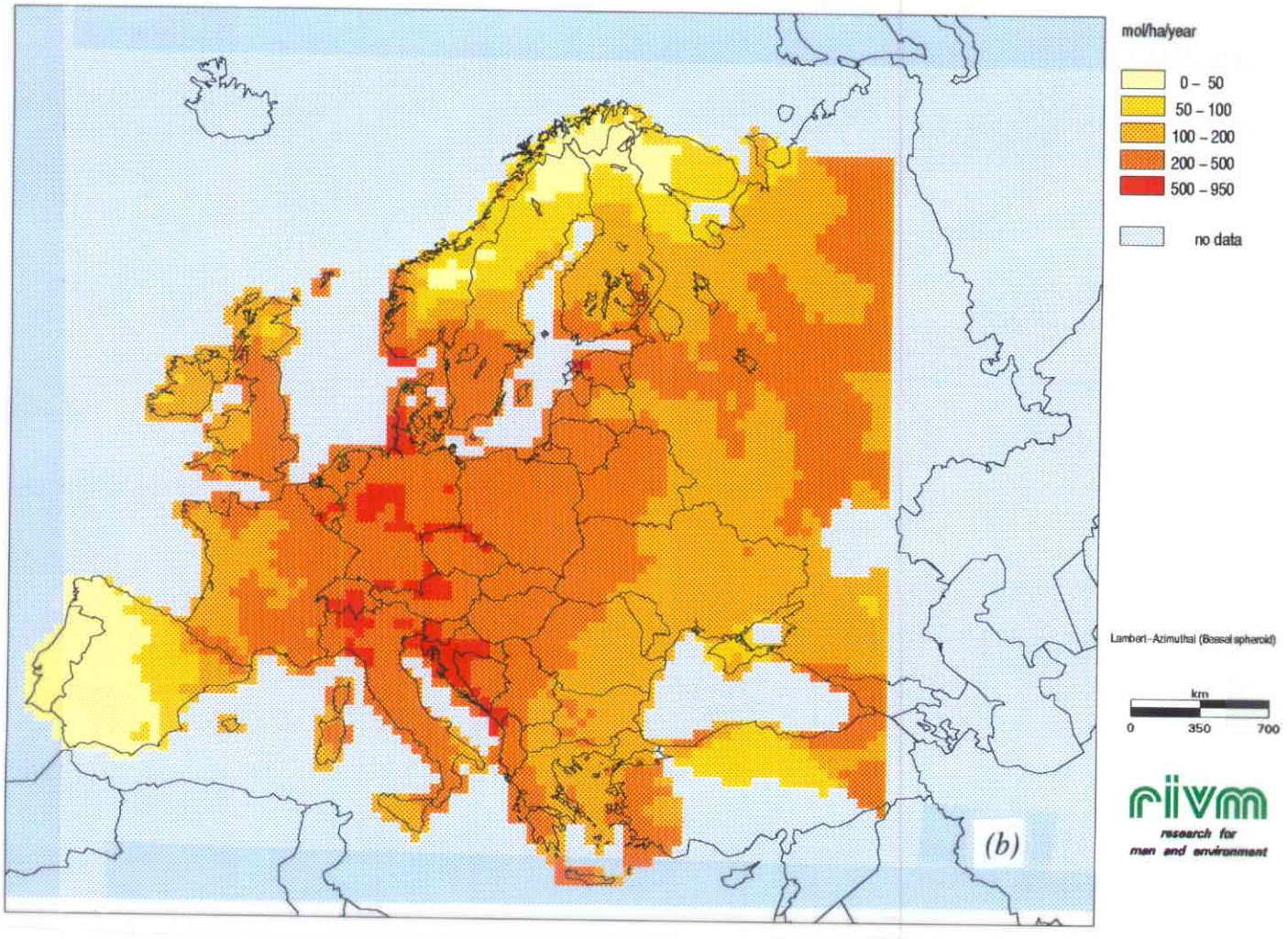

Fig. 7: Maps of annual mean wet deposition fluxes of non-marine sulphate (a), nitrate (b) and ammonium (c)

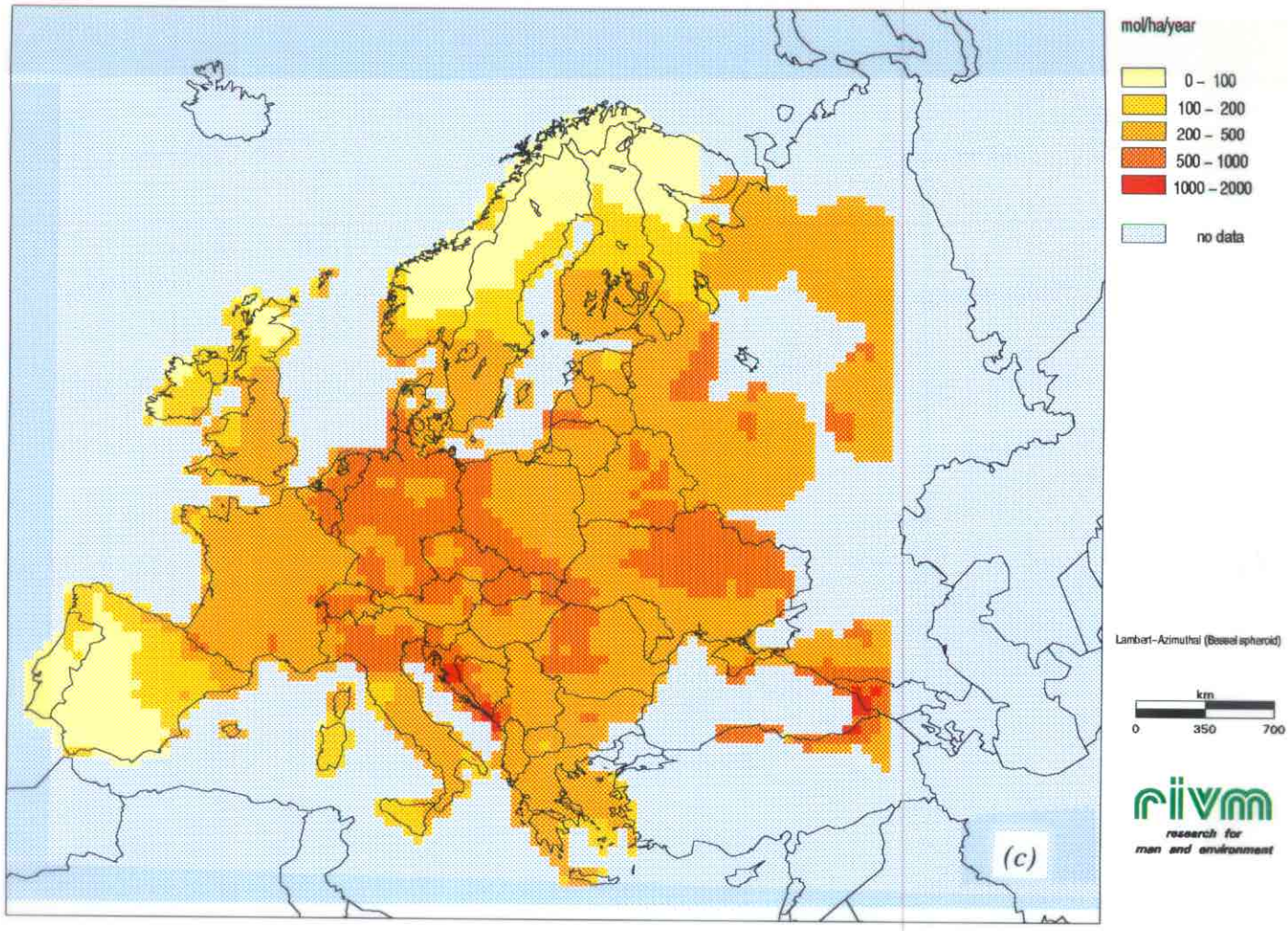

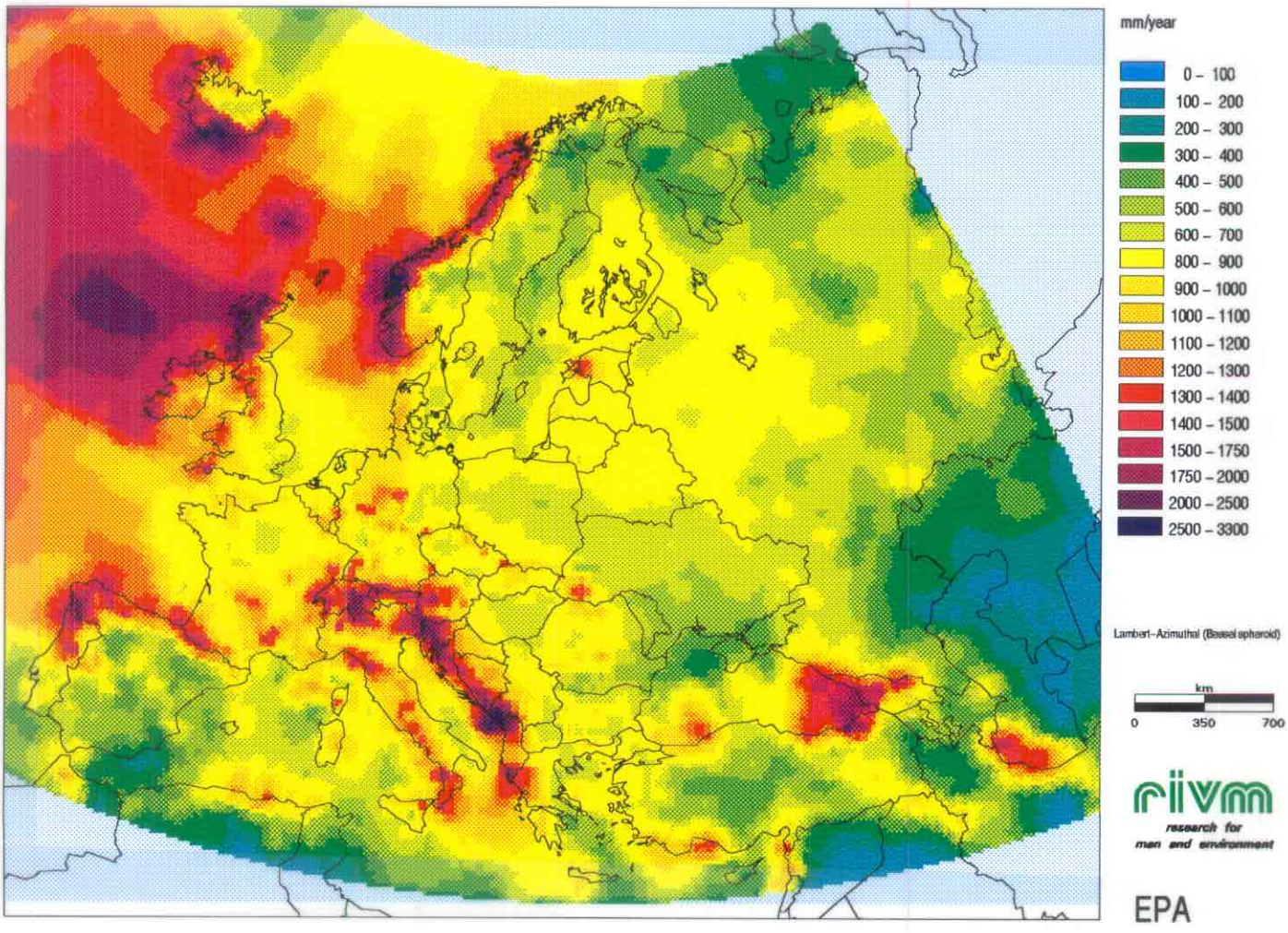

Fig. 8: EPA long-term mean precipitation map.

At RIVM, another dataset that contains interpolated values of long-term annual mean precipitation amounts, based on several thousands of measurements, was available (Legates and Willmott, 1990). This EPA map (developed at the Environmental Protection Agency, U.S.A.) is based on validated monthly mean precipitation amounts measured from 1920 to 1980. Data were screened for coding errors and a procedure was carried out to correct for gauge-induced biases to remove systematic errors caused by wind, wetting on the interior walls of the gauge and evaporation from the gauge. These corrected values were interpolated to a 0.5 degree of longitude by 0.5 degree of latitude grid. In this map (Figure 8), areas with large precipitation amounts in coastal and mountainous areas (due to orographic effects) can be recognised. It was thought that the most accurate results could be obtained by using a combination of the ODS and EPA datasets.

The general idea was to explore whether there were systematic differences between 1989 data and the long-term averages. To determine the deviations of the ODS data (considering 1989) from the long-term mean EPA data, and whether these deviations were systematic (i.e. whether consistent areas with larger or smaller values could be recognised), the following procedure was carried out. At first data from individual ODS stations were summed to receive total annual precipitation amounts for each station. In some cases many 6-h values were stored as missing values in the data files. If more than 25% of the observations of a particular station were missing, the station was not taken into account. For each remaining station a rainfall amount proportional to the percentage of missing data was added. For example, if for a certain station data coverage is 75% and the stored precipitation amount is 600 mm, then the value used in the comparison procedure equals 750 mm. If a station was situated at an altitude greater than 500 m it was not taken into account as well, because at high altitudes measurements might differ from EPA to a large extent. This might be the case in mountainous areas where very large precipitation amounts can be measured locally at ODS stations (point data), whereas in the EPA database (grids) the average of a block is concerned. After application of these selection criteria, 866 out of the total of 1297 available ODS stations remained. With ArcInfo, a map was created (Appendix 6) which shows sites where deviations of the ODS values are larger than ±30% with respect to the EPA values and sites where deviations are smaller than ±30%. A deviation less than ±30% was considered to be acceptable and explainable by natural annual fluctuations. Of the remaining 866 stations, 419 appeared to fall within these limits, 258 deviated more than -30%, and 189 deviated more than +30%. The deviation was 45% on average. These deviations were not systematic in space (i.e. dark and pale spots are distributed in a somewhat random way), although in some areas (like Central Europe) negative deviations dominate. Over the whole of Europe the balance is fairly correct as the summed total of all positive deviations almost equals the summed total of all negative deviations (the average deviation is +3%). Therefore, no correction of the EPA data was performed. However, the map obtained in combination with Figure 9 yields an indication of the order of the uncertainty that is introduced by using long-term mean data instead of data from 1989. The uncertainties introduced by using the long-term mean values can be considerable, but they are not systematic.

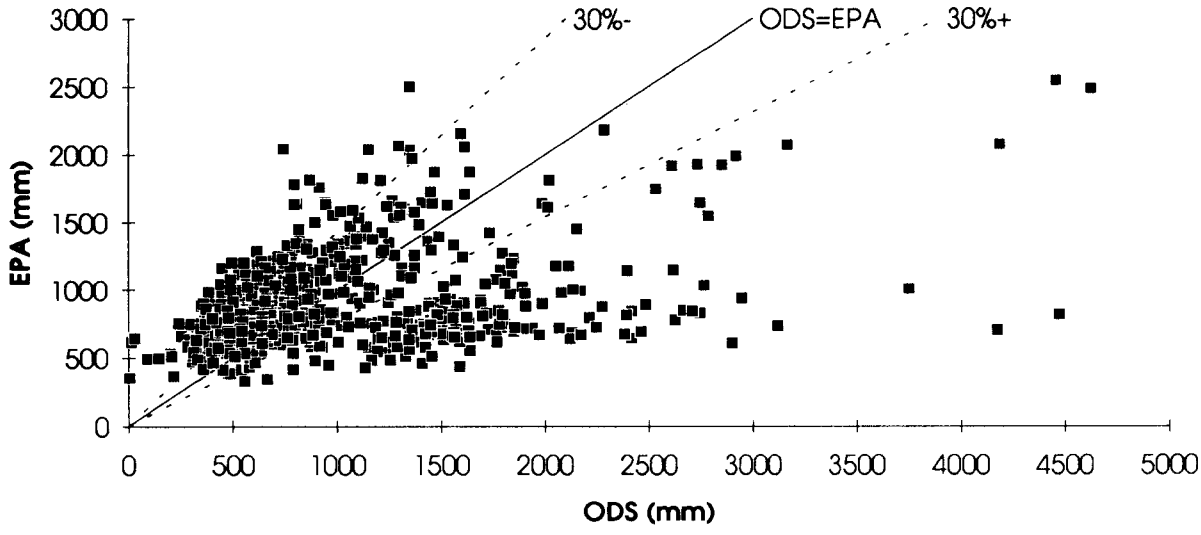

Figure 9: Scatter-plot of the total annual precipitation amounts of EPA vs. ODS.

8. DISCUSSION

8.1 Description of spatial patterns

Concentration and wet deposition maps of all components are presented in Appendix 5. The maps of the four acidifying components (i.e. non-marine sulphate, nitrate, ammonium and hydrogen) clearly resemble European emission and climate patterns. In the concentration maps large emission sources can be recognised, whereas in the flux maps climate patterns and orographic effects are also observed. In mountainous areas large fluxes due to orographic rains can be seen. Especially in former Yugoslavia the large long-term mean precipitation amounts cause large fluxes of each element in the flux maps. Large fluxes can also arise from high concentrations in precipitation.

Considering the non-marine sulphate maps, large fluxes (400-1000 mol/ha per year) can be noticed in Eastern and Central Europe (Germany, Poland, Czech and Slovak Republics, Austria, Hungary, north Italy and former Yugoslavia). Especially the border area Germany-Poland-Czech Republic (known as the Black Triangle) is a zone of large sulphate pollution due to the burning of brown coal. Large sulphate concentrations are mainly caused by SO_2 emissions from industry and power stations (high temperature combustion of fossil fuels). Note the very large non-marine sulphate concentrations and fluxes in Ukraine due to large-scale heavy industry and burning of low quality brown coal (i.e. coal with a high sulphur content). Concentrations and fluxes obtained in Turkey should be interpreted with care, because they are not based on measurements in Turkey itself and are solely the result of the interpolation (in this case extrapolation) from surrounding countries.

Nitrate arises mainly from NO_x emissions from industry, power stations and motor vehicle exhausts (i.e. burning processes). The spatial patterns in the nitrate maps resemble the patterns found in the sulphate maps, but this time also the Netherlands and Southern Scandinavia show rather large fluxes (300-700 mol/ha per year). Again, large concentrations can be observed in the Black Triangle. In Russia nitrate concentrations and fluxes are low compared to sulphate concentrations and fluxes.

Ammonia emissions arise mainly from livestock wastes, with smaller contributions from fertiliser application and the fertiliser producing industry. The largest ammonium fluxes (400-1000 mol/ha per year) can therefore be observed in or near areas with intensive agricultural landuse, e.g. Central Europe. In the Netherlands for example, high ammonium fluxes are found due to the intensive livestock breeding in this country.

In the hydrogen ion concentration map the largest acidity ($pH < 4.4$) can be found in a small zone ranging from southern Scandinavia to northern Italy (Po valley) and in Great Britain. The hydrogen ion concentration is a balancing term corresponding to the concentrations of acidic and neutralising elements and is therefore not related to any single factor. In the western part of the Netherlands the hydrogen ion concentrations are larger ($pH < 4.4$) than in the eastern part ($pH > 4.6$). In the western part the low pH value is caused by industrial emissions from the United Kingdom, whereas in the eastern part neutralisation by ammonia has taken place resulting in a

slightly higher pH value (i.e. lower hydrogen ion concentration).

Lowest fluxes of sulphate, nitrate, ammonium and hydrogen ion (< 200 mol/ha per year) can be found in northern Scandinavia, the Iberian Peninsula, and, to a lesser extent, France and Great Britain (except for the hydrogen ion). Note the spatial patterns of the non-marine sulphate, nitrate and ammonium concentrations in Great Britain. The pattern clearly resembles increasing concentrations eastwards, caused by the influence of industry in the Midlands and the prevailing westerly winds.

For base cations, a division can be made between elements of marine origin (sodium, chloride and to some extent magnesium) and other elements (potassium and calcium), mainly originating from soils, agricultural activities, road dust and industry as well as marine sources. For the elements of marine origin a clear pattern of decreasing fluxes with increasing distance to seas, in particular the Atlantic Ocean, can be observed. This pattern is most distinct for sodium and chloride, especially along the Irish and the northern English coast where fluxes are larger than 3000 mol/ha per year. This is caused by the combined effect of large concentrations together with large precipitation amounts. The remainder of the European continent shows a fairly homogeneous pattern (fluxes varying 0-800 mol/ha per year). Although there is only one measurement site for sodium on Iceland, an inhomogeneous pattern on the flux map can be seen. This is caused solely from the differentiated pattern in the long-term mean precipitation map. The spatial variation in the magnesium fluxes is somewhat more differentiated than the variation in the sodium and chloride fluxes. Besides near seas, large magnesium fluxes (> 100 mol/ha per year) can be observed in Hungary, Ukraine and the former Soviet Union due to large concentrations. Note that the interpolated field in the former Soviet Union is based on only a few measurements. The potassium concentration and flux maps show homogeneous spatial variation almost all over Europe (fluxes varying between 0-75 mol/ha per year). Large fluxes (200-500 mol/ha per year) due to large concentrations can be observed in Ukraine and due to large rainfall amounts in Ireland and Great Britain. In Ukraine also large magnesium and calcium concentrations and fluxes can be seen. Especially for calcium this may be caused by the influence of *(1)* emissions of fly ash from the cement and concrete processing industry, *(2)* locally emitted soil dust (in particular in areas with alkaline soils) and *(3)* transport of desert dust from the Sahara. Besides in Ukraine, the largest calcium fluxes (400-800 mol/ha per year) appear in Italy, Hungary and the Black Triangle. Calcium fluxes are lowest (0-100 mol/ha per year) in Great Britain and Scandinavia .

8.2 Uncertainty analysis

The wet deposition maps are subject to several sources of uncertainty. An estimation of these uncertainties will be made in this section. The uncertainties are divided into three main categories: *(1)* uncertainty associated with the measurements, *(2)* uncertainty associated with assumptions in the methods used, and *(3)* uncertainty caused by the interpolation procedure. Numbers are presented as percentages reflecting the relative deviation from the estimated value for an average grid cell in terms of one standard deviation (σ), implying that the probability that the real value is the estimated value $\pm x\%$, is 68%.

The first source of uncertainty comprises measurement errors and other uncertainties associated with the original data. This can be caused by errors in the field when the samples are collected and in the laboratory when the chemical composition of the samples is analysed. Furthermore, different chemical analytical methods were used by the laboratories in different countries to analyse the chemical composition of the samples, hampering intercomparison between data. De Ridder *et al.*, (1984) reported systematic differences of approximately 10% between the same samples analysed at three different laboratories in the Netherlands. Mosello *et al.* (1994) report an experiment in which 98 laboratories from 18 different countries participated in a study to reveal the magnitude of systematic differences between results analysed in different laboratories. They found differences of about 10% for SO_4^{2-}, NH_4^+ and Ca^{2+} concentrations; 15% for NO_3^-, Na^+ and K^+; 25% for Cl^- and even up to 50% for Mg^{2+} concentrations.

Besides, data at about 500 locations originated from 1989, while at other locations data of other years or an average of several years were used. For the acidifying components, Kovar and Puxbaum (1992) showed that in the Alps the yearly variability in concentration only adds an uncertainty of approximately 10% at the most to the overall uncertainty. In the United Kingdom the annual mean of the acidifying components at individual sites varied by ± 10-20% between years (UK Review Group on Acid Rain, 1990). The variability in the average European concentrations is smaller than that for individual sites because the variability is smoothed by the averaging over Europe in the interpolation procedure. Concentrations of the base cations, however, appear to be more variable than acidifying components. In 1987 the network mean concentration in the United Kingdom was approximately 40% smaller than in 1986, probably due to meteorological conditions (particularly wind speed) (UK Review Group on Acid Rain, 1990). The uncertainty introduced by these factors collectively for an average 50x50 km grid cell is assumed to be 20% for concentrations of acidifying components and 40% for concentrations of base cations.

The second uncertainty source comprises errors caused by assumptions in the methods used. Major error sources might be *(a)* the representativeness of the sites and *(b)* the usage of long-term mean precipitation amounts instead of year-specific data. Besides, *(c)* the seeder-feeder mechanism and *(d)* problems in high rainfall areas were not taken into account because there is a lack of relevant information on a European scale. Furthermore, the influence of *(e)* topography (altitude), as well as the uncertainty introduced by *(f)* not capturing snow in the precipitation samplers and *(g)* the derivation of correction factors for the contribution of dry deposition to bulk precipitation samplers are considered. Finally, *(h)* uncertainty in sulphate concentration introduced by correction for the influence of sea salt by using interpolated sodium concentrations is taken into account.

ad. a) The representativeness of the sites is determined by two components. First, it can be questionable whether results obtained at a particular measurement site are representative for the area surrounding that point. This might lead to uncertainties, e.g. when a sample is taken near sources, while it should represent a large area where sources are sparse. Second, although the rainfall measurement technique is not a very complex one, the collection of representative rainfall measurements for a specific area

is difficult and can lead to uncertainty, because nearby objects like trees, houses and hills can change rainfall amounts systematically by their influence on turbulent transport of rain drops. For this reason it is recommended to position rainfall samplers at a distance of at least four times the height of the nearest porous obstacle and at a distance of at least eight times the height of the nearest vast obstacle. Furthermore it is recommended to measure precipitation amounts using a standard meteorological device situated 40 cm above the ground (WMO, 1971). The uncertainty in representativeness for an average 50x50 km grid cell is assumed to approximate 30%.

ad. b) The usage of long-term mean precipitation amounts instead of year-specific data introduces an uncertainty of 45% on average. However, locally large deviations can occur. Of all 867 stations, 19 ODS stations deviate more than ±200% from EPA and 90 stations deviate more than ±100%. Over the whole of Europe the precipitation amount balance is fairly correct as the summed total of all positive deviations almost equals the summed total of all negative deviations (the average deviation is 3%). However, strictly speaking these values cannot be regarded as average relative uncertainties, as ODS is not a correct standard for average precipitation amounts in 1989. Deviations between ODS and EPA are therefore caused by uncertainty in ODS as well as uncertainty in EPA. The values can thus be considered as 'maximum average uncertainties' introduced by the usage of long-term mean data instead of year-specific data. The uncertainty introduced in the interpolation procedure performed by EPA is thought to be of minor importance.

ad. c) In upland areas in northwest Europe a substantial proportion of rainfall originates from scavenging of cap cloud by the seeder-feeder process (Browning *et al.,* 1974). The effect of orography on rainfall composition has been investigated experimentally in Great Dun Fell in the United Kingdom. The work showed that concentrations of major ions in rain increased with altitude by a factor of 2 to 3 over the height range 200 to 850 m above sea level (asl) (UK Review Group on Acid Rain, 1990). The four major ions SO_4^{2-}, NO_3^-, NH_4^+ and H^+, behaved in approximately the same way. Over this height range the amount of rain roughly doubled due to orographic effects, so that wet deposition increased by a factor of 4 to 6 (Dollard *et al.*, 1983; Fowler *et al.,* 1988). The increase in concentration of major ions at high altitude occurs when the cap cloud (feeder) droplets contain larger concentrations than rain from higher levels (seeder). In this process, aerosols containing elements mentioned above (and all other ions) are lifted by hills and activated into orographic clouds. Cloud droplets in the orographic (feeder) cloud are efficiently scavenged by precipitation falling from a higher level. For upland areas where orographic enhancement of rainfall is an important contributor to wet deposition, the additional scavenging of pollutant from orographic cloud is therefore expected to increase wet deposition above the values that would be predicted when chemical composition is assumed to be constant with altitude. Large uncertainties remain, and the values mentioned should be regarded as providing an initial estimate and applicable only to regions with similar climate, precipitation and topography as the United Kingdom. Dore *et al.* (1992) mapped wet deposition in the United Kingdom, incorporating the seeder-feeder effect over mountainous terrain. Over high ground they found an increase in wet deposition of 41% to 76% compared to the situation when ion concentrations are considered to be constant with height. The areas with large enhancements represent a relatively small fraction of the land area and have therefore

only a small impact on the total pollutant budget. The uncertainty introduced by ignoring the seeder-feeder process in the concentration mapping in this study is smaller than the values reported by Dore *et al.* (1992), as local wet deposition enhancements will be smoothed out when data are interpolated to a grid with 50x50 km blocks. If measurement sites are located in areas where wet deposition is enhanced by the seeder-feeder process there is no underestimation. However, in practice, sites are mostly located in lowland areas. The seeder-feeder mechanism is not incorporated in the maps compiled in this study.

ad. d) In high rainfall areas (e.g. in mountainous areas and near coasts) concentrations decrease as a result of diminishing below-cloud scavenging. To obtain wet deposition fluxes, interpolated concentration fields were multiplied by rainfall amounts from EPA. In this way there is no physical coupling between concentration and precipitation amounts. As a result, precipitation amounts are multiplied by a constant concentration, leading to an overestimation in high rainfall areas. This is the case when (high) concentrations from areas with low precipitation amounts are interpolated to areas with large precipitation amounts. The contrary, i.e. underestimation in low rainfall areas, is possible as well. However, the former is more likely to occur, as most high rainfall areas are located at large distances from major anthropogenic pollution sources (background areas). In areas where sampler density is low, underestimation is expected to be largest. In the areas concerned this uncertainty is assumed to be about 20%.

ad. e) Unlike the uplands of northwest Europe, concentrations in precipitation in the Alps generally decrease with increasing altitude. In regions with large mountains, snow and rain chemistry reveal marked vertical gradients in composition (Ronseaux and Delmas, 1988; Puxbaum and Kovar, 1991). For these regions the very high elevation snows (>2000 m) are in general less polluted than those on lower slopes because the majority of the pollutant burden is restricted to the boundary layer. This effect might lead to an overestimation which is assumed to approximate 20%. Besides, because of the differentiated topography in mountainous areas, the spatial variability of annual precipitation amounts is fairly large. To calculate accurate wet deposition fluxes in these areas it is therefore necessary to use precipitation maps based on a large number of measurements (Kovar *et al.,* 1991). However, in general at high altitudes sampler density is low due to large maintenance costs and sampling difficulties. A better result might be obtained by using a digital terrain model (DTM) in combination with an empirical relationship between altitude and annual rainfall amount (Behr, 1990). In the Alps, the highest rainfall amounts are observed in the pre- and high Alpine areas along the northern and southern Alps, whereas in the valleys in the centre of the Alps the smallest rainfall amounts are measured (Kovar *et al.,* 1991). In Alpine areas, the spatial variability of ion concentrations is small compared to the variability in rainfall amounts. Generally, concentrations in the Alps are smaller than outside the Alps. Concentrations increase to the north, south and especially the southeast (Kovar *et al.,* 1991).

ad. f) Large wind velocities prevents snowfall being captured by the funnels of samplers. Especially in the winter season, this leads to an underestimation of rainfall amounts in mountainous areas. Depending on altitude and wind conditions of the sites, the underestimation will vary between 0 and 30% (Kovar *et al.,* 1991). For

snow, good data can be obtained by using specially designed snow collectors situated at ground level (Lövblad *et al.*, 1994).

ad. g) The uncertainty introduced by the method to derive correction factors for the contribution of dry deposition to bulk precipitation samplers is a combination of *(1)* uncertainty in the measurements, *(2)* uncertainty in the derivation method itself and *(3)* uncertainty in the processes that regulate the difference. The dependence of the wet-only to bulk ratio of sodium and chloride on the distance to the coast shows that the most important process must be particle deposition. This would mean that the highest uncertainty in bulk samplers will be in places where particle concentrations are high. If gases are important, especially for wet funnels, is not known. Buijsman (1989) reports that application of dry deposition correction factors introduces 10-20% uncertainty in the Netherlands, depending on the location of the station. Together with uncertainty introduced by *(2)* and *(3)*, total uncertainty is estimated to be 30%.

ad. h) For sulphate, additional uncertainty is added in the non-marine sulphate calculation procedure, as interpolated sodium values were used to correct for the contribution of sea salt for about 200 locations. This uncertainty is assumed to be of minor importance compared to other sources of uncertainty as *(1)* only 200 sites are concerned, and *(2)* the correction causes a decrease in sulphate concentration of 25% at the maximum. Only at high sodium concentration levels will the interpolation error caused by the interpolation procedure have some impact. Besides, the 200 locations are randomly distributed over Europe, hampering quantification of the introduced uncertainty.

The third source of uncertainty is a result of uncertainties inherent to the interpolation procedure, because derived values are nothing more than an estimation of the expected value at locations where no measurements were made. This uncertainty is expressed as kriging variances. It is assumed that the data satisfy the intrinsic hypothesis and that the variogram model is well chosen. The extent to which the intrinsic hypothesis holds cannot be quantified. As the original values were transformed to their common logarithms to stabilise the variances, all subsequent analyses were performed on the transformed values. The retransformation of the data (from log- to original values) was performed by taking the exponent. In this way the median value of the block is obtained (Journel and Huijbregts, 1978). Because the original data were distributed skew, with some large outliers of high concentrations, the median gives a more representative block value than the mean does. The interpolation errors can be quantified in kriging standard deviation maps or can be used to map confidence intervals to give an idea on the reliability of the interpolation. Smallest errors occur where data are numerous and largest errors where data are sparse. In some regions where no information is available, the errors are large and one may wonder whether to leave the area on the map of estimated concentrations blank or accept the large uncertainties associated with the concerned estimation. In this study these uncertainties were accepted because a map covering the whole of Europe was demanded, and interpolation was performed even in areas with large interpolation errors. Because interpolation was performed on the concentration data, kriging variances were available only for the interpolated concentration fields (not for the wet deposition flux fields). The kriging variances cannot be transformed back to the original values by just taking the exponent. A cumbersome procedure is needed and

interpretation of the results will be difficult (Journel and Huijbregts, 1978). Therefore, for non-marine sulphate, nitrate and ammonium concentrations, 68% confidence intervals were calculated (the estimation ±2 standard deviations, providing the upper and lower boundary). When the upper and lower boundaries of a particular element at a particular location are compared, the probability that the actual value would fall within the range between both values is approximately 68%. Calculation of confidence intervals has the advantage that one is forced to involve confidentiality information in the interpretation of the results. Besides, interpretation of upper and lower boundaries is easier than interpretation of kriging variances alone.

For non-marine sulphate the average relative error varies between 15% in western Europe to 35% in the largest part of the southwest and southeast of Europe (only very locally in the former Soviet Union do uncertainties exceed 50%). For Western Europe for example, a relative error of 15% means that there is a possibility of approximately 68% that the actual values vary between the interpolated value ± 0.15 * the interpolated value. Relative nitrate interpolation errors vary from 10% to 30%, ammonium errors from 15% and 40% (except locally in the former Soviet Union). A wide interval (i.e. large uncertainties) may be caused by *(1)* small-scale differences in the concentration field (so that even in areas with a large number of measurement sites the estimation of the average block value is more variable), *(2)* a lack of measurement sites (so that even in areas with only large-scale differences the average block value is based on too few measurements to derive a confident result) or *(3)* a combination of these factors. For all components, the confidence interval is rather large in southeast Europe (e.g. Greece), Eastern Europe and the former Soviet Union. Sometimes no data are available at all, whereas in other cases data quality can be questionable. In these areas the interpolation error is the largest source of uncertainty. For ammonium, large differences might also be caused by the characteristics of the emission sources of NH_3, i.e. many local sources showing strong variation.

8.3 Total uncertainty in the wet deposition maps

To assess the total uncertainty in the wet deposition maps is very difficult and therefore the estimates themselves are uncertain as well. The numbers presented here should therefore be regarded as a best guess based on expert judgement. To assess the total uncertainty a division into three categories is made, i.e. *(a)* west, northwest and Central Europe as 'good quality areas' where data quality is assumed to be high and sufficient (representative) data is present, *(b)* areas at the edges of the maps, i.e. east, southeast and southwest Europe as 'poor quality areas', where less data is available of which the representativeness and quality can be questionable and *(c)* mountainous areas (e.g. the Alps) and upland areas (e.g. United Kingdom and Scandinavia), even though located in areas with many data, as 'complex terrain areas with additional uncertainties'. Total uncertainty in concentrations and total uncertainty in rainfall amounts have been estimated separately. For both variables the most dominating uncertainty (which could be quantified either in this study or in the literature) was taken to represent total uncertainty, as all uncertainties are distributed around the same mean. In this approach uncertainties are assumed to reflect random errors. i.e. non-systematic errors. The mathematical procedure followed for the error propagation can be summarised as follows. Total uncertainty in concentrations (Q_a) and total

uncertainty in rainfall amounts (Q_b) were squared and added. The square root of the result is the resulting total uncertainty in the wet deposition fluxes (Q_{tot}) (equation 9).

$$Q_{tot} = \sqrt{(Q_a^2 + Q_b^2)} \quad (9)$$

This equation is only valid if it is assumed that there is no correlation between the variables. If the variables are correlated an extra term must be added: R times the product of individual errors, where R is the correlation coefficient between the variables (equation 10).

$$Q_{tot} = \sqrt{(Q_a^2 + Q_b^2 + 2\,R\,Q_a\,Q_b)} \quad (10)$$

In the case of calculation of the wet deposition fluxes the correlation coefficient is unknown. Therefore, two cases are considered, first a propagation of errors without correlation (conservative), and second, a propagation with full positive correlation (worst case). The numbers of total uncertainty are presented as percentages which show the total relative deviation from the estimated value in terms of 1 standard deviation, i.e. the probability is 68% that the real value is the estimated value ± *x*%. As the estimates are rather crude, no distinction between different components was made. In the conservative case *(1)*, the overall uncertainty for an average 50x50 km grid cell is estimated to be 50% in west, northwest and Central Europe, whereas in the worst case *(2)* the overall uncertainty is estimated to be 70% here. In areas at the edges of the maps, i.e. east, southeast and southwest Europe, *(1)* is estimated to be 60% and *(2)* 80%, whereas in complex terrain areas *(1)* is estimated to be 70% and *(2)* 100%. These values are summarised in Table 7.

Table 7: *Total uncertainty in concentration and rainfall amount per average grid cell of 50x50 km for different areas, as well as total uncertainty in wet deposition in the conservative and the worst cases*

Area	**Concentration (%)**	**Rainfall amount (%)**	**Total: Conservative (%)**	**Worst (%)**
(a)	30	40	50	70
(b)	40	40	60	80
(c)	50	50	70	100

(a) refers to west, northwest and Central Europe, (b) to east, southeast and southwest Europe and (c) to complex terrain areas.

8.4 Comparison with the EMEP long-range transport model

A comparison was made between wet deposition fluxes resulting from this study, and results obtained by the EMEP long-range transport model. The EMEP model only deals with non-marine sulphate, nitrate and ammonium fluxes. The maps resulting

from calculations by EMEP have a grid resolution of 150x150 km (Appendix 7). A way of comparison between both methods can be obtained from scatter-plots in which the averages of the new values within one EMEP grid cell of 150x150 km are plotted against the EMEP values (Appendix 8). It is obvious that the results obtained in this study are much higher than results obtained by the EMEP model. Average fluxes are about 75% higher for sulphate, 20% for nitrate and 55% for ammonium. The regression lines deviate from the 1:1 relationship to a considerable extent as the slope value is far from one. In Table 7 the average fluxes for each component are considered for the new results as well as the EMEP results. The table also shows the correlation coefficients between the results obtained by both methods and the slope of the regression line.

Table 8: Comparison between average fluxes obtained in this study and EMEP

Component	**Flux: this study**	**Flux: EMEP**	**r^2**	**a**
Sulphate	274	155	0.31	0.49
Nitrate	213	175	0.56	0.82
Ammonium	283	182	0.57	0.67

(r^2) denotes Pearson correlation coefficients between results obtained by both methods and (a) the slope of the regression lines. Fluxes in mol/ha per year.

Explanations for these differences cannot be given in this stage. The differences may be caused by the usage of long-term mean precipitation amounts by EPA in this study. This dataset contains very high values locally in former Yugoslavia, Pyrenees, Alps and Italy, leading to an overestimation of wet deposition fluxes in these areas compared to values calculated by the EMEP model. EMEP model results were probably obtained by calculation with lower rainfall amounts than amounts used in this study. Besides, multiplication of rainfall amounts by a constant concentration may also lead to an overestimation in high rainfall areas (i.e. near coasts and in mountainous areas) because these areas are mostly located at large distances from major anthropogenic pollution sources (background areas). This leads to an overestimation of wet deposition fluxes when high concentrations (from low precipitation areas near sources) are interpolated to background areas (where concentrations are lower) and subsequently multiplied by high rainfall amounts. In areas where sampler density is low, underestimation is expected to be largest. Furthermore, as the EMEP model is based on emission amounts by all separate countries in Europe, differences may be explained by underestimation of emissions from Eastern Europe and the former Soviet Union. Another reason may be the lack of measurement sites in the former Soviet Union of which representativeness may also be uncertain, possibly leading to inaccurate wet deposition fluxes in this study.

Iversen *et al.* (1991) compare EMEP model results with EMEP measurement data. For non-marine sulphate they noticed an underestimation, particularly for low

concentration levels, because no background concentration in precipitation is assumed in the EMEP model. This effect is more important in remote areas. The model seems to underestimate the measured concentrations at coastal sites due to the marine component from sea spray, natural emissions of reduced sulphur from the sea and underestimation of the emissions from ship traffic by the model. Schaug *et al.,* (1993) have also compared the measurements and model results. They conclude that the model underestimates at coastal sites, and overestimates in the source regions in western and Central parts of Europe. Nitrate shows a similar behaviour as sulphate (Schaug *et al.,* 1993; Iversen *et al.,* 1991), although the underestimation is smaller. The reason for the (small) underestimation by the model at coastal sites may be that the model lacks a chemical mechanism for the conversion of nitric acid to particulate nitrate over sea, and the transport of nitrate in particles over longer distances than nitric acid (Schaug *et al.,* 1993). For ammonium, the model seems to underestimate the measured concentrations, but no strong conclusions about this difference can be drawn because the emissions on which the model is based are very uncertain compared to those for sulphur dioxide and nitrogen oxides, and measurement sites are situated in rural areas where local emissions are often strong (Iversen *et al.,* 1991).

These results are difficult to compare with results obtained in this study because Iversen *et al.* (1991) and Schaug *et al.* (1993) compare EMEP model concentration results with EMEP measured concentrations at individual sites, whereas in this study fluxes per grid cell are compared with fluxes obtained by the EMEP model. However, they report generally underestimations of sulphate, nitrate and ammonium, particularly for low concentration levels, and at coastal sites. On average the underestimation is 23%, 8% and 33%, respectively (Iversen *et al.*, 1991).

9. CONCLUSIONS AND RECOMMENDATIONS

9.1 Conclusions

Results obtained from sites scattered over Europe have allowed us to map regional-scale variations in concentration and fluxes of non-marine sulphate, nitrate, ammonium, hydrogen ion, sodium, chloride, magnesium, potassium and calcium on a European scale.

The results are satisfactory in the sense that the observed patterns agree well with what would be expected from prior knowledge of European emissions and climate patterns. Large nitrate and sulphate fluxes were observed (particularly) in the Black Triangle and former Yugoslavia. In Ukraine also large sulphate fluxes were found. Ammonium fluxes were largest in Central Europe. The influence of salt water bodies was evident in the sodium, chloride and magnesium maps. Large calcium fluxes were found in southeast Europe, probably caused by the influence of soil dust from calcareous soils and desert dust from the Sahara.

An extensive uncertainty analysis to assess the quality of the maps was performed. When it is assumed that concentration in rain and rainfall amounts are not correlated (conservative case) total uncertainties per average 50x50 km grid cell range from 50% in west, northwest and Central Europe to 60% in east, southeast and southwest Europe, and 70% in complex terrain areas. When an error propagation with full positive correlation (worst case) is concerned, total uncertainties range from 70% in west, northwest and Central Europe to 80% in east, southeast and southwest Europe, and 100% in complex terrain areas

A comparison with EMEP long-range transport model results has shown systematic differences. Average fluxes are about 75% higher for sulphate, 20% for nitrate and 55% for ammonium.

9.2 Recommendations

The quality of the maps might be improved by:

1. Investigation of data quality and data representativeness.
More information on data quality at the different sites as well as information on the representativeness of those sites should be available to be able to improve the quality of the results and to make a more accurate estimate of the overall uncertainty.
2. Extension of the number of measurement sites.
To eliminate blank areas in the maps, more measurement sites are needed. These sites must be evenly distributed in space and they must be representative for the area they make predictions for in the interpolation procedure. However, new sites will not be available in the short term. Furthermore, the measurement techniques used should be the same everywhere, improving comparability between results.
3. Calculation of wet deposition using 1989 precipitation data:
Section 7.2 described problems to correct the long-term mean precipitation map by using data from 1989. Efforts should be made to collect more confident 1989 rainfall

amount data.

4. Improvement of bulk/wet-only correction factors.

One possibility to improve the bulk/wet-only correction factors is to try to find a relationship between the correction factors and the amount of dry deposition. Bulk samplers probably collect more dry deposition if particle and gas concentrations are larger. Especially the factors for sodium and chloride are hard to determine because they are influenced largely by sea. Another possibility to improve the factors is to perform a kriging interpolation on only the concentrations measured by bulk samplers. In areas where the kriging variances will be small (which means that in these areas bulk samplers are nearby) the interpolated concentration values can be compared to the values measured with wet-only samplers located in that area. In this way a relationship between the two types of samplers can be inferred.

5. Investigation of the distribution of the spatial variation.

The distribution of the spatial variation in concentrations can be investigated. If the variance appears not to be homogeneously distributed over Europe (i.e. the spatial correlation between the measurements is different in separate parts of Europe), different variograms can be constructed for each separate part of Europe, with separate parameter values. However, it is difficult to trace these separate parts and it is a problem to link the different variograms to each other in spatial terms, i.e. how can one handle the transition zones between the areas described by separate variograms.

6. Incorporation of anisotropy in the variogram modelling.

Wet deposition is influenced by several factors, e.g. large-scale weather patterns and orography. When different variograms have been obtained for separate parts of Europe, anisotropy can be taken into account in the variogram modelling procedure to obscure directional differences. On the other hand, at some locations in Europe sampling density may be too low to allow variogram differentiation in different directions.

7. Reduction of kriging errors.

In some geostatistical software packages the search radius for interpolation can be divided into sectors. A minimum and a maximum number of measurements within each sector necessary for interpolation can be expressed. In this way the interpolation is forced to use information from each direction. This option ensures interpolation instead of extrapolation. The interpolation result will change to a reasonable extent, especially at the edges of the maps. Besides, some datapoints near the coast can only be used for interpolation inland because they lack information in a seaward direction. A comparison between maps derived in this way and maps developed in this study can be carried out. The kriging errors will diminish, but a map covering the whole of Europe cannot be obtained (i.e. the maps will be 'smaller') because some measurements can no longer 'fully' be used.

ACKNOWLEDGEMENTS

All persons delivering data used to compile the European wet deposition maps are acknowledged for their contribution. Thanks go to: A. Widhalm (Austria), M. Bíba (Czech Republic), E. Bieber (Germany), E. O'Carroll (Ireland), R. Carvalho (Portugal), N. Cénac (France), P. Coddeville (France), E. Dambrine (France), D. Fottová (Czech Republic), M. Frolova (Latvia), J.Führer (Switzerland), R. Gehrig (Switzerland), M. McGettigan (Ireland), L. Granat (Sweden), P. Grennfelt (Sweden), L. Horváth (Hungary), D. Hrcek (Slovenia), Z. Ikonomova (Bulgaria), J. Irwin (United Kingdom), J. Iwanek (Poland), O. Järvinen (Finland), D. Kallweit (Germany), K. Kindbom (Sweden), A. Kovar (Austria), R. Lavrinenko (Russia), M. Mitosinkova (Slovak Republic), D. Möller (Germany), R. Mosello (Italy), H. Puxbaum (Austria), A. Reissell (Finland), M. Reuther (Germany), E. Roekens (Belgium), L.Saare (Estonia), J. Santroch (Czech Republic), V. Smirnioudi (Greece), I. Stratan (Moldava), K. Torseth (Norway), E. Ulrich (France), J. Vrubel (Czech Republic), T. Vukovic (Yugoslavia), H. Wielogorska (Poland) and D. Wintermeyer (Germany). D. Karssenberg is kindly thanked for his helpful comments on the draft version of the report. Information used originated from questionnaires as well as from the following reports:

Bowman J. (1991), Acid Sensitive Surface Waters in Ireland, The impact of a major new sulphur emission on sensitive surface waters in an unacidified region; Environmental Research Unit, Dublin.

Brüggemann E. (1993), Abschlußbericht zum Förderungsvorhaben BMfT: Wissenschaftliches Begleitprogramm zur Sanierung der Atmosphäre über den neuen Bundesländern (SANA), Aufbau und Betrieb eines Meßnetzes zur Bestimmung des flächenhaften Eintrags und der zeitlichen Trends von Schadstoffen durch Niederschläge; Inst. für Troposphärenforschung e.V., Leipzig Prj. B. 2.1.

Brüggemann E. (1993), Quantitativer Einfluß verschiedener Emissionsgebiete auf die chemische Zusammensetzung der nassen Deposition sowie Trendberechnungen anhand mehrjähriger Meßreihen; Auswirkungen lufthygienischer Sanierungsmaßnahmen in den neuen Bundesländern, Abschlußbericht für den Zeitraum 1991/1992; Verbundprojekt SANA, Projekt: Nasse Deposition, prj. B 2.2.

Campbell G.W., Stedman J.R., Irwin J.G. (1992), Acid Deposition in the United Kingdom; Warren Spring Laboratory, LR 865 (AP) DoE Contract No PECD/7/12/76, Crown, Middlesex.

Coddeville P., Guillermo R. and Houdret JL. (1993), Les Retombees Atmosferiques en France, Réseau MERA 1990; Ecole des Mines de Douai.

Dambrine E. (1992), Etablissement d'un réseau de collecte et d'analyse de la pluie et des pluviolessivats dans les Vosges; Rapport Technique Definitif, Commission des Communautes Europeennes, Direction Généreale VI, Décision no. 8960. Fr 005.0 (Code INRA 4278 B), INRA Centre de Nancy.

Granat L. (1989), Luft- och nederbördskemiska stationsnätet inom PMK; Stockholms Universitet, Meteorologiska institutionen, Rapport från verksamheten 1989, Naturvårdsverket Rapport 3789.

Hrcek D. (1992), Air Pollution in Slovenia: April 1991 - March 1992, Ministry of Environment and Regional Planning; Hydrometeorological Institute of Slovenia.

I.H.E. (1991), Regennet 01/04/90 - 31/3/91; Instituut voor hygiëne en epidemiologie, afdeling lucht, Brussels.

I.N.M.G. (1989), Investigaçao Meteorologica de Apoio à Defesa de Ambiente, Instituto Nacional de Meteorologia e geofisica, Estudos do Clima, Divisao de Protecçao do Ar, Boletim do Projecto I_2 do Piddac, nos 61, 62, 63, 64 (I, II, III, IV Trim., 1989).

Järvinen O., Vänni T. (1990), Sadeveden Pitoisuus- ja Laskeuma- Arvot Soumessa Vuonna 1989; Vesi- ja Ympäristöhallituksen Monistesarja, Helsinki, Nro 236.

Kallaste T., Roots O., Saar J., Saare L. (1992), Air Pollution in Estonia 1985-1990; Environmental Report 3, Environment Data Centre, National Board of Waters and the Environment, Helsinki.

Klockow D., Wintermeyer D. (1990), Erstellung von Depositionskarten für die Bundesrepublik Deutschland; Abschlußbericht zum Vorhaben, Gefördert durch das Bundesministerium für Forschung und Technologie, Dortmund, Nr. 0339232 A.

Leinonen L., Junto S. (1991), Ilmanlaadun Tuloksia Tausta-Asemilta, Results of Air Quality at Background Stations January - June 1989 and July - December 1989; Finish Meteorological Institute - Air Quality Department, Helsinki.

Lochman V. (1993), Pollutant fall-out into forest ecosystems as related to changes in forest soils; Lesnictví-Forestry, Volume 39, No.2.

Mosello R., Morselli L. (1992), Documenta dell'Istituto Italiano de Idrobiologia Dott. Marco De Marchi, N.33, Situazione degli Srudi Sulla Chimica delle Deposizioni Atmosferiche Umide nel 1989 in Italia, Consiglio Nazionale delle Richerche, Pallanza, Pubblicazione n.5.

N.A.B.E.L. (1992), Luftbelastung 1992, Schriftenreihe umwelt nr. 207, BUWAL, Bern, Switzerland.

Nilsson J. (1986), Miljørapport 1986: 11; Nordic Council of Ministers, Copenhagen.

Persson K., Lövblad G. and Munthe J. (1993), Luft- och nederbördskemiska stationsnätet inom PMK; IVL, Göteborg, Sweden.

Schaug J., Pedersen U., Skjelmoen J.E. (1991), EMEP Co-operative programme for monitoring and evaluation of the long-range transmission of air pollutants in Europe, Data Report 1989, part 1: Annual Summaries, Norwegian Institute for Air Research, EMEP/CCC-Report 2/91.

S.F.T. (1991), Overvåking av langtransportert forurenset luft og nedbor, Årsrapport 1989, Statlig program for forurensningsovervåking, Rapport 437/91.

United Kingdom Review Group on Acid Rain (1990) Acid Deposition in the United Kingdom 1986-1988, Third Report of the United Kingdom Review Group on Acid Rain; Warren Spring Laboratory, Stevenage, UK.

Ulrich E., Williot B. (1993), Les Depots Atmospheriques en France de 1850 à 1990, Dépôts en milieu rural et en fôret, Dépots dans les zones industrialisées et urbaines; Imprimerie de l'Office National des Fôrets.

REFERENCES

Asman W.A.H. (1985), De verhoging van de NH_4 concentratie in regen in gebieden met hoge NH_3 emissie; Instituut voor Meteorologie en Oceanografie, Universiteit van Utrecht, Rapport R 85-12.

Barnard W.R., Stensland G.J., Gatz D.F. (1986) Water, Air and Soil Pollution, 30, 285.

Behr O. (1990) Ermittlung von Niederschlagsverteilungen und Gebietsniederschlägen unter Einbeziehung digitaler Geländeinformationen, Institut für Hydraulik der Technische Universität, Vienna.

Browning K.A., Hill F.F., Pardoe C.W. (1974), Structure and mechanism of precipitation and the effect of orography in a winter-time warm sector; Q J Roy Met Soc, 100, 309 - 330.

Buijsman E. (1982), Zure regen: atmosferische processen; Instituut voor Meteorologie en Oceanografie, Universiteit van Utrecht, Rapport V 82-29.

Buijsman E. (1989), Onderbouwende informatie over het landelijk meetnet luchtkwaliteit 1: Het landelijk meetnet regenwatersamenstelling, National Institute of Public Health and Environmental Protection, Bilthoven, The Netherlands, Report no. 228703006.

Buijsman E., Erisman J.W. (1986) Ammonium wet deposition flux in Europe; Institute for Meteorology and Oceanography, University of Utrecht, The Netherlands, Report no. R-86-5.

Burrough P.A. (1986), Principles of Geographical Information Systems for Land Resources Assessment; Clarendon Press, Oxford.

Clark A.G., Lambert D.R. (1988), Local factors influencing the chemistry of precipitation; In: Perry, R., Harrison, R.M., Bell, J.N.B., Lester, J.M. (eds.), Acid rain: scientific and technical advances, Selpter, London.

Cressie N.A.C. (1993), Statistics for Spatial Data; Wiley & Sons, Inc., New York.

Deursen W.P.A. van, Wesseling C.G. (1992), The PC-raster package; Department of Physical Geography, University of Utrecht, The Netherlands.

Dollard G.J., Unsworth M.H., Harvey M.J. (1983), Pollutant transfer in upland regions by occult precipitation; Nature, 302, 241-243.

Dore A.J., Choularton T.W., Fowler D. (1992), An improved wet deposition map of the United Kingdom incorporating the seeder-feeder effect over mountainous terrain; Atmospheric Environment, 26A, (8), 1375-1381.

Draaijers, G.P.J., Erisman, J.W. (1993), Atmospheric sulphur deposition to forest stands: throughfall measurements, Atmospheric Environment, 27A, (1), 43-55.

Englund E., Sparks A. (1991), GEO-EAS 1.2.1 Geostatistical Environmental Assessment Software, Users Guide; Environmental Monitoring Systems Laboratory, Office of Research and Development, U.S. Environmental Protection Agency, Las Vegas, Nevada.

Fowler D. (1984), Transfer to terrestrial surfaces; Philos Trans R Soc London, B305, 281-297.

Fowler D., Cape J.N., Leith I.D., Choularton T.W., Gay M.J., Jones A. (1988), The influence of altitude on rainfall composition at Great Dun Fel, Atmospheric Environment, 22, 1355-1362.

Garland J.A. (1978), Dry and wet removal of sulphur dioxide to land and water surfaces, Proc R Soc London, A354, 245-268.

Gatz D.F., Barnard W.R., Stensland G.J. (1986) Water, Air and Soil Pollution, 30, 245.

Georgii H.W., Grosch S., Schmitt G. (1986), Assessment of wet and dry pollutant deposition to forests in the Federal Republic of Germany; Institute für Meteorologie und Geophysik, J.W. Goethe Universität, Frankfurt.

Grennfelt P., Larsson S., Leyton P., Olsson B. (1985), Atmospheric deposition in the Lake Gärdsjön area, SW Sweden, Ecol Bull 37, 101-108.

Hendry C.D. and Brezonik P.L. (1980) Environmental Science Technology, 14, 843.

Hicks B.B., Baldocchi D.D., Meyers T.P., Hosker J.R.P., Matt D.R. (1987), A preliminary multiple resistance routine for deriving dry deposition velocities from measured quantities; Water Air Soil Pollut 36, 311-330.

Isaaks E.H., Srivastava R.M. (1989), Applied Geostatistics; Oxford University Press, New York/Oxford.

Iversen T., Halvorsen N., Mylona S., Sandnes H. (1991), Calculated budgets for airborne acidifying components in Europe, 1985, 1987, 1988, 1989 and 1990; Meteorological Synthesizing Centre-West, Norwegian Meteorological Institute, Oslo.

Journel A.G., Huijbregts Ch.J. (1978), Mining Geostatistics; Academic Press, London.

Karssenberg D. (1994), Kriging partial realizations of non-stationary random fields using maps of square root difference and exploratory data analysis; University of Utrecht, The Netherlands.

KNMI/RIVM (1989), Chemische samenstelling van de neerslag over Nederland; Annual Report 1988, De Bilt/Bilthoven, The Netherlands, Report no. 228703012.

Kovar A., Kasper A., Puxbaum H. , Fuchs G., Kalina M., Gregori M. (1991), Kartierung der deposition von SO_X, NO_X, NH_X und basischen kationen in Österreich; Technische Universität Wien, Institut für Analytische Chemie Abteilung für Umweltanalytik im auftrag des Umweltbundesambtes, Vienna.

Kovar A., Puxbaum H. (1992), Nasse Deposition im Ostalpenraum, Untersuchung der nassen deposition atmosphärischer spurenstoffe im bereich der arge Alp und der arbeitsgemeinschaft Alpen-Adria; Institut für Analytische Chemie der Technischen Universität Vienna, Abteilung für Umweltanalytik, im auftrag des Bayerischen Staatsministerium für Landesentwicklung und Umweltfragen, Vienna/Munich.

Legates D.R., Willmott C.J. (1990), Mean seasonal and spatial variability in gauge-corrected, global precipitation, Int J Climatol, 10, 111-123.

Lövblad G., Erisman J.W., Fowler D. (1992), Models and Methods for the Quantification of Atmospheric Input to Ecosystems; An International workshop on the deposition of acidifying substances, Göteborg, 3-6 November 1992.

Lövblad et al (1994), Submanual on deposition on ICP forests level 2 plots, IVL, Göteborg, Sweden.

Matheron G. (1971) The theory of regionalized variables and its applications, les Cahiers du Centre de Morphologie; Mathematique de Fontainebleau, Ecole des Mines de Paris, V.5.

Moldan (1980), In: Drablös D., Tollan A. (eds.), Ecological impact of acid precipitation; SNSF-project, Norway.

Mosello R., Marchetto A., Tartari G.A. (1988), Bulk and wet atmospheric deposition chemistry at Pallanza (Italy); Water Air Soil Pollut 42, 137-151.

Mosello R., Bianchi M., Geiss H., Marchetto A., Tartari G.A., Serrini G., Serrini Lanza G., Muntau H. (1994), Acid Rain Analysis: Results of the third interlaboratory exercise, Aquacon-Medbas-Subproject N. 6 (Analytical Quality Control and Assessment Studies in the Mediterrain Basin), Pallanza, Italy.

Munger J.W., Eisenreich S.J. (1983) Environmental Science Technology, 17, 32A.

Nilsson J., Grennfelt P. (eds) (1988), Critical Loads for Sulphur and Nitrogen; Report from a workshop held at Skokloster, Sweden, 19-24 March 1988. NORD miljorapport 1988: 15, Nordic Council of Ministers, Copenhagen.

Pebesma E.J. (1994), GSTAT 1.1 - Multivariate Geostatistical Toolbox; National Institute for Public Health and Environmental Protection, Bilthoven, The Netherlands.

Potma C.J.M. (1993), Description of the ECMWF/WMO Global Observational Data Set, and associated data extraction and interpolation procedures; National Institute of Public Health and Environmental Protection, Bilthoven, The Netherlands, Report no. 722401001, .

Pul W.A.J. van, Potma C.W.M., Leeuwen E.P. van, Draaijers G.P.J., Erisman J.W. (1995), EDACS: European Deposition maps of Acidifying Compounds on a Small scale. Model description and preliminary results; National Institute of Public Health and Environmental Protection, Bilthoven, The Netherlands, Report no. 722401005.

Puxbaum H., Kovar A. (1991) Seasonal trend of snowfall composition at the high alpine observatory Sonnblick (3106 m a.s.l., eastern alps). In: Borell, P. *et al.* (eds.), Proc Eurotrac Symposium '90, SPB Academic Publishing bv, pp 61-66.

Ridder T.B. de, Baard J.H., Buishand T.A. (1984), The impact of sample strategy and analysis protocol on concentrations in rainwater; Royal Meteorological Institute of the Netherlands, Report no. TR-55.

Ronseaux F., Delmas R.J. (1988), Chemical composition of bulk atmospheric deposition to snow at Col de la Brevna (Mt Blanc); In: Unsworth M.H., Fowler D. (eds.), Acid deposition at high elevation sites, Kluwer, pp 491-510.

Ruijgrok W., Visser H., Römer F.G. (1990), Comparison of bulk and wet-only samplers for trend detection in wet deposition; Proc Workshop on Cloud Chemistry and Wet Deposition, Utrecht, The Netherlands, 10-12 april, 1990.

Sandnes H. (1993), Calculated Budgets for Airborne Acidifying Components in Europe, 1985, 1987, 1988, 1989, 1990, 1991 and 1992; Det Norske Meteorologiske Institutt, Oslo, Technical Report no. 109.

Schaug J., Pedersen U., Skjelmoen J.E. (1991) EMEP Co-operative programme for monitoring and evaluation of the long-range transmission of air pollutants in Europe, Data Report 1989, part 1: Annual Summaries; Norwegian Institute for Air Research, EMEP/CCC-Report 2/91.

Schaug J., Iversen T., Pedersen U. (1993), Comparison of measurements and model results for airborne sulphur and nitrogen components with kriging; Atmospheric Environment, 27A, (6), 831-844.

Slanina J., Keuken M.P., Arends B., Veltkamp A.C., Weyers G.P. (1990), Report on the contribution of ECN to the second phase of the Dutch priority programme on acidification; ECN, Petten, The Netherlands.

Stedman J.R., Heyes C.J., Irwin J.G. (1990), A comparison of bulk and wet-only precipitation collectors at rural sites in the United Kingdom; Water Air Soil Pollut 52, 377-395.

United Kingdom Review Group on Acid Rain (1990), Acid Deposition in the United Kingdom, Third Report of the United Kingdom Review Group on Acid Rain; Prepared at the request of the Department of the Environment, UK.

Webster R., Campbell G.W., Irwin J.G. (1991), Spatial Analysis and mapping the annual mean concentrations of acidity and major ions precipitation over the United Kingdom in 1986; Environ Mon Assess 16, 1-17.

Webster R., Oliver M.A. (1990), Statistical Methods in Soil & Land Resources Survey; Oxford University Press.

WMO (1971), Guide to meteorological instrument and observing practices; WMO - No. 8, TP. 3, Geneva.

APPENDICES

Appendix 1: The questionnaire: Wet deposition measurement/monitoring in Europe.

QUESTIONNAIRE
WET DEPOSITION MEASUREMENTS/MONITORING IN EUROPE

NOTE

If you think you are not the right person to fill in this questionnaire, please send this questionnaire to the people responsible for the wet deposition measurements/monitoring network in your institute.

If your institute is not dealing with wet deposition measurements at all, only fill in page 1 of this questionnaire indicating persons/institutes responsible for the management of wet deposition measurements in your country.

■ **Person who answered this questionnaire:**

Name: .....
Institute: .....
Department: .....
Street: .....
P.O. box: .....
Postcode: .....
City: .....
Country: .....
Telephone: .....
Fax: .....

■ **If different from above, name and address of the person/organization responsible for the management of the wet deposition measurements in your country:**

Name: .....
Institute: .....
Department: .....
Street: .....
P.O. box: .....
Postcode: .....
City: .....
Country: .....
Telephone: .....
Fax: .....

■ **How many measurement sites are there in your wet deposition monitoring network?**

.....

■ **Since when does this network exist?**

.....

■ **What kind of samplers are used in the network?**

Bulk	Wet/only
o	o

■ **Which components are measured in this network?**

SO_4^{2-}	NO_3^-	NH_4^+	Na^+	Cl^-	Mg^{2+}	Ca^{2+}	K^+	HCO_3^-	PO_4^{3-}
o	o	o	o	o	o	o	o	o	o

pH	Conductivity	N-total	S-total	C-total
o	o	o	o	o

Al^{3+}	Fe^{3+}	Cu^+	Hg^{2+}	Co	Ni	Pb^{4+}	Zn^{2+}	Mo	Mn^{4+}	Cd^{2+}
o	o	o	o	o	o	o	o	o	o	

■ **Is there any report or publication available with technical background information about the network?**

Yes	No
o	o

■ **Does this report/publication contain information about:**

Exact location (longitude, latitude) of each site	o
Height above sea level of each measurement site	o
Characteristics of the vicinity of each site	o
Sample methodology	o
Analytical procedure	o
Data management	o

■ **We would be very pleased if you can send us above mentioned technical background report/publication. Otherwise, please indicate author(s), title, and the way it can be obtained:**

.....
.....

■ **Are there any reports or publications available with results from the measurement/monitoring activities?**

Yes	No
o	o

■ **Do these reports/publications contain information about yearly average wet deposition fluxes for each measurement site in your country?**

Yes	No
o	o

■ **We will be very pleased if you can send us above mentioned reports/publications with results for 1989. In the second instance we are interested to receive results for 1990, 1991 and 1992. Otherwise, please indicate authors(s), titles, and the way these reports/publications can be obtained:**

.....
.....

- **If no reports/publications with average wet deposition fluxes for 1989 (and/or 1990, 1991, 1992) for each measurement site in your country exist, please fill in the attached table.**

- **Please provide any further information which might be relevant for us:**

  .....
  .....
  .....
  .....
  .....
  .....

NOTE

If you are interested in more information on this project please let us know.

End of questionnaire

Appendix 2: X-Y plots between elements that are strongly correlated.

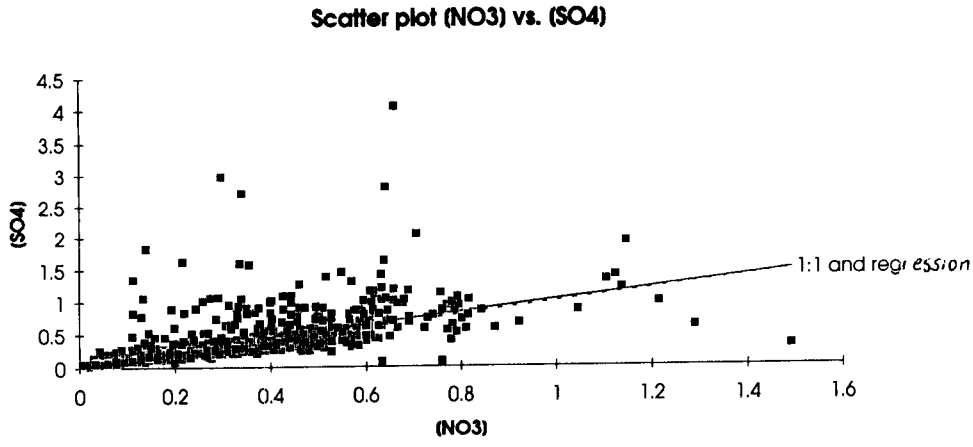

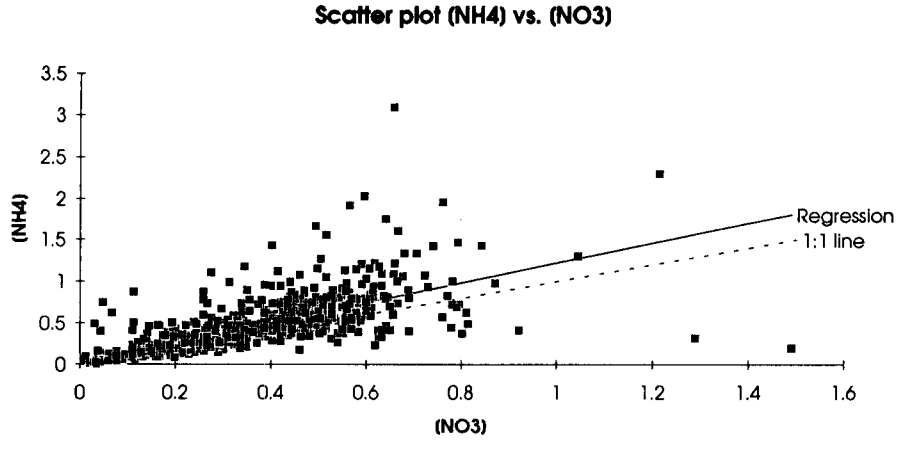

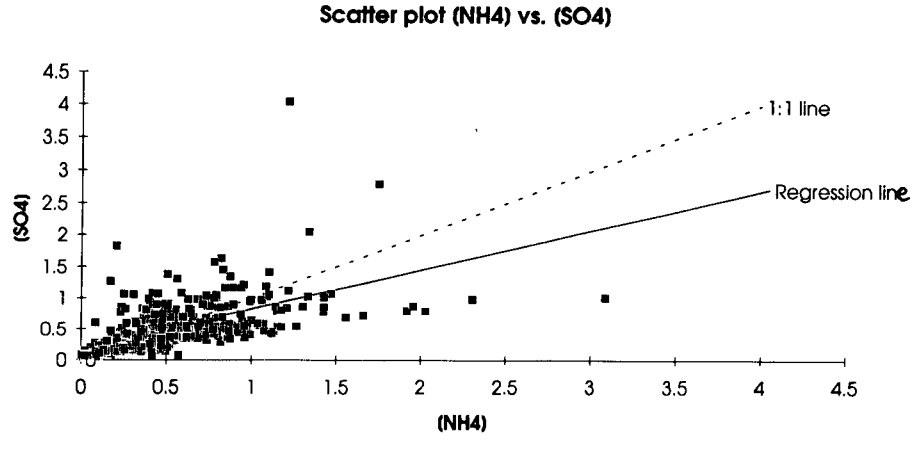

Scatter plot (Na) vs. (Cl)

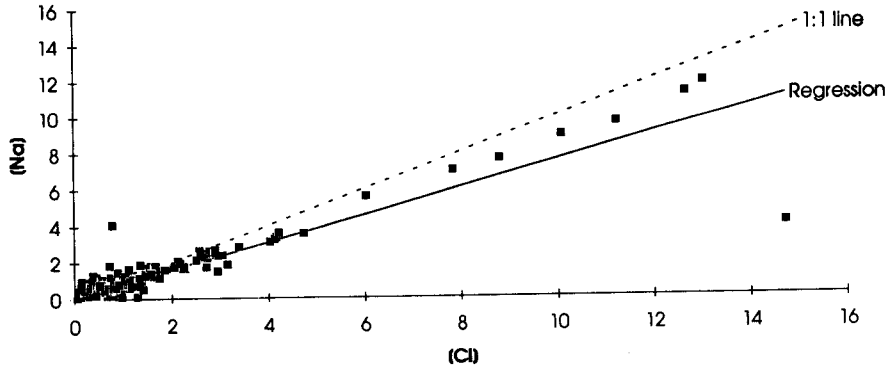

Scatter plot (Na) vs. (Mg)

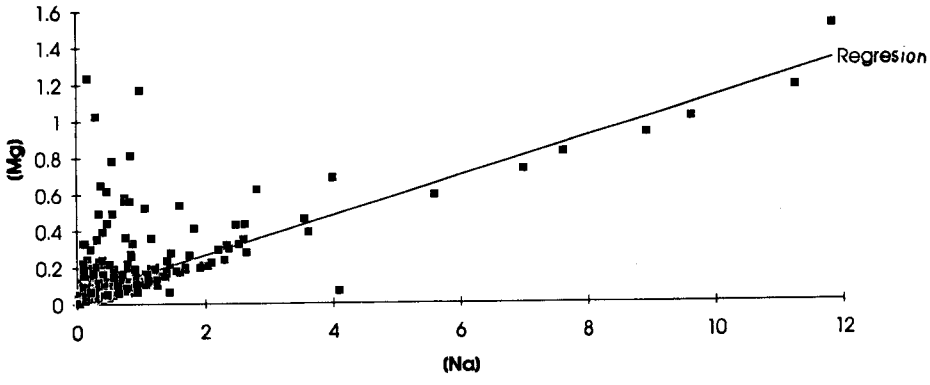

Scatter plot (Cl) vs. (Mg)

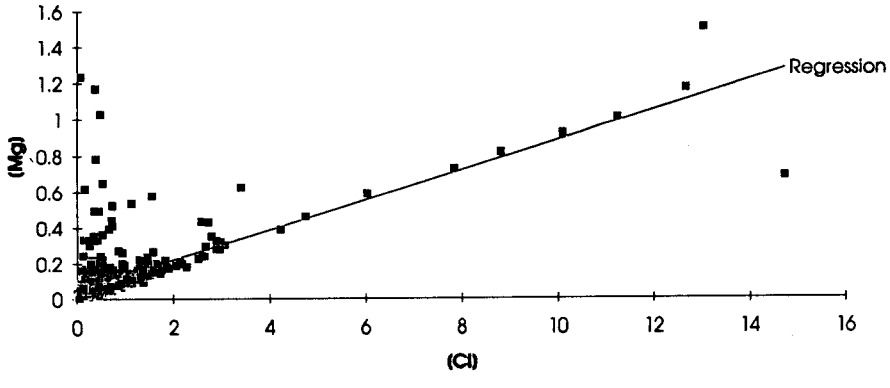

Appendix 3: Description of the kriging interpolation technique

For applying the kriging interpolation technique, the first step is to decide on a suitable function for $m(\mathbf{x})$. In the simplest case, where no trend is present, $m(\mathbf{x})$ equals the mean value in the sampling area and the average or expected difference between any two places, **x** and **x+h**, separated by a distance vector **h**, will be zero:

$$E[Z(x) - Z(x+h)] = 0 \qquad (1)$$

Also, it is assumed that the variance of differences depends only on the distance between sites (**h**) (which is also called the *lag*), so that:

$$E[\{Z(x) - Z(x+h)\}^2] = E[\{\varepsilon'(x) - \varepsilon'(x+h)\}^2] = 2\gamma(h) \qquad (2)$$

where $\gamma(\mathbf{h})$ is a function known as the *semi-variance*. It is the variance per site when sites are considered in pairs. It is known as semi-variance because it is half the variance of the difference between such pairs. The function $\gamma(\mathbf{h})$ that relates γ to the lag is the semi-variogram, increasingly known just as the variogram. The two conditions, stationarity of difference and variance of differences, define the requirements for the *intrinsic hypothesis* of Regionalised Variable theory. This means that once structural effects have been accounted for, the remaining variation is homogeneous in its variation so that differences between sites are merely a function of the difference between them. Although there are some doubts about the validity of these assumptions (for concentrations in precipitation for example, the variance of differences also depends on the altitude of the sites), kriging can be applied because the interpolation weights obtained are better than those obtained by other, more simple methods.

Suppose that a property Z is measured at numerous places $\mathbf{x}_1$, $\mathbf{x}_2$,... to give the values $Z(\mathbf{x}_1)$, $Z(\mathbf{x}_2)$,... . Suppose also that there are n pairs of measurements at places separated by the lag **h**. Then for that lag the semi-variance can be estimated by:

$$\gamma(h) = \frac{1}{2n}\sum_{i=1}^{n}\{Z(x_i) - Z(x_i + h)\}^2 \qquad (3)$$

If the procedure is repeated for several different lags, an ordered set of semi-variances is obtained, and these constitute the experimental semi-variogram. So the experimental variogram is estimated at discrete values of the lag. However, the underlying variogram is continuous, and as it is needed to evaluate semi-variances at numerous intermediate lags some continuous function must be found to describe it. If for example mean precipitation acidity was measured at two sites, placed at random 50 km apart, the difference will, on average, be smaller than if the sites were 200 km apart. This is quantified in the semi-variance function. This function is essential for determining optimal weights for interpolation. In the variogram the limiting semi-variance is known as the *sill*; it implies that at these values of the lag there is no spatial dependence between the data points because all estimates of variances of differences are invariant with distance. The separation is called the *range*. This is a

critically important part of the semi-variogram because it describes at what distance inter-site differences become spatially dependent. Within the range, usually denoted by the symbol *a*, the closer together the sites, the more similar they are likely to be. Hence, if the distance separating an unvisited site from a data point is greater than the range, then that data point can make no useful contribution to the interpolation because it is too far away. The non-zero intercept is known as the *nugget*. The nugget-variance (ε') describes the variation that is random and not spatially correlated at the shortest sampling interval used.

Given the often large, short-range nature of air pollution variation that contributes to nugget variance, simple kriging results in maps which have many sharp spikes or pits at the data points (Burrough, 1986). This can be overcome by modifying the kriging equations to estimate an average value of Z over a block B. The estimation variances obtained for block kriging are usually substantially less than for point kriging. The average value of Z over a block B is given by:

$$Z(x_b) = \frac{Z(x)dx}{\int_B areaB} \tag{4}$$

A kriged estimate is a weighted sum of data: if there are n values $z(\mathbf{x}_i)$, i=1,2,...,n then the estimate for some block B is:

$$\hat{z}(B) = \sum_{i=1}^{n} \lambda_i z(x_i) \tag{5}$$

To avoid bias the weights, λ_i sum to 1. The estimation variance is:

$$\sigma^2{}_B = E\left[\left\{z(B) - \hat{z}(B)\right\}^2\right] = 2\sum_{i=1}^{n} \lambda_i \bar{\gamma}(x_i, B) - \sum_{i=1}^{n}\sum_{j=1}^{n} \lambda_i \lambda_j \gamma(x_i, x_j) - \bar{\gamma}(B, B) \tag{6}$$

where $\gamma(\mathbf{x_i},\mathbf{x_j})$ is the semi-variance between the sampling sites x_i and x_j, $\gamma(\mathbf{x_i},B)$ is the average semi-variance between the sampling sites and the block to be estimated, and γ (B,B) is the average semi-variance within the block, i.e. the within-block variance. This variance is minimised subject to the non-bias condition when:

$$\sum_{i=1}^{n} \lambda_i \gamma(x_i, x_j) + \psi = \bar{\gamma}(x_j, B) \quad \textbf{for all } j \tag{7}$$

where ψ is the Langrange multiplier associated with the minimisation. When this set of linear equations (kriging equations) are solved, the weights are obtained which can be inserted into equation (5) to give $z(B)$. An estimate of the kriging variance is also obtained by :

$$\sigma^2{}_B = \sum_{i=1}^{n} \bar{\gamma}(x_i, B) + \psi - \bar{\gamma}(B, B) \tag{9}$$

Appendix 4:

Histograms of the log-transformed data

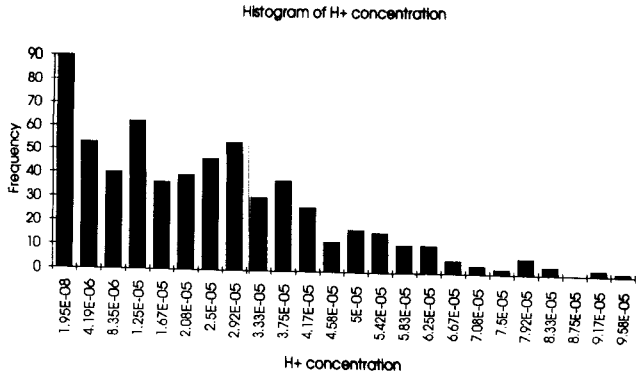

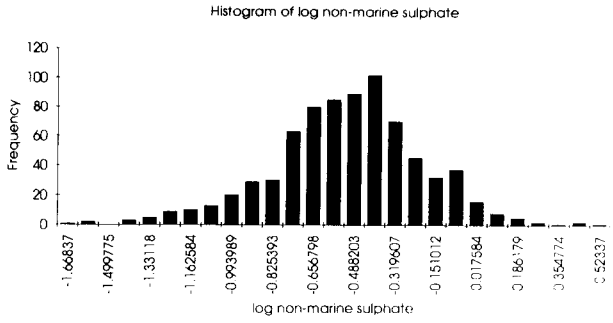

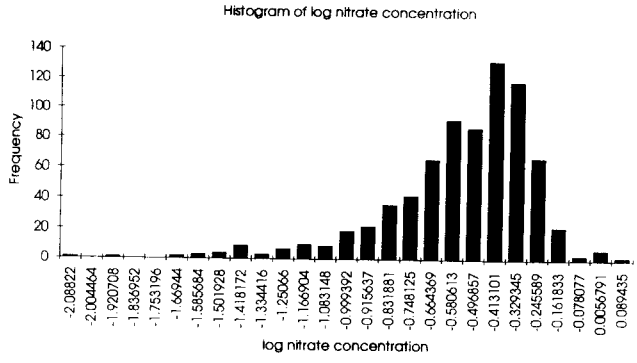

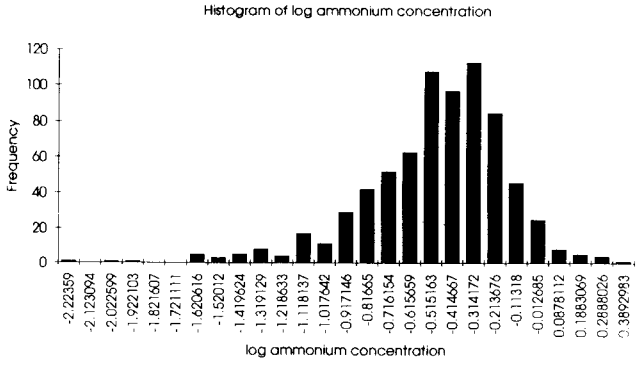

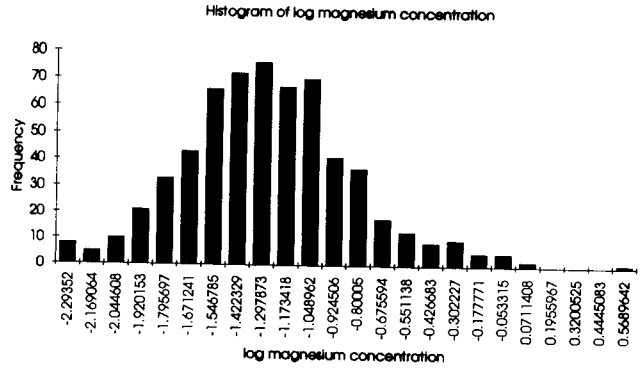

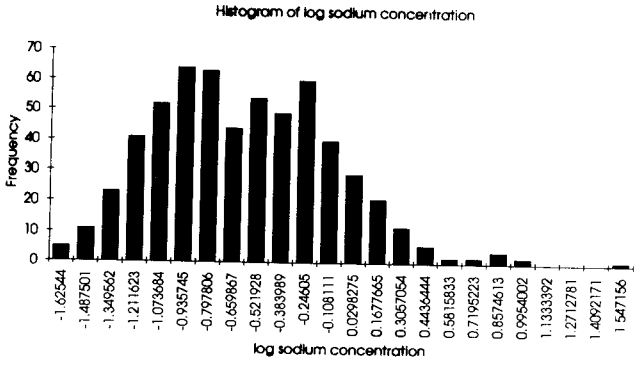

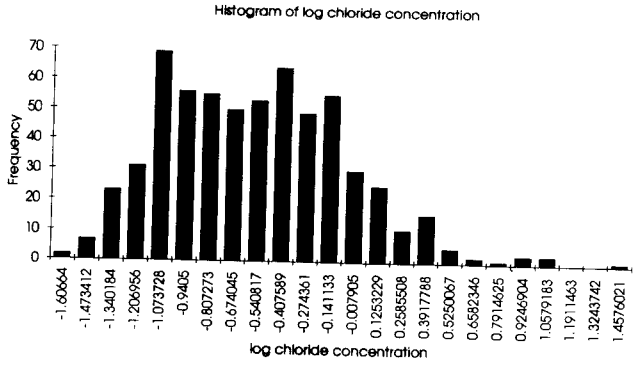

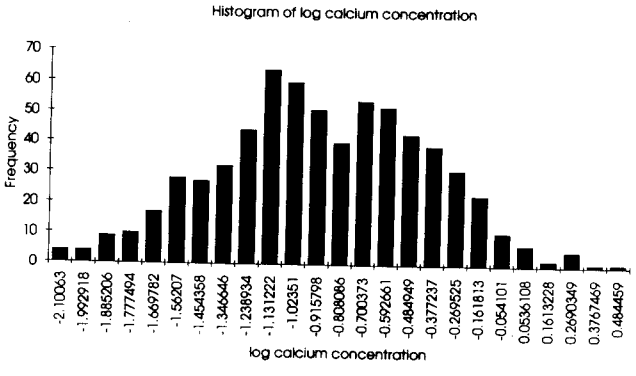

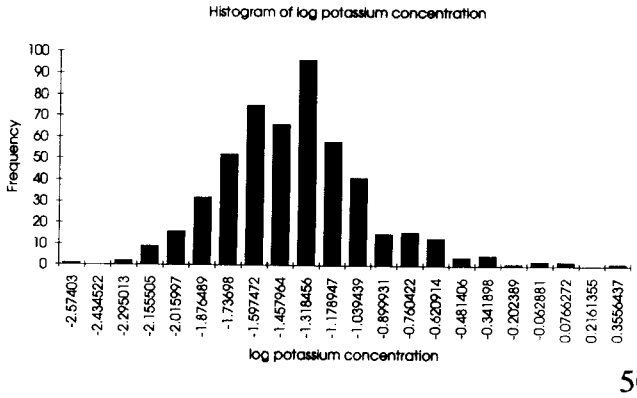

Appendix 5: Concentrations in rain and wet deposition fluxes mapped for each component.

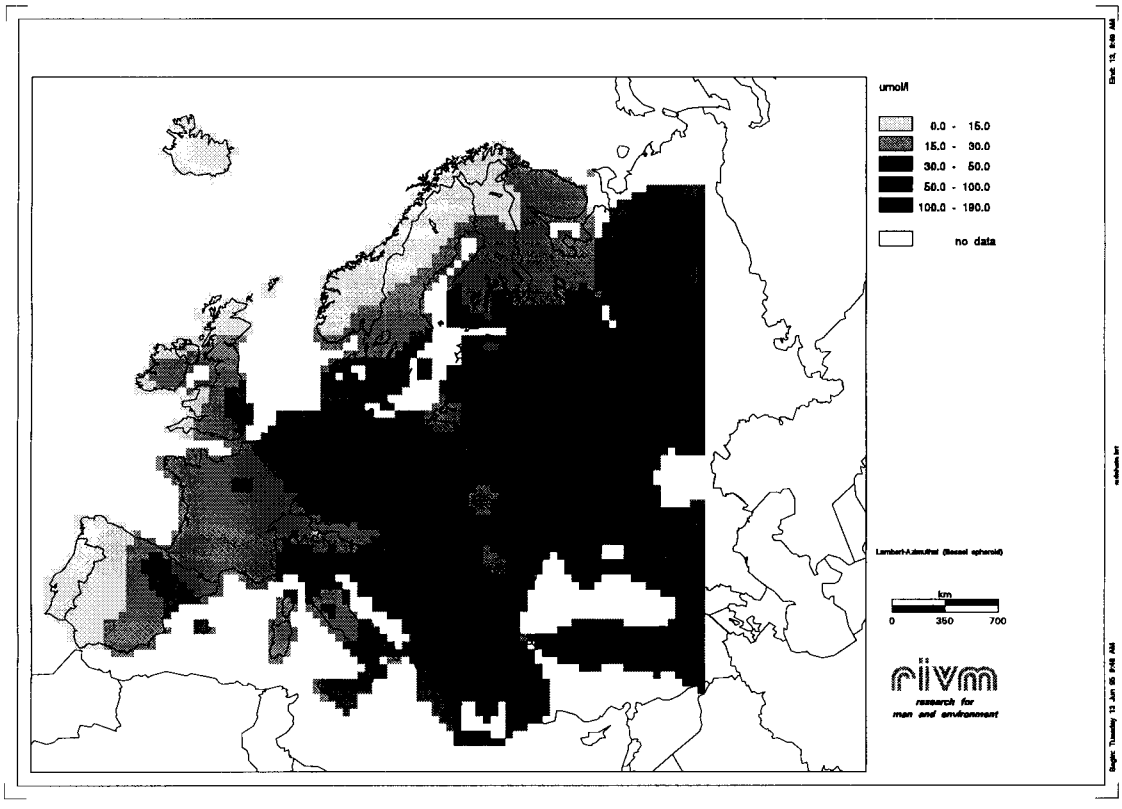

Non-marine sulphate concentrations on a 50x50 km basis in 1989 in µmol l^{-1}.

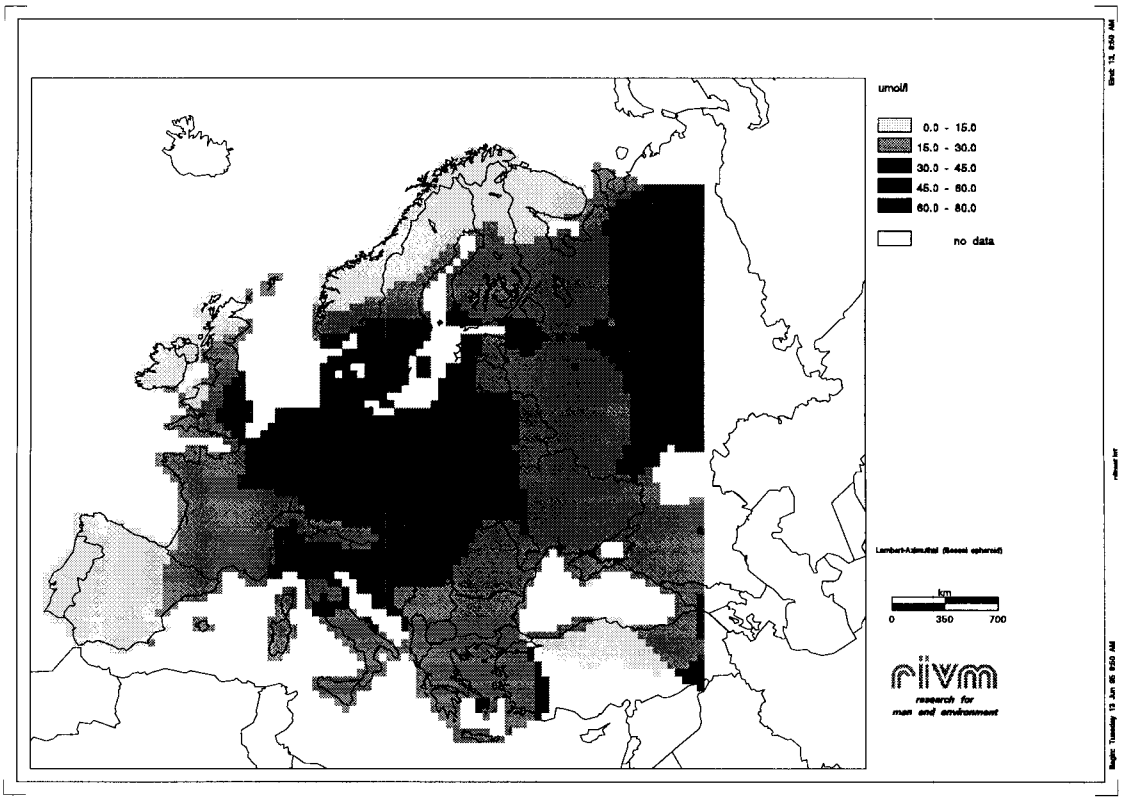

Nitrate concentrations on a 50x50 km basis in 1989 in µmol l^{-1}.

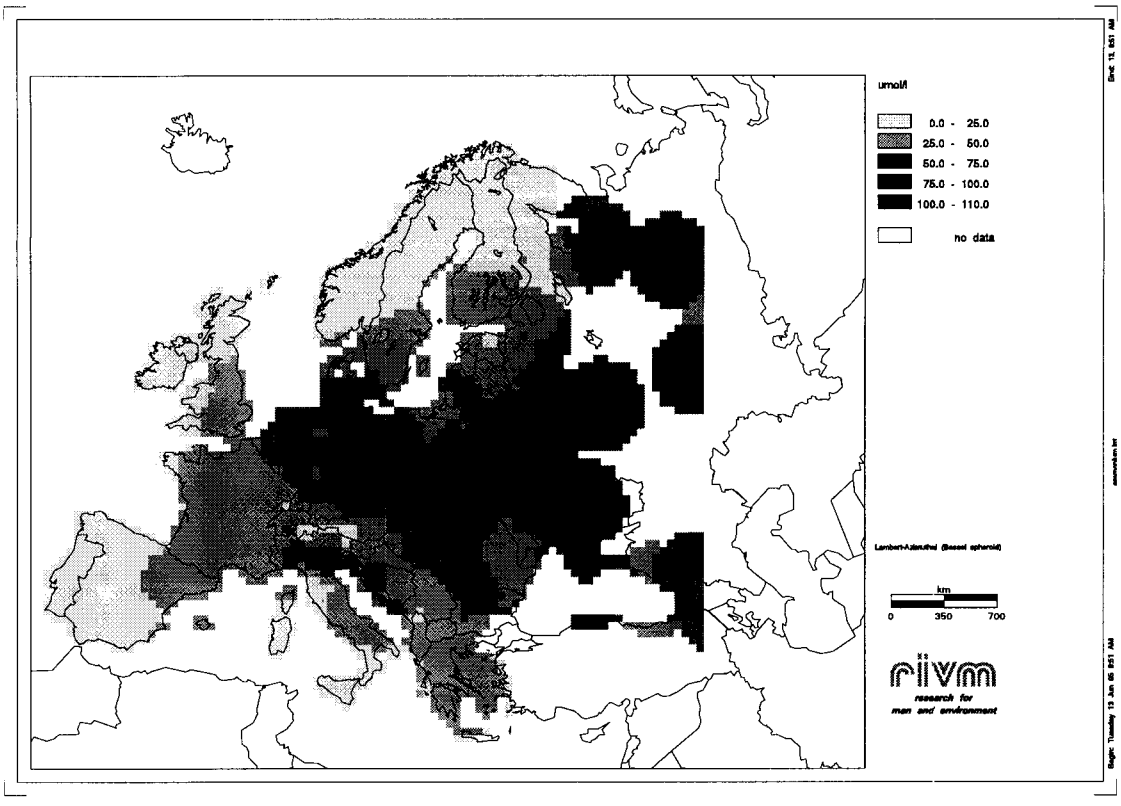

Ammonium concentrations on a 50x50 km basis in 1989 in µmol l^{-1}.

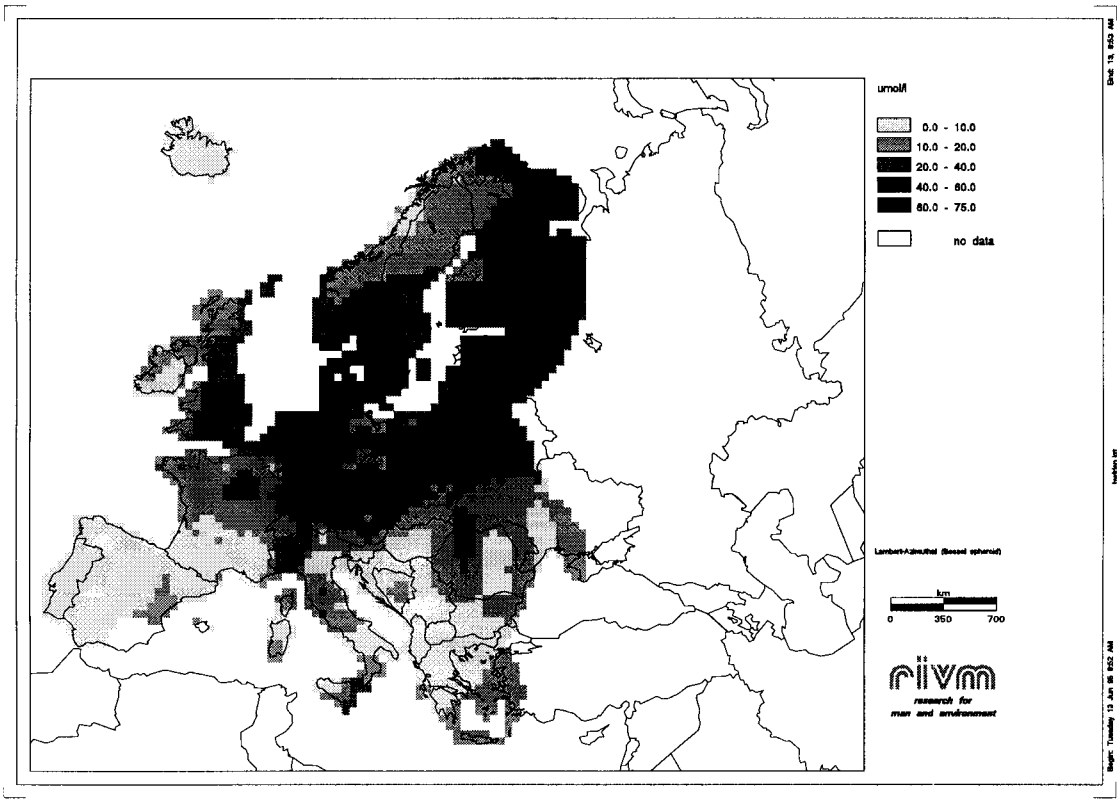

Hydrogen ion concentrations on a 50x50 km basis in 1989 in µmol l^{-1}.

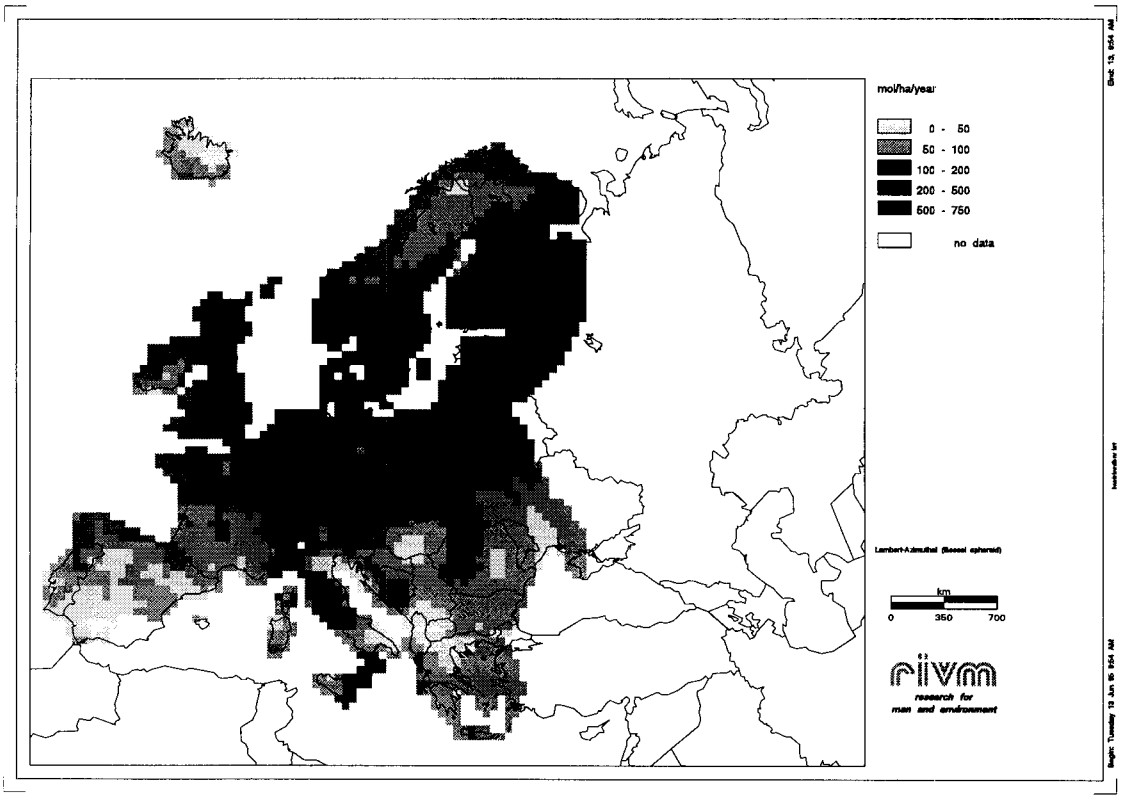

Wet deposition of hydrogen ion on a 50x50 km basis in 1989 in mol ha^{-1} a^{-1}.

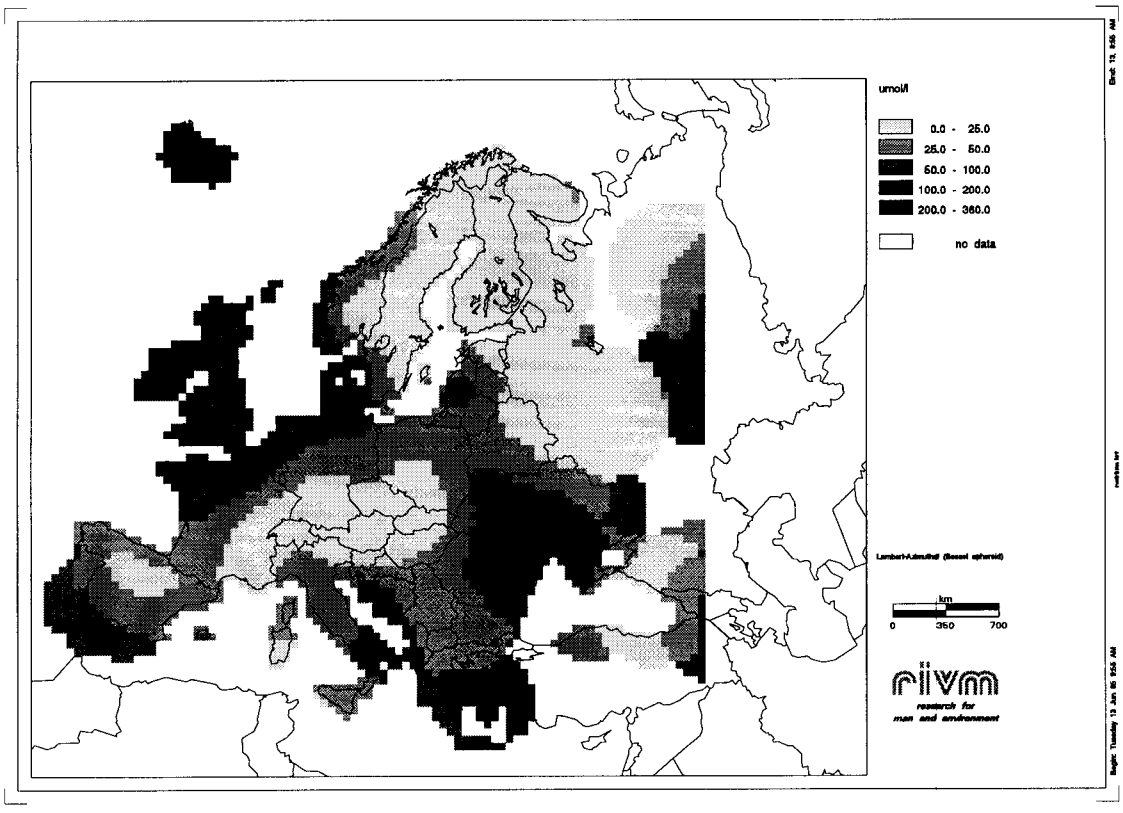

Sodium concentrations on a 50x50 km basis in 1989 in µmol l^{-1}.

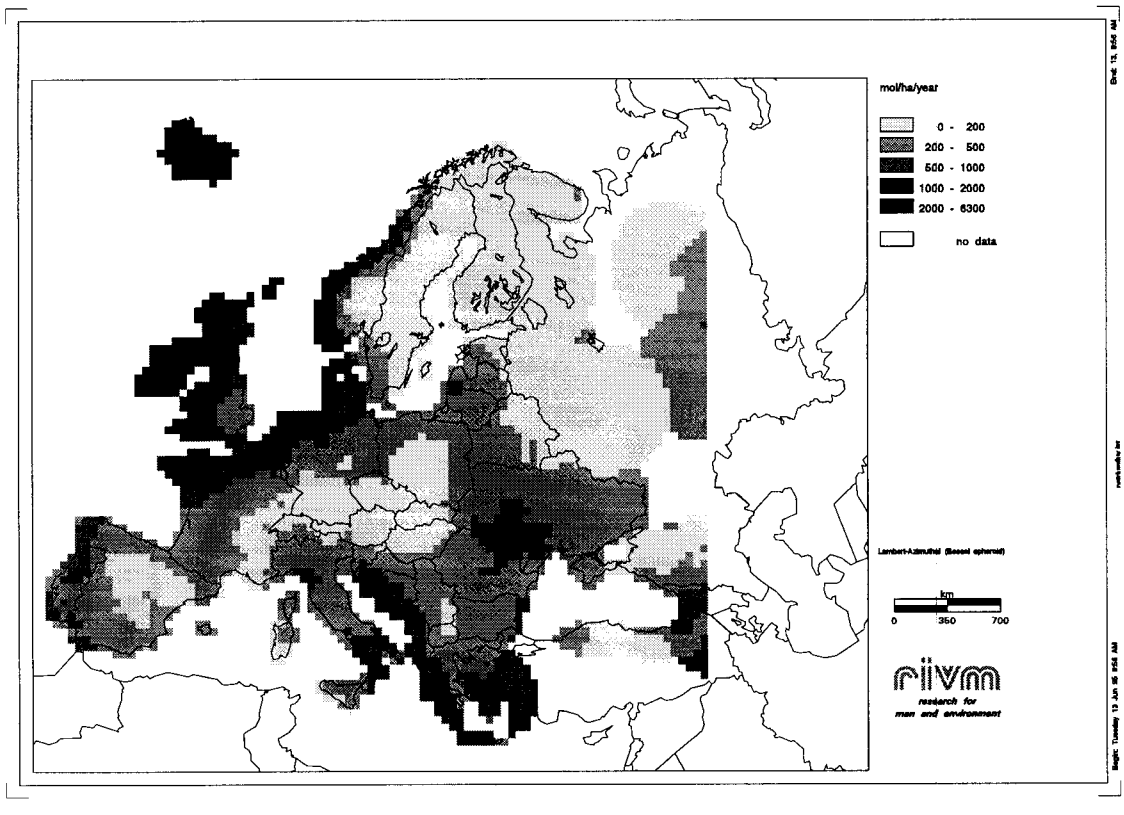

Wet deposition of sodium on a 50x50 km basis in 1989 in mol ha^{-1} a^{-1}.

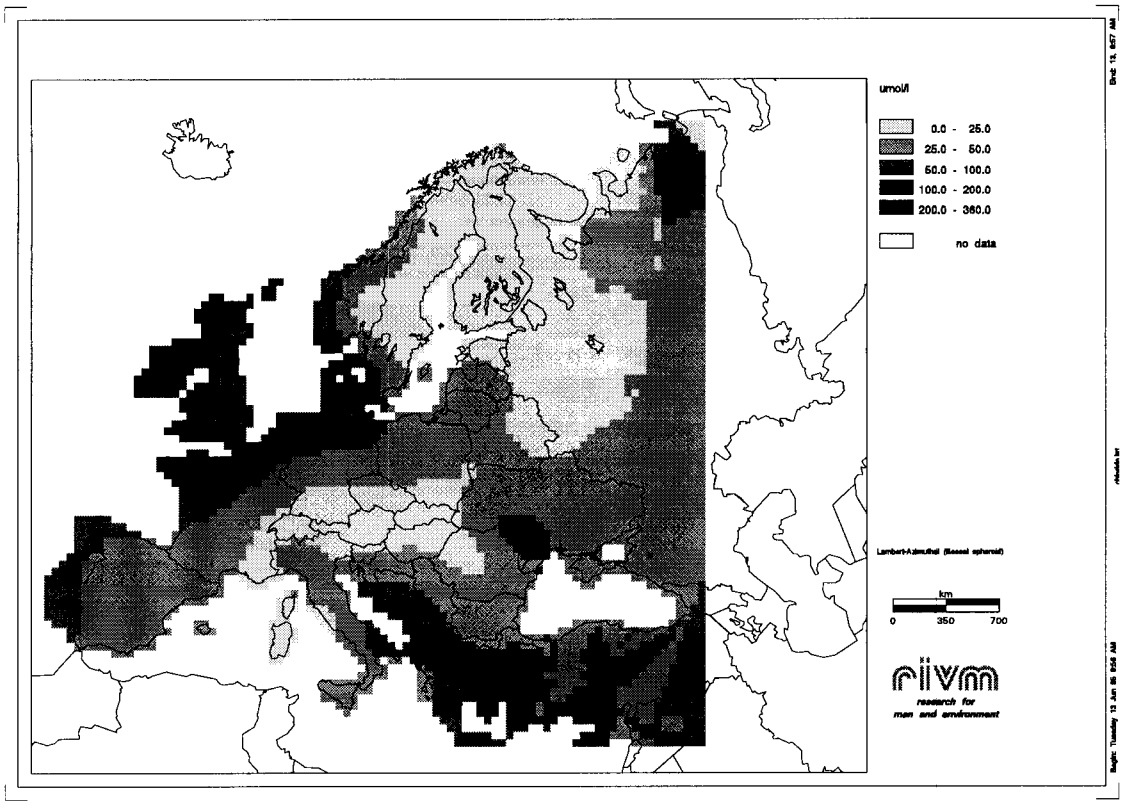

Chloride concentrations on a 50x50 km basis in 1989 in µmol l^{-1}.

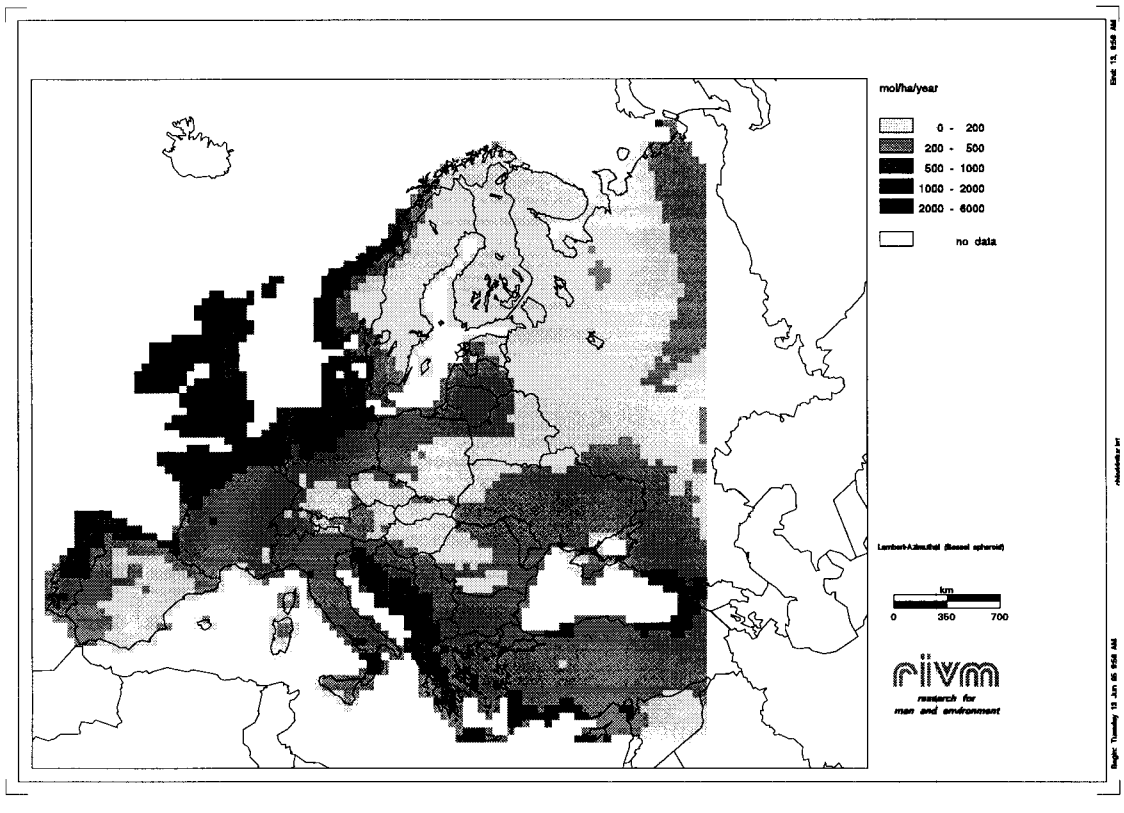

Wet deposition of chloride on a 50x50 km basis in 1989 in mol ha^{-1} a^{-1}.

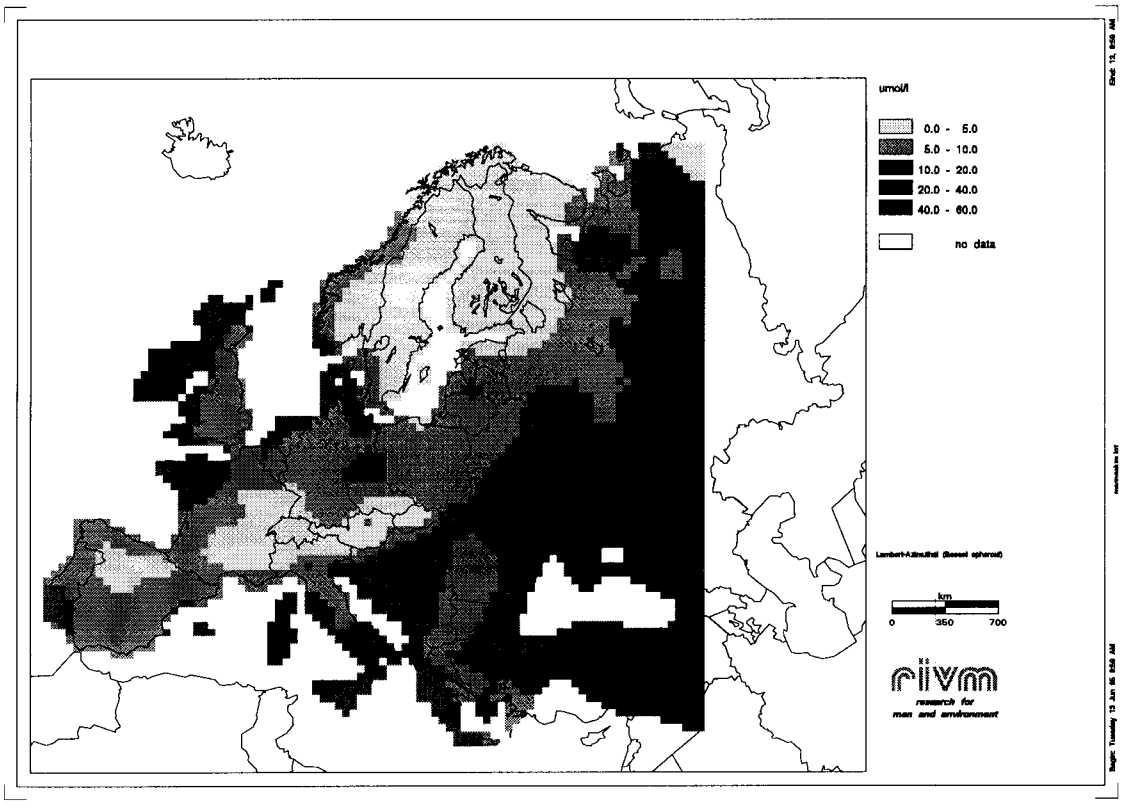

Magnesium concentrations on a 50x50 km basis in 1989 in µmol l^{-1}.

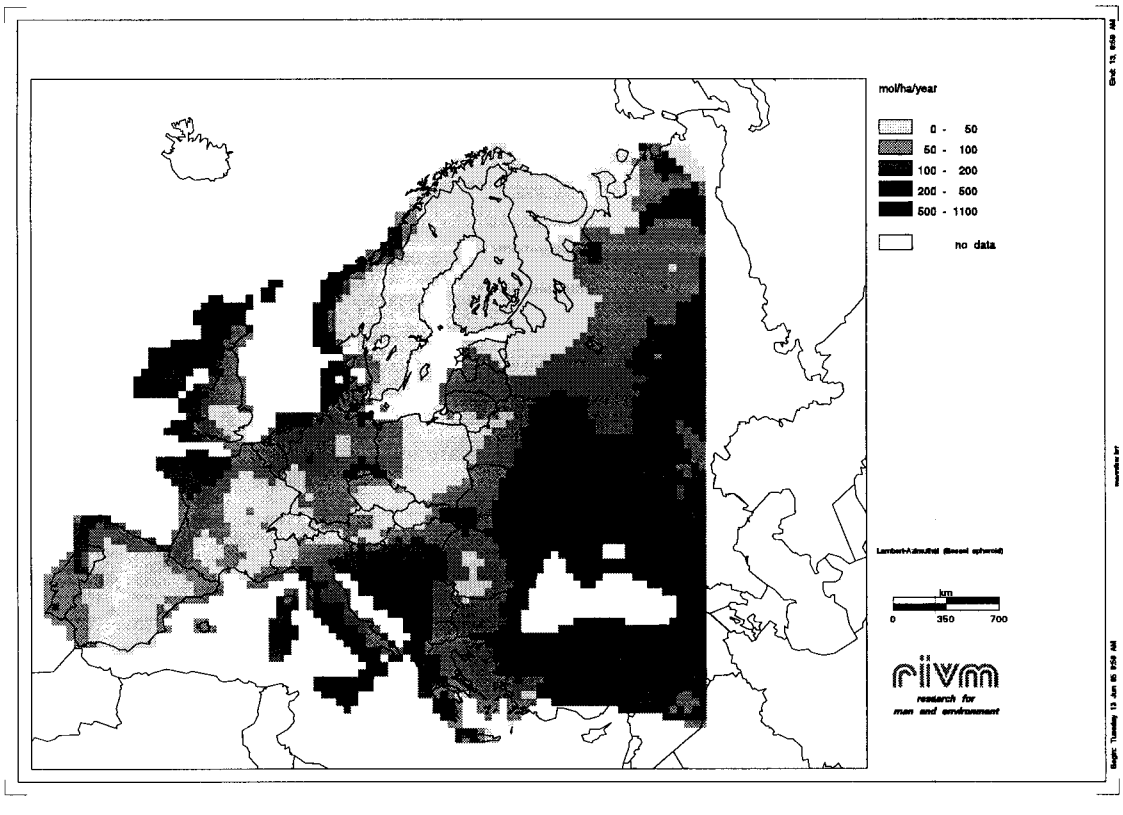

Wet deposition of magnesium on a 50x50 km basis in 1989 in mol ha^{-1} a^{-1}.

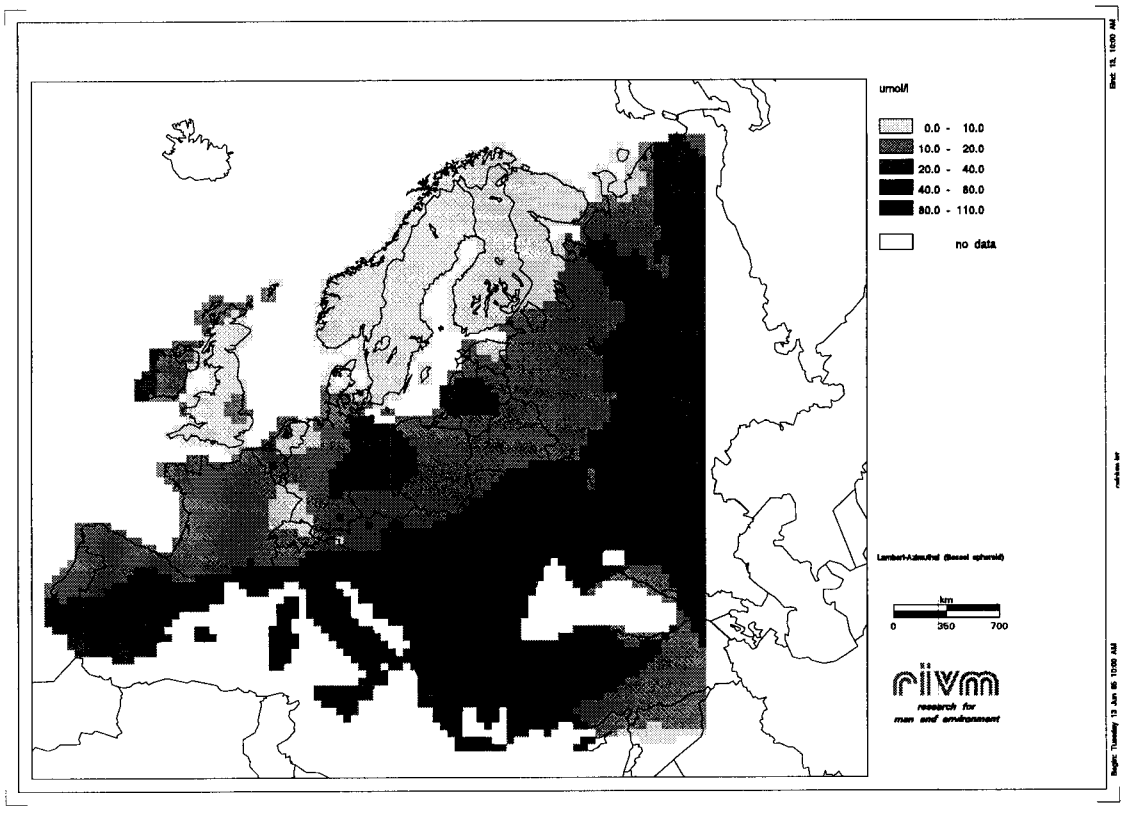

Calcium concentrations on a 50x50 km basis in 1989 in µmol l^{-1}.

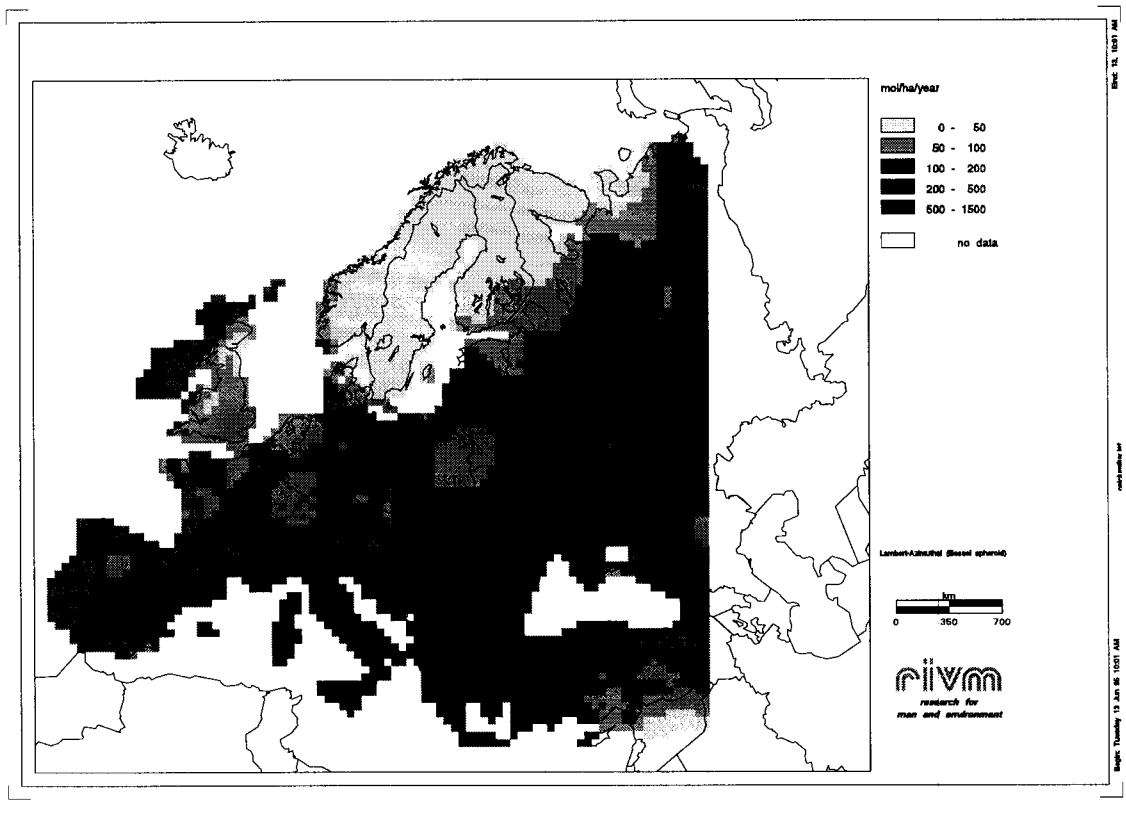

Wet deposition of calcium on a 50x50 km basis in 1989 in mol ha^{-1} a^{-1}.

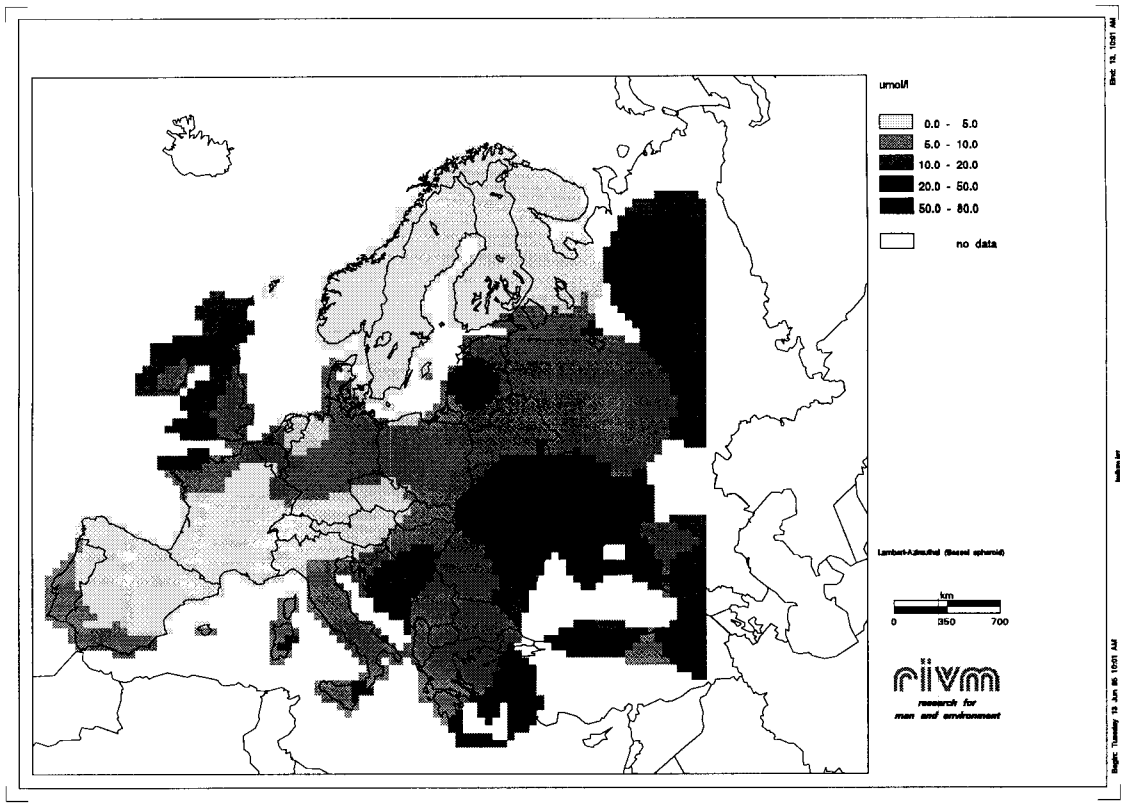

Potassium concentrations on a 50x50 km basis in 1989 in µmol l^{-1}.

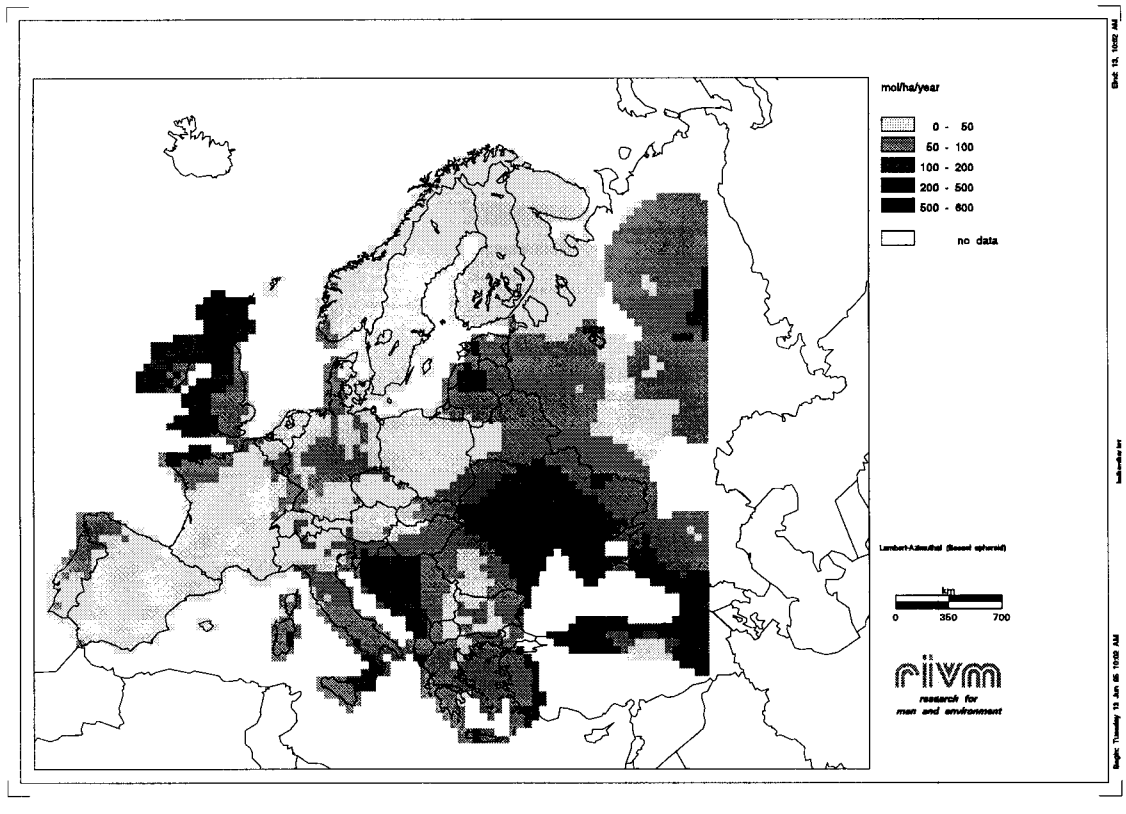

Wet deposition of potassium on a 50x50 km basis in 1989 in mol ha^{-1} a^{-1}.

Appendix 6: Map of deviations between 1989 rainfall amount data by ODS and the long-term yearly mean precipitation amount data by EPA.

rivm
research for man and environment

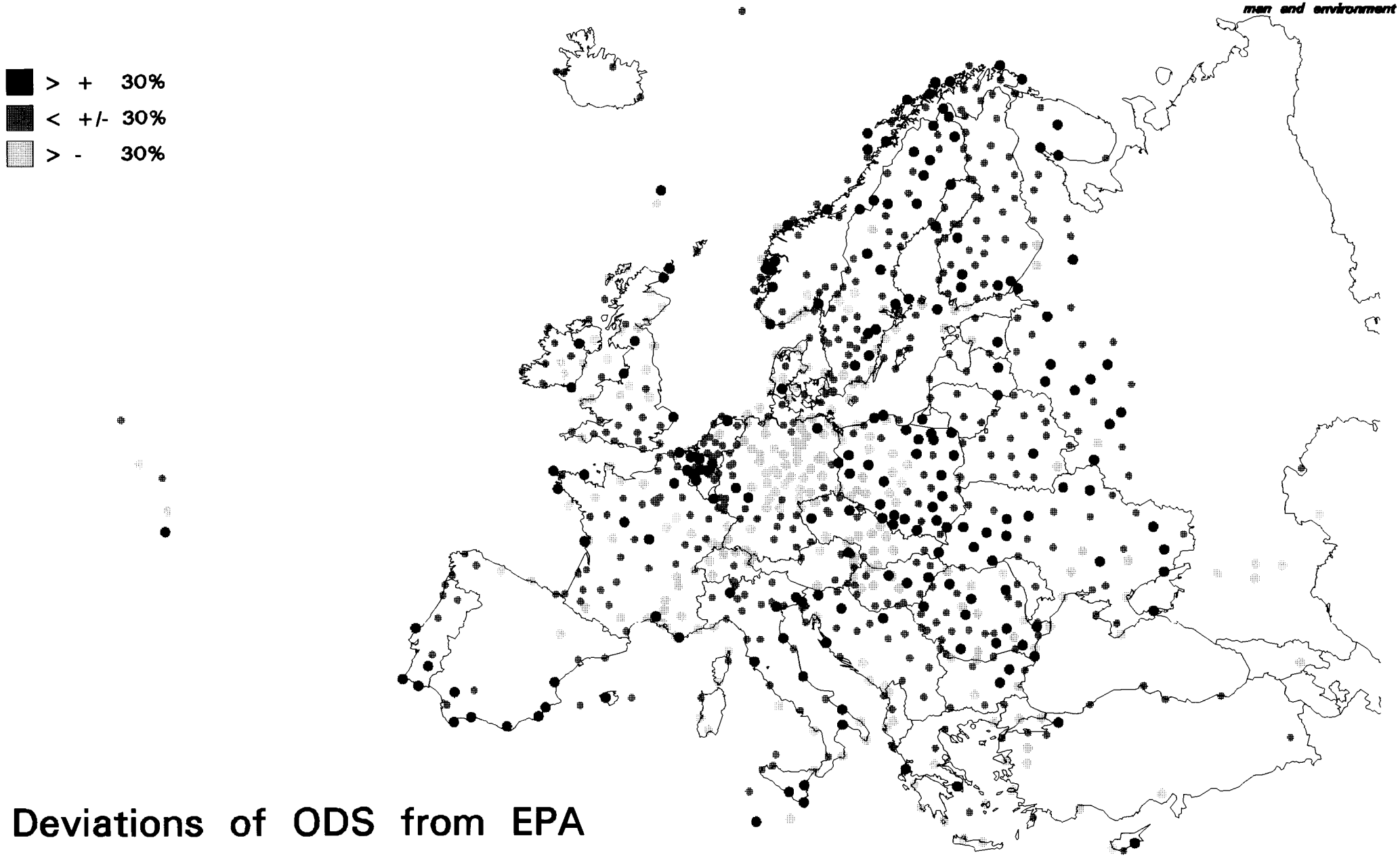

Deviations of ODS from EPA

APPENDIX 7: EMEP WET DEPOSITION IN 1989 BASED ON MODEL RESULTS

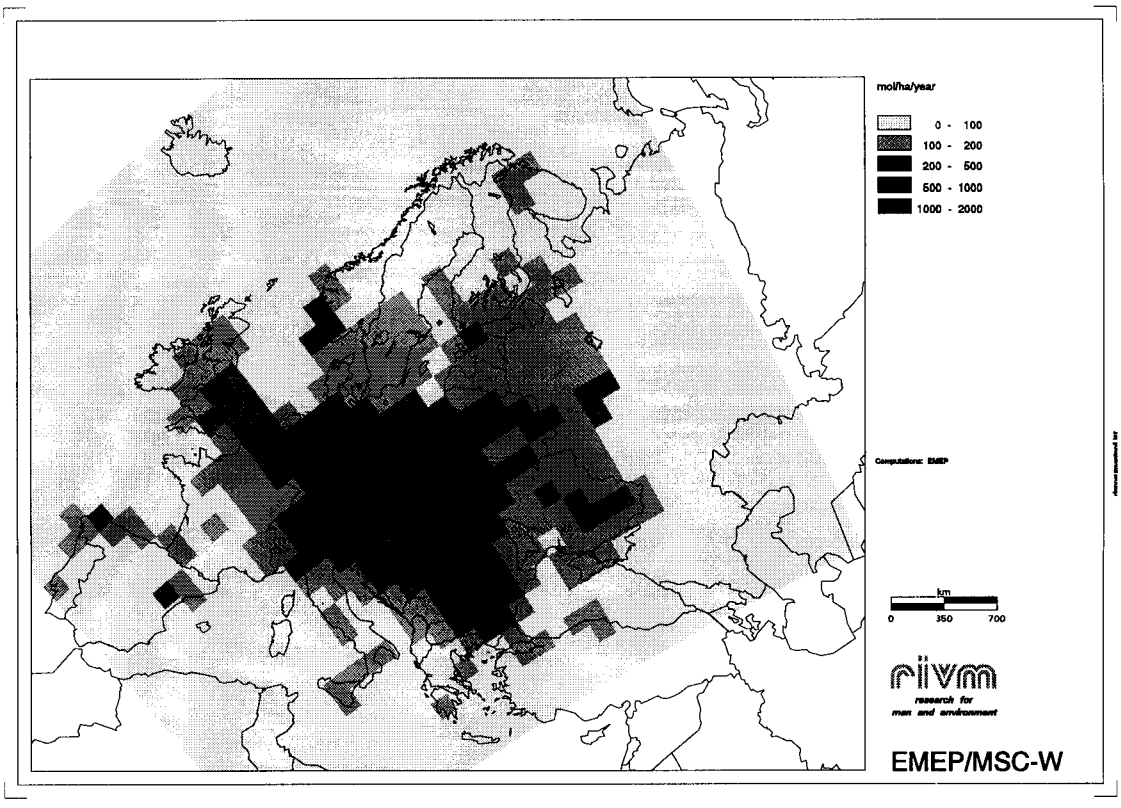

EMEP wet deposition of sulphate on a 150x150 km basis in 1989 in mol ha^{-1} a^{-1}.

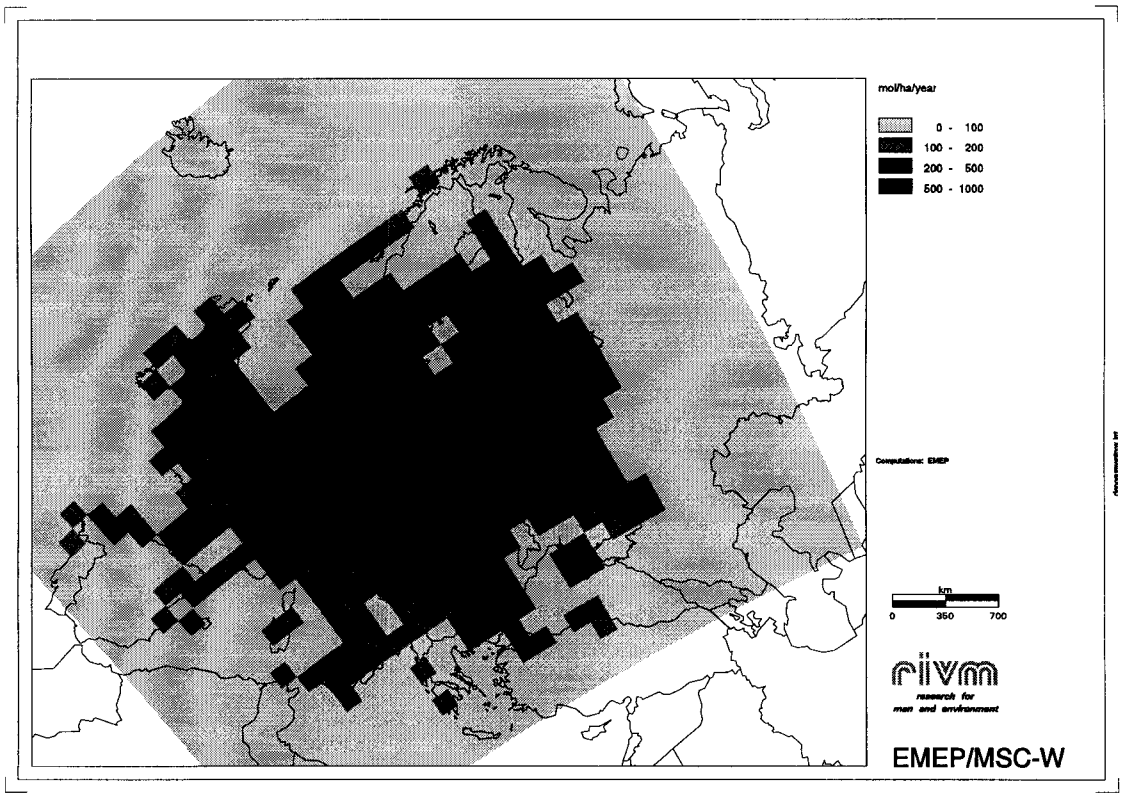

EMEP wet deposition of nitrate on a 150x150 km basis in 1989 in mol ha^{-1} a^{-1}.

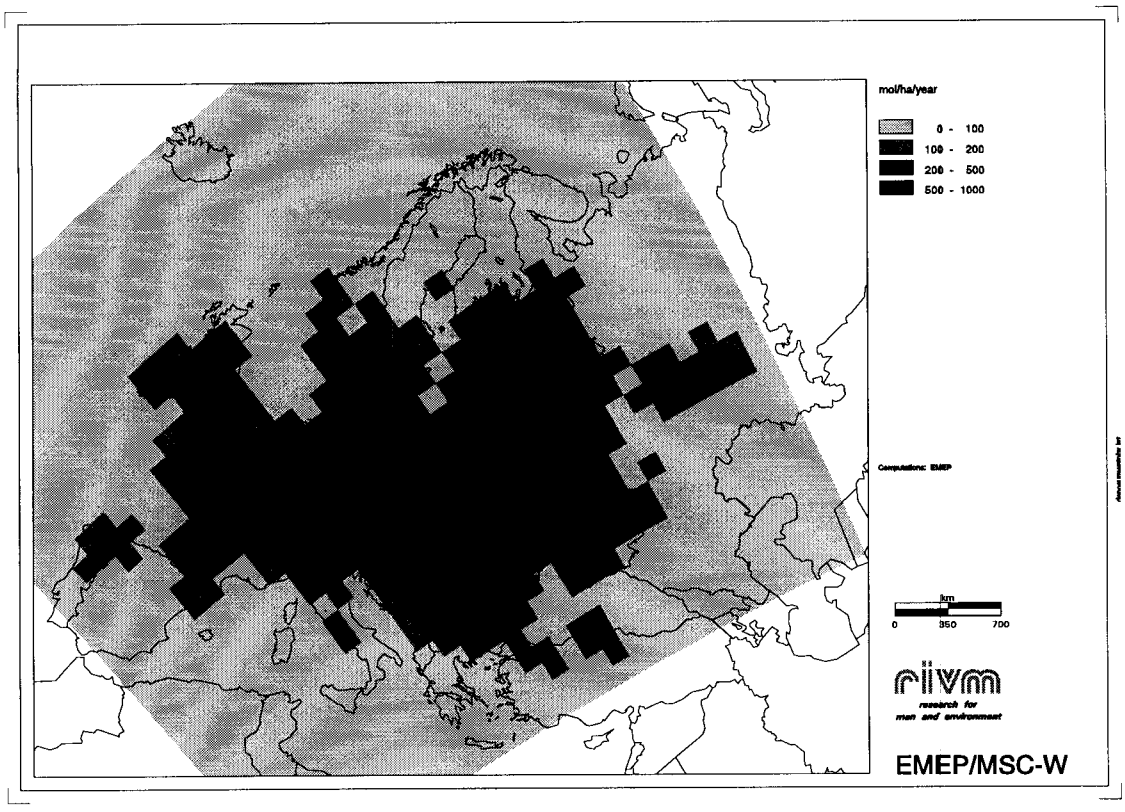

EMEP wet deposition of ammonium on a 150x150 km basis in 1989 in mol ha^{-1} a^{-1}.

Appendix 8: X-Y plots between EMEP values and the average of the new values within one EMEP cell.

SO4 flux: RIVM vs. EMEP

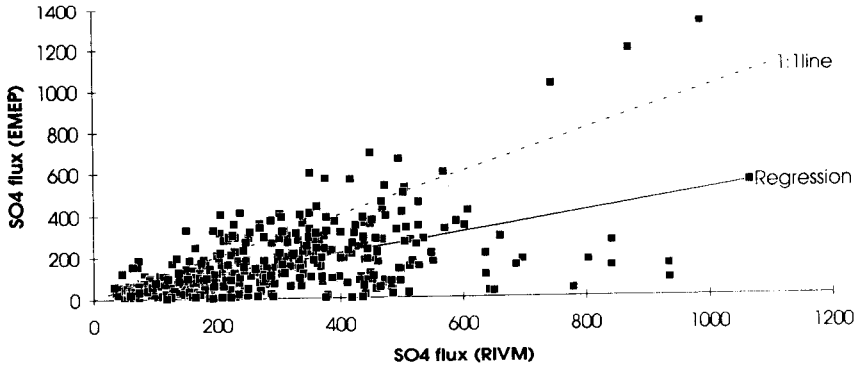

NO3 flux: RIVM vs. EMEP

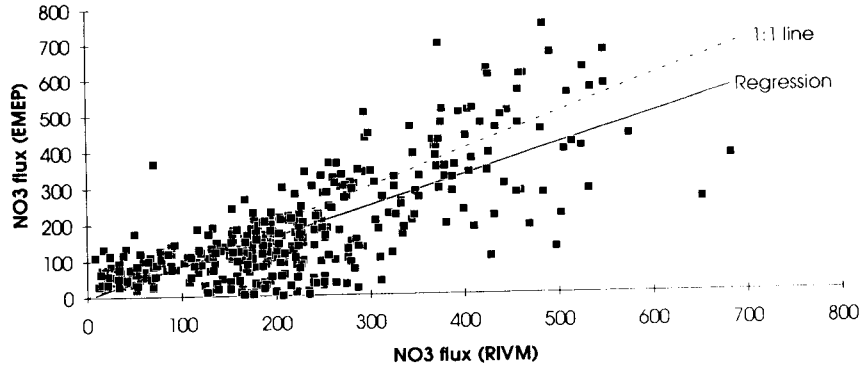

NH4 flux: RIVM vs. EMEP